

5-3-2019

Life History Patterns and the Spatial and Trophic Ecology of Batoids in a Northern Gulf of Mexico Estuary

Matthew Bernard Jargowsky

Follow this and additional works at: <https://scholarsjunction.msstate.edu/td>

Recommended Citation

Jargowsky, Matthew Bernard, "Life History Patterns and the Spatial and Trophic Ecology of Batoids in a Northern Gulf of Mexico Estuary" (2019). *Theses and Dissertations*. 2946.
<https://scholarsjunction.msstate.edu/td/2946>

This Graduate Thesis - Open Access is brought to you for free and open access by the Theses and Dissertations at Scholars Junction. It has been accepted for inclusion in Theses and Dissertations by an authorized administrator of Scholars Junction. For more information, please contact scholcomm@msstate.libanswers.com.

Life history patterns and the spatial and trophic ecology of batoids in a
northern Gulf of Mexico estuary

By

Matthew Bernard Jargowsky

A Thesis
Submitted to the Faculty of
Mississippi State University
in Partial Fulfillment of the Requirements
for the Degree of Master of Science
in Wildlife, Fisheries and Aquaculture
in the Department of Wildlife, Fisheries and Aquaculture

Mississippi State, Mississippi

May 2019

Copyright by
Matthew Bernard Jargowsky
2019

Life history patterns and the spatial and trophic ecology of batoids in a
northern Gulf of Mexico estuary

By

Matthew Bernard Jargowsky

Approved:

J. Marcus Drymon
(Major Professor)

Michael E. Colvin
(Committee Member)

Matthew J. Ajemian
(Committee Member)

Kevin M. Hunt
(Graduate Coordinator)

George M. Hopper
Dean
College of Forest Resources

Name: Matthew Bernard Jargowsky

Date of Degree: May 3, 2019

Institution: Mississippi State University

Major Field: Wildlife, Fisheries, and Aquaculture

Major Professor: J. Marcus Drymon

Title of Study: Life history patterns and the spatial and trophic ecology of batoids in a northern Gulf of Mexico estuary

Pages in Study 121

Candidate for Degree of Master of Science

Mobile Bay is a dynamic estuary home to a diverse faunal assemblage, which includes several species of batoid fishes (Chondrichthyes: Batoidea). To better understand the dynamics of this batoid assemblage, batoids were opportunistically sampled from 440 trawls performed in and around Mobile Bay from 2016 to 2017. The species *Hypanus sabinus* and *Gymnura lessae* were the most common batoids collected (86% of catch). PERMANOVA analysis found the variables day length, location, year, and water temperature best described catch variability. Furthermore, stomach contents from *Gymnura lessae* were sampled to investigate its diet. Most prey were heavily degraded, thus DNA metabarcoding was used to enhance prey identification. Most prey (88.3%) were from the families Sciaenidae and Engraulidae, and the variables season and sex best explained the dietary variability. These data will be necessary for modeling potential habitat and dietary shifts of Mobile Bay's batoids as climate change and anthropogenic disturbances alter estuaries.

ACKNOWLEDGEMENTS

Thank you to Dr. J. Marcus Drymon for granting me the opportunity to pursue my master's degree and for all the support and guidance over the years. Thank you to my committee members, Dr. Michael Colvin and Dr. Matthew Ajemian for their help developing and constructing my thesis. Thank you to the National Fish and Wildlife Foundation for funding the project. Thank you to everyone at Discovery Hall Programs at the Dauphin Island Sea Lab (DISL) for allowing me to sample batoids from their trawls as without their help, none of this research would have been possible. Thank you to all the DISL boat captains, Jonathan Wittmann, Tom Guoba, Rodney Collier, and Russell Wilson for their countless hours spent collecting these hazardous species and recording batoid catch for me.

Thank you to Dr. Sean Powers and everyone at the Fisheries Ecology Lab who has helped me with various parts of my project and given me guidance over the years, specifically Crystal Hightower, Trey Spearman, Pearce Cooper, Reid Nelson, Sarah White, Courtney Buckley, Mariah Livernois, Justin McDonald, Dr. Mark Albins, Dr. Meagan Schrandt, Dr. Kelly Boyle, Deepa Shrestha, and Stan Bosarge. Thank you to all the past interns and undergraduate volunteers who helped me sample batoids over the years: Brandy Malbrough, Kyle Hafstad, Tristan Garriga, Oliver Ho, Michelle Louie, Lauren Still, Trish Vosburg, Jacob Eagleton, Kelly Nichols, Ed Kim, Desaray Swanson,

Andrew Fuehring, Locke Revels, Kathleen Gill, Katya Jagolta, Kirsten Humphries, Frank D'Alonzo, and Cameron McPhail. Thank you to Emily Seubert for all your hard work in the field, allowing me to spend as many days as possible on land writing. Thank you to Dr. Joe Bizzarro for helping me with diet analysis and Dr. Kristene Parsons for sharing your knowledge of butterfly rays with me.

Thank you to my parents, Michael and Lori Jargowsky, for all the continuous support throughout the years, fostering my love of nature, and always pushing me to do my best. Thank you to my brothers, Mike and Ben Jargowsky, for your continuous friendship. Thank you to my Aunt Trish, Trish Repici, and Nona, Lucy Jargowsky, for your constant love and encouragement. Thank you to my Mommom and Poppop, John and Lorie McKiernan, for all your love and support and the summer trips to Acadia National Park, which were some of the best weeks of my life and really reinforced my love of nature. Thank you to the Amanda Jefferson, the love of my life, for pushing me to be the best scientist that I can be and making the time I've spent living on the Gulf Coast with you as wonderful as its been. Finally, thank you to all my friends and extended family not already mentioned for your support.

TABLE OF CONTENTS

ACKNOWLEDGEMENTS.....	ii
LIST OF TABLES.....	vi
LIST OF FIGURES	viii
CHAPTER	
I. LIFE HISTORY PATTERNS OF COASTAL BATOIDS AND THE SPATIAL AND ENVIRONMENTAL FACTORS INFLUENCING THE ASSEMBLAGE IN A NORTHERN GULF OF MEXICO ESTUARY.....	1
Introduction	1
Methods	3
Study Area.....	3
Sampling Methods.....	4
Side-Scan Sonar.....	5
Data Analysis.....	5
Results	8
Trawl Catch	8
Side-Scan Sonar.....	9
PERMANOVA.....	9
Age, Growth, and Reproduction.....	11
Occupancy Modeling.....	13
Discussion.....	14
Tables	22
Figures	33
II. DIETARY HABITS OF <i>GYMNURA LESSAE</i> REVEALED THROUGH DNA METABARCODING OF STOMACH CONTENTS	59
Introduction	59
Methods	62
Sampling Methods.....	62
DNA Metabarcoding	63
Data Analysis.....	66
Results	68
Sample Collection	68

DNA Metabarcoding	69
Sample Size Sufficiency	69
Diet Analysis	70
PERMANOVA.....	71
Discussion.....	74
Tables	80
Figures	88
REFERENCES	100
APPENDIX	
A. FT. MORGAN SIDE-SCAN SONAR ANALYSIS CRUISE REPORTED (CRUISE WI201808-L1).....	109
Introduction	110
Methods	110
Results	111
Tables	113
Figures	119

LIST OF TABLES

Table 1.1	Total number of batoids captured in 440 fishery-independent trawls performed in and around Mobile Bay, Alabama, from February 2016 to November 2017.	22
Table 1.2	Catch data of the four most common batoids, separated by sex and maturity.	24
Table 1.3	PERMANOVA results for all batoids whose numerical catch accounted for at least 5% of the total catch from trawls in and around Mobile Bay, February 2016 to November 2017.	24
Table 1.4	PERMANOVA results for mature <i>Gymnura lessae</i> caught from trawls in and around Mobile Bay, February 2016 to November 2017.	24
Table 1.5	PERMANOVA results for immature <i>Gymnura lessae</i> caught from trawls in and around Mobile Bay, February 2016 to November 2017.	24
Table 1.6	PERMANOVA results for <i>Hypanus sabinus</i> caught from trawls in and around Mobile Bay, February 2016 to November 2017.	24
Table 1.7	Results of CCA analysis on batoid catch data using significant response variables from the PERMANOVA analysis.	29
Table 1.8	Results of the negative binomial GLM for <i>Gymnura lessae</i> catch in the Channel zone modeled to test for differences in catch based on maturity stage with increasing day length.	29
Table 1.9	Top occupancy models for <i>Hypanus sabinus</i> for trawls near the mouth of Mobile Bay from 2016 to 2017 with covariates listed for the parameters occupancy (ψ), local colonization (γ), local extinction (ϵ), and detection (p).	30
Table 1.10	Top occupancy models for <i>Gymnura lessae</i> for trawls near the mouth of Mobile Bay from 2016 to 2017 with covariates listed for the parameters occupancy (ψ), local colonization (γ), local extinction (ϵ), and detection (p).	30

Table 1.11	Top occupancy models for <i>Narcine bancroftii</i> for trawls near the mouth of Mobile Bay from 2016 to 2017 with covariates listed for the parameters occupancy (ψ), local colonization (γ), local extinction (ϵ), and detection (p).	30
Table 1.12	Top occupancy models for <i>Hypanus say</i> for trawls near the mouth of Mobile Bay from 2016 to 2017 with covariates listed for the parameters occupancy (ψ), local colonization (γ), local extinction (ϵ), and detection (p).	30
Table 2.1	Primers used in this study.	80
Table 2.2	Diet composition of <i>Gymnura lessae</i> collected in Mobile Bay from February 2016 to May 2018 using the results of DNA metabarcoding.	26
Table 2.3	Diet composition of <i>Gymnura lessae</i> collected in Mobile Bay from February 2016 to May 2018 using free otoliths as a measure of prey species consumption.	82
Table 2.4	PERMANOVA models for the diet composition of <i>Gymnura lessae</i> using the results of DNA metabarcoding.	28
Table 2.5	PERMANOVA models for the diet composition of <i>Gymnura lessae</i> using free otoliths as a measure of prey species consumption.	84
Table 2.6	PERMANOVA results for the metabarcoding and otolith data pooled into a single dataset to test for differences in diet based on sampling method.	85
Table 2.7	Results of CCA analysis on the metabarcoding data based on the response variables found to be significant in the metabarcoding data PERMANOVA analysis.	85
Table 2.8	Results of CCA analysis on the otolith data based on the response variables found to be significant in both the otolith and metabarcoding data PERMANOVA analysis.	86
Table 2.9	Results of CCA analysis on the metabarcoding data based on the response variables found to be significant in the otolith data PERMANOVA analysis.	87
Table A.1	Contacts in the report.	113
Table A.2	Full contact analysis.	114

LIST OF FIGURES

Figure 1.1	Map of Mobile Bay, Alabama.	33
Figure 1.2	Copy of the partitioned map of Mobile Bay, Alabama, used to record trawl locations throughout the length of the survey.	34
Figure 1.3	Number of trawls per month for each of the four sampling zones used in data analysis.	35
Figure 1.4	Image of the sea floor captured during the side-scan sonar survey of the Channel, including trawl scars marked with white lines.	36
Figure 1.5	Image of the sea floor captured during the side-scan sonar survey of the Channel with outlined depth contours.	37
Figure 1.6	Image of the sea floor captured during the side-scan sonar survey of the Channel showing sediment composition.....	38
Figure 1.7	Interaction plots for a) <i>Hypanus sabinus</i> and b) <i>Gymnura lessae</i> catch for each zone plotted against day length pooled by hour.	39
Figure 1.8	Interaction plots for a) <i>Hypanus sabinus</i> and b) <i>Gymnura lessae</i> catch for day length pooled by hour plotted by temperature binned by 5 °C increments.....	40
Figure 1.9	Interaction plots for a) <i>Hypanus sabinus</i> and b) <i>Gymnura lessae</i> catch for each zone plotted by temperature binned by 5 °C increments.....	41
Figure 1.10	Interaction plots for <i>Narcine bancroftii</i> catch for temperature binned by 5 °C increments plotted by year.	42
Figure 1.11	Interaction plots for a) <i>Hypanus sabinus</i> and b) <i>Gymnura lessae</i> catch for each zone plotted by year.....	43
Figure 1.12	Interaction plots for immature <i>Gymnura lessae</i> catch for day length pooled by hour plotted against temperature binned by 5 °C increments.....	44

Figure 1.13	CCA biplot of the catch data showing the relationships between the response variables and batoid species for the variables found to be significant in the PERMANOVA analysis.....	45
Figure 1.14	Logistic regression fit to sex-specific binomial maturity data for a) female <i>Hypanus sabinus</i> , b) male <i>Hypanus sabinus</i> , c) female <i>Gymnura lessae</i> , d) male <i>Gymnura lessae</i> , e) female <i>Narcine bancroftii</i> , f) male <i>Narcine bancroftii</i> , g) female <i>Hypanus say</i> , h) male <i>Hypanus say</i>	46
Figure 1.15	Length frequency plots for <i>Hypanus sabinus</i> , <i>Gymnura lessae</i> , <i>Narcine bancroftii</i> , and <i>Hypanus say</i>	47
Figure 1.16	<i>Gymnura lessae</i> young sampled in early summer.	48
Figure 1.17	<i>Gymnura lessae</i> young sampled in late summer and presumably a few month in development, still yellow in color.	49
Figure 1.18	<i>Gymnura lessae</i> young sampled in October, which appears close to full term and is now brown in color.	50
Figure 1.19	Estimates from the negative binomial GLM modeled for <i>Gymnura lessae</i> catch in the Channel zone with increasing day length to test for differences in catch based on maturity stage.	51
Figure 1.20	A von Bertalanffy growth function (VBGF) fit to female <i>Gymnura lessae</i> length frequency data using a simulated annealing algorithm, where $L_0 = 17.7$, $L_\infty = 86.7$, $k = 0.50$, and $t_0 = 0.07$, plotted over a) the binned and restructured data used to fit the VBGF and b) a scatter plot of individual disc widths plotted by date of capture.....	52
Figure 1.21	A von Bertalanffy growth function (VBGF) fit to male <i>Gymnura lessae</i> length frequency data using a simulated annealing algorithm, where $L_0 = 17.7$, $L_\infty = 42.9$, $k = 1.12$, and $t_0 = 0.05$, plotted over a) the binned and restructured data used to fit the VBGF and b) a scatter plot of individual disc widths plotted by date of capture.....	53
Figure 1.22	Outputs of the best fitting occupancy model for <i>Hypanus sabinus</i> for the parameters a) initial occupancy, local colonization, and local extinction probability, b) detection probability by day length for 2016, and c) 2017.....	54

Figure 1.23	Outputs of the best fitting occupancy model for <i>Gymnura lessae</i> for the parameters a) initial occupancy and local colonization, b) local extinction probability by year, c) detection probability by date for 2016, d) 2017, e) detection probability by day length for 2016, and f) 2017.55	55
Figure 1.24	Outputs of the best fitting occupancy model for <i>Narcine bancroftii</i> for the parameters a) initial occupancy, local colonization, and local extinction probability, b) detection probability by day length, and c) detection probability by date.56	56
Figure 1.25	Outputs of the best fitting occupancy model for <i>Hypanus say</i> for the parameters a) initial occupancy, local colonization, and local extinction probability, b) detection probability by date for 2016, and c) detection probability by date for 2017.57	57
Figure 2.1	Cumulative prey curves for <i>Gymnura lessae</i> sampled from February 2016 to May 2018 based on the metabarcoding data with prey categories representing distinct species for increasing number of ray stomachs sampled for a) all stomachs, b) stomachs from males, and c) stomachs from females.....88	88
Figure 2.2	Cumulative prey curves for <i>Gymnura lessae</i> sampled from February 2016 to May 2018 based on the otolith data with prey categories representing distinct species for increasing number of ray stomachs sampled for a) all stomachs, b) stomachs from males, and c) stomachs from females.89	89
Figure 2.3	Interaction plots for the metabarcoding data comparing the variables season and sex using mean prey consumption, represented by %N, for the prey species a) <i>Micropogonias undulatus</i> , b) <i>Anchoa hepsetus</i> , and c) <i>Leiostomus xanthurus</i> plotted against season.90	90
Figure 2.4	Interaction plots for the otolith data comparing the variables season and sex using mean prey consumption, represented by %N, for the prey species a) <i>Micropogonias undulatus</i> , b) <i>Anchoa spp.</i> , and c) <i>Leiostomus xanthurus</i> plotted against season.91	91
Figure 2.5	Interaction plots for the metabarcoding data comparing the variables day length and sex using mean prey consumption, represented by %N, for the prey species a) <i>Micropogonias undulatus</i> , b) <i>Anchoa hepsetus</i> , and c) <i>Leiostomus xanthurus</i> plotted against day length pooled by hour.92	92

Figure 2.6	Interaction plots for the otolith data comparing the variables day length and sex using mean prey consumption, represented by %N, for the prey species a) <i>Micropogonias undulatus</i> , b) <i>Anchoa hepsetus</i> , and c) <i>Leiostomus xanthurus</i> plotted against day length pooled by hour.....	93
Figure 2.7	CCA biplots of the metabarcoding data showing the relationships between the response variables found to be significant in the metabarcoding data PERMANOVA analysis and prey species for a) percent number, %N, and b) percent weight, %W, for <i>Gymnura lessae</i>	94
Figure 2.8	CCA biplots of the otolith data showing the relationships between the response variables and prey species / genus for %N showing the variables found to be significant in the PERMANOVA analysis for a) the otolith data and b) the metabarcoding data for <i>Gymnura lessae</i>	95
Figure 2.9	CCA biplots of the metabarcoding data showing the relationships between the response variables found to be significant in the otolith data PERMANOVA analysis and prey species for a) percent number, %N, and b) percent weight, %W, for <i>Gymnura lessae</i>	96
Figure 2.10	Snapshot of trawl contents taken during sampling showing differences in relative body size of <i>Leiostomus xanthurus</i> , larger bodied fish with distinct black spot located above pectoral fin, compared to <i>Anchoa hepsetus</i> , semi-translucent fish with a distinct horizontal silver stripe, and <i>Micropogonias undulatus</i> , smaller bodied fish without distinct black spot located above its pectoral fin.	97
Figure 2.11	Picture of a prey item, <i>Cynoscion arenarius</i> , relative to the body cavity of the <i>Gymnura lessae</i> that consumed it, which was too large to fit completely into the batoids stomach resulting in only partial digestion of the prey.	98
Figure A.1	Survey extent of the Ft. Morgan Sonar Survey outlined in orange.....	119
Figure A.2	Actual cruise track for the Ft. Morgan Sonar Survey.	120
Figure A.3	Contacts identified within the Ft. Morgan Sonar Survey.	121

CHAPTER I
LIFE HISTORY PATTERNS OF COASTAL BATOIDS AND THE SPATIAL AND
ENVIRONMENTAL FACTORS INFLUENCING THE ASSEMBLAGE IN A
NORTHERN GULF OF MEXICO ESTUARY

Introduction

Batooids, superorder Batoidea, are an understudied group of cartilaginous fishes present in all oceanic ecosystems (Last et al. 2016). The International Union for the Conservation of Nature (IUCN) lists 47% of all batoids to be “Data Deficient” and of those where sufficient data exists, 38% are listed as “Threatened” and 22% are listed as “Near Threatened” (Dulvy et al. 2014). As is often the case with sharks, priorities for batoid research are frequently skewed towards charismatic species, such as the manta rays, *Mobula* spp., rather than more abundant benthic species (Flowers et al. 2016). Despite a basic lack of ecological information for many batoid populations, most coastal ecosystems support a suite of different batoid species, many of which occupy distinct ecological niches (Vaudo and Heithaus 2011; Humphries et al. 2016). Furthermore, many of these species undertake seasonal migrations or emigrate offshore, making their ecological role on these coastal ecosystems difficult to quantify (Funicelli 1975; Schwartz 1990). Like most coastal ecosystems, many estuaries in the northern Gulf of Mexico support a diverse batoid assemblage, including dietary generalist and specialists

that forage on a variety of prey ranging from polychaetes to fish (Funicelli 1975; Ajemian and Powers 2012). These mesopredators play vital roles in their ecosystems through both their foraging habits and as important prey for many large predatory sharks (Strong Jr et al. 1990). Moreover, the foraging activities of these batoids can disturb sediments and create feeding pits, which free trapped organic particles for benthic invertebrates (Thrush et al. 1991; O’Shea et al. 2012). These feeding pits can alter benthic communities, increase biodiversity, and suppress the dominance of polychaetes in the substrate (VanBlaricom 1982). Other species have a commensal relationship with these batoids, feeding on organisms flushed to the surface by the feeding events (Thrush et al. 1991; Kajiura et al. 2009). In addition, while most batoids are continuous or active feeders, using a foraging strategy that generally produces a weak prey response, some are ambush predators as well, employing a foraging strategy that is known to elicit a greater effect on prey through nonconsumptive effects (Preisser et al. 2007; Jacobsen and Bennett 2013).

Assessing coastal batoid populations is challenging as most species lack basic life history information. For example, in the northern Gulf of Mexico, age and growth information only exists for a single species, *Rhinoptera bonasus* (Neer and Thompson 2005). This lack of life history information is critical, because while elasmobranchs are often regarded as being susceptible to exploitation given slow growth, late age of maturity, and low reproductive rates, this is not always the case, particularly with small coastal elasmobranchs such as batoids (Frisk 2010). In the absence of age and growth studies, age at maturity can be estimated in early maturing viviparous species with synchronous reproductive cycles by systematically sampling all life stages of the species continuously throughout multiple years (Rudloe 1989). Through this process, cohorts can

be grouped by length and growth can be monitored through length frequency distributions until growth begins to plateau (Pauly and David 1981). This information can be valuable for determining the resilience of a species to anthropogenic disturbances (Carlson et al. 2017).

Estuaries in the northern Gulf of Mexico are changing and will continue to change in the future (Fodrie et al. 2010). With increasing climate change (ocean acidification, warming water) and anthropogenic disturbances (coastal development, fisheries exploitation), monitoring the batoid assemblage will be crucial for understanding the health of coastal ecosystems (Pörtner 2008). This study aims to increase our knowledge of how temporal and environmental factors influence the coastal batoid assemblage in a northern Gulf of Mexico estuary and to provide insight into some of their life history patterns. These data are necessary for modeling potential habitat shifts as waters continue to warm in this region.

Methods

Study Area

Mobile Bay is one of the largest estuaries in the United States (Figure 1.1). It is relatively shallow with an average depth of 3 m, with the exception of the shipping channel, which splits the bay in half, where the average depth is 12 m (Schroeder and Wiseman Jr 1988). The estuary receives the sixth greatest annual freshwater discharge in North America from the Mobile River system to the north while simultaneously receiving saltwater inputs from the Gulf of Mexico to the south (Park et al. 2007). These freshwater and saltwater inputs cause the salinity in the estuary to range from 0 to 35 ppt throughout

the year, which leads to extreme seasonal stratification, causing hypoxic and anoxic events during summer months (Schroeder and Wiseman Jr 1988; Cowan et al. 1996).

Sampling Methods

From 2016 to 2017 batoid species were opportunistically sampled from trawls performed in and around Mobile Bay by Discovery Hall Programs at the Dauphin Island Sea Lab. All trawls were conducted off the 65 ft R/V *Alabama Discovery* using a 25 ft otter trawl between the hours of 0800 to 1700 with between one to five trawls completed per day. Tow times were approximately 30 minutes in duration and performed in 5 to 10 meters of water at approximately 2.5 knots. Individual tow times, depths, speeds, and exact positions were not recorded. Rather, trawl locations were noted using a partitioned map of Mobile Bay (Figure 1.2). All batoids caught were identified to species and counted; most were sacrificed for additional life history studies. For these individuals, measurements were taken for disc width and weight, followed by the determination of sex and maturity. Maturity in males was determined by the calcification of the claspers and the development of the testes. For females, maturity was determined by the development of the ovaries, oviduct, uterus, size of vitellogenic ova, and the presence of ova or embryos in the uterus. This study was performed in accordance with Alabama state laws and under the IACUC protocols (IACUC Board Reference Number 974304) approved by the University of South Alabama. All efforts were taken to reduce animal suffering during handling. Water temperature data were collected from the nearest environmental monitoring station, accessed at mymobilebay.com.

Side-Scan Sonar

A side-scan sonar survey was performed in the Channel, located as described in Figure 1.2. The survey followed the path typically trawled by the captains in that zone, to collect data on bottom features, contours and sediment composition. Transects were conducted aboard the 46 ft R/V *E.O. Wilson* on August 24, 2018, and data analysis was conducted in SonarWiz7. Side-scan sonar analysis involved fine-tuning data appearance, including adjustments to gain normalization, track bottom type, align transects, identify targets with vertical relief, and identify broad-scale bottom features, including changes in sediment composition. After analysis, contact and feature shapefiles as well as the GeoTiff files were imported into QGIS 3.0 and clipped by the area of interest's extent, giving them a cleaner appearance (QGIS Development Team 2018). A copy of the side-scan sonar cruise report is included as Appendix A.

Data Analysis

For community assemblage comparisons, individual trawls were treated as individual sampling events and batoid species catch abundances were treated as the response variables. To avoid bias due to low sample size among factors and variables, catch was only examined for trawl locations with greater than 50 sampling events and for species whose numerical catch accounted for at least 5% of the total catch (Barley et al. 2017). To test for differences in catch based on sex, a binomial test was used. Sex-specific disc width at 50% maturity (DW_{50}) was determined for each species meeting those requirements by fitting a logistic regression to binomial maturity data using the packages, 'FSA' (Ogle et al. 2018) and 'car' (Fox and Weisberg 2007), in the software

program R (v. 3.5.1) (R Core Team 2016). For community analysis, catch was fourth-root transformed, to reduce the effects of multivariate dispersion, and then the Bray-Curtis coefficient was used to create a similarity matrix (Clarke and Warwick 2001).

A Permutational multivariate analysis of variance (PERMANOVA) was used to test for differences in the batoid assemblage across the response variables year, trawls/day, location, day length, and water temperature. The response variables year, trawls/day, and location were treated as factors and the variables day length and water temperature were treated as covariates. For species with sufficient data, these same response variables were also tested using a univariate PERMANOVA with Euclidean distances to examine differences in life history stage (immature and transitional vs mature) and individual species. All PERMANOVAs were permuted 9999 times using the Vegan Community Ecology package (Oksanen et al. 2018) in R. Differences were considered significant if p-values were < 0.05 . A final model was then created using step-wise model selection to determine what combination of response variables best explained the variability in the data (Burnham and Anderson 2003; Bizzarro et al. 2017). Permutation tests for heterogeneity of multivariate group dispersions were run to test all response variables as PERMANOVA is known to be sensitive to sample dispersion (Anderson and Walsh 2013). A canonical correspondence analysis (CCA) was used to complement the results of the PERMANOVA analysis and help determine the association of batoid species and the response variables (Braak and Verdonschot 1995). The significance of the overall model, each canonical axis, and each response variable was determined by permutating the data 9999 times. Biplots were then created for examining correlations between the response variables and each species. A Generalized Linear

Model with a negative binomial distribution and a log link was created using the package ‘Mass’ (Venables and Ripley 2002) in R to test for differences in catch between maturity stages for the variable day length (Hilbe 2011).

To determine relative age at maturity, cohort data were analyzed using the ‘TropFishR’ package (Mildenberger et al. 2017) for data poor stock assessments in R. A von Bertalanffy growth function was fit to sex-specific length frequency data, pooled by month, with the growth parameters length-at-age 0 (L_0), asymptotic length (L_∞), the growth coefficient (k), and the theoretical time at age zero (t_0) estimated using a simulated annealing algorithm (Xiang et al. 2013; Smart et al. 2016).

$$L_t = L_0 + (L_\infty - L_0)(1 - e^{-k(t-t_0)}) \quad (1.1)$$

L_0 was fixed for each sex and estimated by averaging the smallest free-living individual and the largest *in utero* found in this study (Jacobsen et al. 2009; Yokota and Carvalho 2017).

Occupancy modeling and analysis was done in R using the package ‘unmarked’ (Fiske and Chandler 2011). For each species, a multi-season occupancy model was created, with each season being defined as a two-month sampling period (February to March, April to May, June to July, August to September, and October to November, years 2016-2017) (MacKenzie et al. 2003). The number of replicates per site per season varied from 0-41, with a mean of 9.5 replicates; however, while some sites had 0 replicates for one sampling period, no sites had 0 replicates for a season when combining both years. For the parameters local colonization and extinction, the covariates year and average day length were modeled, and for detection, the covariates year, day length, and date were modeled. All continuous variables were standardized prior to analysis. For each

species null, single, and multi covariate models were created and then ranked using Akaike Information Criterion (AIC). The top model was defined as the model with the lowest AIC when also accounting for a two AIC unit increase for every additional parameter included in the model (Arnold 2010; Fish et al. 2018). Model fit was tested using the McKenzie and Bailey goodness-of-fit test extended to dynamic (multiple season) occupancy models in the ‘AICcmodavg’ package using 1000 bootstrap samples (Mazerolle 2017).

Results

Trawl Catch

In total, from February 2016 to November 2017, 440 trawls were performed and 1427 batoids, comprising of seven different species, were caught (Table 1.1). Of the eighteen zones listed in the partitioned map of Mobile Bay, only four sites, Little Dauphin Island, Sand Island, Channel, and North Fort Morgan (zones 12, 13, 14, and 15 respectively on the map) were sampled frequently enough for data analysis (Figure 1.3). In addition, of the seven batoid species caught, only four, *Gymnura lessae*, *Hypanus sabinus*, *Hypanus say*, and *Narcine bancroftii*, were caught frequently enough to be included in data analysis. Significantly more males than females were caught for all those species except for *H. say* (Table 1.2). Both mature and immature male *H. sabinus* were caught at significantly higher rates. *N. bancroftii* showed evidence of aggregation and both cohort and sexual segregation, with over two-thirds of their total catch consisting of mature males and over half of their total catch coming from just four individual trawls, of which 85.7% were mature males.

Side-Scan Sonar

Side-scan sonar was performed in the Channel given the prevalence of trawls from that area (156 of 440 trawls) and the relatively high catch per unit effort (CPUE) (5.11 batoids/trawl) (Figure 1.3). A total of twenty-two transects were performed, revealing five sunken artificial objects and faint trawl scarring (Figure 1.4). The depth along the trawl path increased from 4 m in the northeast section to greater than 10 m near the mouth of the bay (Figure 1.5). There is also a steep drop off near the mouth of the channel where the depth is greater than 10 m, despite being less than 0.25 km from land. Lastly, there is a shift in the sediment composition along the trawl path as the northeast portion of the path is primarily mud, whereas the southern portion is primarily sand (Figure 1.6).

PERMANOVA

For the PERMANOVA model that included all batoid species whose numerical catch accounted for at least 5% of the total catch, none of the five variables were found to have heterogeneity of multivariate group dispersion and the variables year, zone, water temperature, and day length were found to be significant (Table 1.3). In addition, the interaction terms day length x zone, day length x temperature, temperature x year, temperature x zone, and zone x year were all found to be significant. The final model explained 27.8% of the catch variability and included the variables day length, zone, year, and temperature, as well as the interaction terms day length x zone, zone x year, and day length x temperature.

PERMANOVA analysis was also conducted on immature *G. lessae*, mature *G. lessae*, and *H. sabinus* to test if these cohorts / species were affected by certain variables differently than the batoid assemblage as a whole. For the PERMANOVA that examined just mature *G. lessae* catch, the variables temperature and day length were the only variables found to be significant that did not also have evidence of heterogeneity of multivariate group dispersion (Table 1.4). The final model included just the variable temperature and explained 8% of the catch variability. For the PERMANOVA that examined just immature *G. lessae* catch, only the variable day length was found to be significant and not have evidence of heterogeneity of multivariate group dispersion (Table 1.5). The final model included both the variables day length and temperature, as well as their interaction term, and explained 14% of the catch variability. Lastly, the PERMANOVA examining just *H. sabinus* catch found only the variable day length to be significant and not also have evidence of heterogeneity of multivariate group dispersion (Table 1.6). The final model included both the variables day length and temperature and explained 7.1% of the catch variability.

Interaction plots were created for all significant interactions in the PERMANOVA analysis where none of the variables had heterogeneity of multivariate group dispersion. The interaction plots for day length x zone show an interaction for *H. sabinus* at Sand Island when comparing catch at 11-hour day lengths to 12 and 13-hour days (Figure 1.7). In addition, catch for *G. lessae* showed a drastic increase at the Channel during 14-hour days, that is not present in the other day lengths. The interaction plots for day length x temperature shows an interaction between 25 °C and 30 °C with increasing day lengths for both *G. lessae* and *H. sabinus* (Figure 1.8).

The interaction for temperature x year is best explained by the interaction plot for *N. bancroftii*, which shows catch was lower in 2016 than 2017 when water temperatures were cooler, but higher when temperatures were warmer (Figure 1.9). Interaction plots for temperature x zone show an interaction for both *G. lessae* and *H. sabinus* at North Fort Morgan and for *H. sabinus* at Little Dauphin Island (Figure 1.10). Interaction plots for zone x year show an interaction for *G. lessae* at the Channel and for *H. sabinus* at the Channel and at Little Dauphin Island (Figure 1.11). Lastly, the interaction plot for day length and temperature for immature *G. lessae* shows an interaction at all temperatures except for 15 °C to 20 °C (Figure 1.12).

The overall CCA model for the catch data using variables found to be significant in the PERMANOVA analysis was significant (Table 1.7). Both axes, CCA1 and CCA2, and the response variables day length, the zones Channel, Sand Island, and North Fort Morgan, and year were all significant. The model explained 16.5% of the overall catch variability. Of all variables, day length explained the greatest amount of catch variation, followed by the zone Channel, and both were positively correlated with all species, except for *H. sabinus*, which was negatively correlated with day length (Figure 1.13). Other correlations were seen with *H. say* and temperature, as well as *H. sabinus* and the zone Sand Island.

Age, Growth, and Reproduction

Disc width at fifty percent maturity (DW_{50}) was calculated for each of the four batoid species examined in detail (Figure 1.14). *H. sabinus* matured at 23.8 cm disc width in males and 25.4 cm disc width in females. *G. lessae* in this study matured at 34.0 cm

disc width in males and 47.9 cm disc width in females. *N. bancroftii* matured at 15.2 cm in males and 17.1 cm disc width in females. *H. say* matured at 39.6 cm and females matured at 47.9 cm. While the distribution of disc widths of both sexes for *H. sabinus* and *N. bancroftii* appeared uniform, female *G. lessae* and *H. say* were often much larger than the males (Figure 1.15).

G. lessae was the only batoid species of which enough mature females were sampled to adequately describe their reproduction. Unlike *G. micrura* in Brazil and *G. lessae* in the southern Gulf of Mexico, which were reported to have an asynchronous reproductive cycle, *G. lessae* in this study had a synchronous reproductive cycle (Yokota et al. 2012; Cu-Salazar et al. 2014). When female *G. lessae* re-emigrate back to our study area in April, females were either already gravid, with two functional uteri, or have large vitellogenic ova present in their left ovary, indicating that they would become gravid shortly. Of the twenty-two mature females sampled in the month of May, 95.5% were gravid. All young sampled in May and June were small and underdeveloped (Figure 1.16). By mid to late summer, young were much more developed and were yellow in color (Figure 1.17).

In late September, the dorsal coloration of the young turned from yellow to brown, resembling that of wild *G. lessae* (Figure 1.18). Concurrently, vitellogenic ova in the left ovary of mature females began to greatly increase in size. In October, most young appear close to full term, and a range of color from yellowish-brown to completely brown. All mature females sampled in October were gravid, except for some smaller females that were either born the previous winter or were born two winters prior, but did not mature quick enough in their first year of growth to start reproduction one year after

birth. The smallest gravid female in this study had a disc width of 51.5 cm and was caught with near full-term young in late September. The largest measured unborn young was sampled in late September and had a disc width of 16.7 cm. The greatest number of young found in an individual uterus was 5; however, most uteri with near full-term young only contained 2 or 3 young. The smallest *G. lessae* caught was 18.7 cm disc width, which is 2 cm larger than the largest unborn young sampled. Based on the raw data, it appeared that mature and immature *G. lessae* showed different patterns in catch with increasing day length; however, this difference was found to be insignificant (Table 1.8, Figure 1.19).

The estimated von Bertalanffy growth function fit to sex-specific length frequency data showed that both female (Figure 1.20) and male (Figure 1.21) *G. lessae* reach DW_{50} in just over one year of growth. Most females (34 of 38) between the estimated ages of 1 and 2 based on size were considered mature (Figure 1.20). Males grew faster than females ($k = 1.12$ vs 0.50). While t_0 was not fixed for either sex, the values obtained from the simulated annealing algorithms were similar ($t_0 = 0.07$ vs 0.05 for females and males respectively).

Occupancy Modeling

The global and best fitting models for all batoid species had non-significant goodness-of-fit test p-values, indicating proper fit (Tables 1.9-1.12). However, all global and best fitting models also had underdispersion, which can indicate a lack of fit. Only the best fitting model for *G. lessae* included any colonization or detection covariates, as they generally increased or had no effect on the AIC of the models.

The best fitting model for *H. sabinus* is difficult to interpret as most parameters have large 95% prediction intervals; however, the estimated values indicate that the species is always present in all zones, which is supported by the catch data (Figure 1.22). *H. sabinus* detection probability was greatest when day length was the shortest. The best fitting model for *G. lessae* suggested that the species experiences localized extinction and colonization events; however, the extinction rate is estimated to be lower than the colonization rate (Figure 1.23). Detection probability was highest for the species halfway through the year and when day length was greatest. It is difficult to make any interpretations for *N. bancroftii* occupancy, as it has large 95% prediction intervals for both initial occupancy and local extinction (Figure 1.24). However, as with *G. lessae*, its highest detection probability is halfway through the year and when day length was greatest. Lastly for *H. say*, as with the other rays, making interpretations about occupancy is difficult due to large 95% prediction intervals (Figure 1.25). However, the detection probability for the species is near zero in the beginning and end of both years, with a high probability of detection halfway through the year.

Discussion

Despite a diverse batoid assemblage, *H. sabinus* and *G. lessae* were the most common species sampled in and around Mobile Bay, comprising of 86.1% of all batoids caught. *H. sabinus* is common throughout its range, and its euryhaline physiology and tolerance to hypoxia allows it to exploit Mobile Bay, which is shallow, brackish, and often hypoxic (Snelson Jr et al. 1988; Johnson and Snelson Jr 1996; Park et al. 2007). *H. sabinus* in this study were found to mature at slightly larger sizes, 1.4 cm and 3.8 cm for

males and females respectively, than those found in Florida coastal lagoons (Snelson Jr et al. 1988). Interestingly, while male *H. sabinus* were caught more often than females in this survey, Funicelli (1975) found the opposite, suggesting that the species exhibits sexual segregation.

Day length best described the catch variability of *H. sabinus*, as its CPUE was highest with decreasing day length. Funicelli (1975) reported that *H. sabinus* catch declined in Mississippi Sound in the winter as rays moved further offshore to the barrier islands due to sensitivities to lower temperatures. Thus, declines in *H. sabinus* catch in our study area, which is adjacent to barrier islands, may be due to individuals moving further into the estuaries when water temperatures increase. This decline is also seen in the best fitting occupancy model for *H. sabinus*, which shows detection probability decreasing with increasing day length, which is most likely driven by changes in overall abundance of the species, changing the likelihood of capturing an individual.

Neonate *H. sabinus* were most abundant in September and October, a month after parturition was reported to take place in Florida (Snelson Jr et al. 1988). They were also generally at least a centimeter larger than their reported size at birth, and given a lack of gravid female *H. sabinus*, parturition may take place outside our sampling area and the neonates that were encountered immigrated to the area about a month after birth. While our *H. sabinus* catch was dominated by immature individuals, mature individuals are likely to be abundant in adjacent habitats. *H. sabinus* in Florida prefer shallower waters (<1 m), so it may be that adult *H. sabinus* were simply located in areas shallower than was trawled (Snelson Jr et al. 1988). Whether neonate and juvenile *H. sabinus* prefer

slightly deeper waters than the adults, or whether they are being competitively excluded requires further investigation (Zaret and Rand 1971).

G. lessae was common in our sampling area, yet not reported in a previous assessment of inshore batoids in the adjacent Mississippi Sound (Funicelli 1975). The distribution of *G. lessae* in Mobile Bay appears to be extremely heterogeneous; for example, *G. lessae* were hyper abundant in the Channel, but largely absent in areas like Sand Island, despite the close proximity of these areas. Their high abundance in the Channel may reflect a habitat preference for areas with strong currents, varying depths, turbidity, or substrate gradients. Understanding the fine-scale microhabitat preferences will aid in the development of accurate population estimates for this species.

While *G. lessae* in our study area were found to mature in about a year, this may not be the case throughout its range. In addition to displaying a different reproductive cycle than seen in other parts of its range, it appears to grow and mature differently in different areas (Yokota and Carvalho 2017). For instance, DW_{50} calculated in this study was larger, 7.1 cm and 7.4 cm for males and females respectively, than reported for *G. micrura* in Brazil, but 8.9 cm smaller for females than reported for *G. lessae* in the southern Gulf of Mexico (Yokota et al. 2012; Cu-Salazar et al. 2014).

Population trends of *G. lessae* in the Northwest Atlantic Ocean and Gulf of Mexico are largely unknown. In 2005, a study found *G. lessae* populations in the northern Gulf of Mexico to have declined over 99% since the 1970's (Shepherd and Myers 2005); however, many conclusions of that study were later refuted as changes in catch were determined to be due to changes in sampling design, rather than declines in the batoids themselves (Carlson et al. 2017). In 2007, a study reported that *G. lessae*

populations off the United States' Atlantic coast had dramatically increased over the previous thirty-five years due to the loss of apex predatory sharks (Myers et al. 2007); however, many conclusions from this study were later refuted as well (Grubbs et al. 2016). Our study does not examine changes in *G. lessae* populations in the northern Gulf of Mexico over time; however, the fact that both males and females are fast growing and early maturing suggests that *G. lessae* has the potential to withstand moderate exploitation, such as bycatch mortality and capture-induced abortion caused by the shrimp fishery (Carlson et al. 2017; Adams et al. 2018).

N. bancroftii in this study were most commonly found in the Channel. This area most closely mirrors their preferred habitat as described in other studies, which is near beach surf zones and sand bars adjacent to passes between estuarine barrier islands (Funicelli 1975; Rudloe 1989). While our study did not find *N. bancroftii* in as high of abundances as Funicelli (1975), this is likely due to the strong habitat preferences and aggregative nature of the species, which may have been missed by our sampling design. This is further supported by over twice as many male *N. bancroftii* being caught than females in this study, whereas Funicelli (1975) reported females to make up 59% of the total catch. It should also be noted that the strong habitat preferences of this species is in large part why it was incorrectly listed as Critically Endangered by the International Union for Conservation of Nature (Shepherd and Myers 2005; Carvalho et al. 2007; Carlson et al. 2017).

Another factor influencing the species catch is that all sampling in this study took place during the day, whereas *N. bancroftii* are most active at night (Rudloe 1989). *N. bancroftii* were least abundant when water temperatures were low, which is likely due to

the batoid emigrating out of our sampling zones to deeper depths when water temperatures decrease (Bigelow and Schroeder 1953). The best fitting occupancy model for *N. bancroftii* and *G. lessae* showed an increase in detection probability when day length was greatest, with peak detection around the middle of the year, indicating higher abundances of these species in our study area during this time.

H. say were encountered less frequently than expected. This may be the result of sampling design as all four of the zones were near the mouth of Mobile Bay, which has widely varying salinities (Cowan et al. 1996). In contrast, *H. say* are generally found in areas with high salinity (Snelson Jr. et al. 1989). In addition, *H. say* are most active at night, and thus their CPUE would likely be higher if sampling occurred at night (Snelson Jr et al. 1989). When compared to *H. say* captured in Florida coastal lagoons, male *H. say* in this study were found to mature at a slightly larger size, 39.6 cm; however, females were found to mature at a slightly smaller size, 47.9 cm (Snelson Jr et al. 1989). *H. say* CPUE was highly correlated with increasing temperatures in our study area, most likely due to the species emigrating out of the area when water temperatures decrease (Funicelli 1975). While day length was not in the best fitting occupancy model for *H. say*, the model showed that the highest detection probability for the species was in the middle of the year.

Both *H. americanus* and *R. bonasus* were caught infrequently in our trawl survey, accounting for only 2.3% of the numerical batoid catch. This low percentage is most likely due to gear and sampling bias, rather than a true reflection of their relative abundance. *R. bonasus* are benthopelagic and are less likely to occupy the benthic portion of the water column sampled by the trawls (Craig et al. 2010). In addition, they are larger

than any of the four most common batoids in our survey and are more apt to avoid capture. However, while this study was not able to draw any conclusions about *R. bonasus*, a previous study on *R. bonasus* in our sampling area already described movement and habitat use by this species (Ajemian and Powers 2016). Using a combination of gill-net and aerial surveys, Ajemian and Powers (2016) found *R. bonasus* displayed strong spatial and seasonal patterns with regards to ontogeny, with adults restricted to barrier islands while juveniles and young-of-the-year exploited inshore regions of the estuary.

H. americanus was most likely caught in low frequencies due to it being the largest of all benthic batoids in this survey, making it less selective towards our gear. Funicelli (1975) also reported that the species was frequently encountered at depths 15 m greater than was sampled in this study (25 m). Lastly, they are also more active at night when sampling was not taking place (Tilley et al. 2013).

Raja eglanteria was absent in our study, despite reports of it once being commonly caught in our study area in the late fall and winter. Its range in the northern Gulf of Mexico is reported to extend from Florida to eastern Texas, so whether this is truly due to a decline in the species range remains to be seen. *R. eglanteria* egg cases were occasionally trawled up in our sampling, so the species is not completely absent in the study area. With warming water temperatures in the northern Gulf of Mexico, it is also possible that the study area no longer supports a suitable habitat for the species (Fodrie et al. 2010). It should be noted that Shepherd and Myers (2005) reported no significant change in the relative abundance of *R. eglanteria* in the northern Gulf of Mexico from 1972 to 2002.

Day length was the most significant variable in the PERMAONVA analysis and is known to cue elasmobranch movement in other species (Grubbs et al. 2005). While seasonal patterns in batoid movement is often attributed to water temperature, day length is less variable than temperature, which can vary at small spatial scales, and might be a better proxy for large scale movements. However, since our analysis relied on temperature data from the nearest environmental monitoring station, rather than measured where the species were caught, some explanatory power may have been lost.

Sampling location explained the greatest amount of catch variability in the trawl data. This may be because our four sample zones have vastly different habitats, due to their positions east and west of the shipping channel and north and south of the barrier islands. The Channel was also the deepest of our four zones, with varying substrate types and depth contours, which may explain the high CPUE in that region.

While the variable year was significant, this was most likely due to changes in sampling design rather than changes in the batoid communities themselves or a depletion effect. In year one, our sampling vessel broke in mid-October, leading to year two completing almost three times the number of trawls after September than in year one. In addition, in year two, there was an abundance of biofouling bryozoan in the Channel zone, leading it to be trawled less often and most likely altering the benthic community.

There were many potential predictors of batoid relative abundance that were not measured due to the opportunistic nature of the study. While our zones indirectly acted as proxies for substrate type, depth, and current speed, these variables have been shown to influence batoid communities and if independently measured would likely explain additional variability (Dedman et al. 2015). In addition, due to the seasonal and sporadic

freshwater inputs into Mobile Bay, salinity also likely plays a large role in how these batoid communities are structured, yet wasn't measured in this study (Cowan et al. 1996). Future efforts to examine the population structure of batoids in Mobile Bay should focus on the role of these factors, among others.

The batoid assemblage near the mouth of Mobile Bay is complex, with evidence of sexual and cohort segregation, dominated by *H. sabinus* and *G. lessae*. Despite their relative proximity to each other, each of our four sampling zones had widely varying batoid communities, indicating the importance of sampling a variety of different habitat types when attempting to quantify batoid diversity. In addition to differences in batoid catch based on zone, day length was also found to be correlated with differences in batoid catch. As average water temperature increases due to climate change, many of these batoid species will likely stay closer to shore in shallow waters for longer periods of time, as decreases in water temperature appear to be the primary stimulus for many of these species to emigrate from the study area (Funicelli 1975; Pörtner 2008). However, how increasing water temperatures will affect the batoid assemblage in Mobile Bay remains to be seen.

Tables

Table 1.1 Total number of batoids captured in 440 fishery-independent trawls performed in and around Mobile Bay, Alabama, from February 2016 to November 2017.

Species	Common Name	Number Caught
<i>Hypanus sabinus</i>	Atlantic stingray	621
<i>Gymnura lessae</i>	Smooth butterfly ray	609
<i>Hypanus say</i>	Bluntnose stingray	91
<i>Narcine bancroftii</i>	Lesser electric ray	71
<i>Hypanus americanus</i>	Southern stingray	17
<i>Rhinoptera bonasus</i>	Cownose ray	16
<i>Aetobatus narinari</i>	Spotted eagle ray	2
Total		1427

Table 1.2 Catch data of the four most common batoids, separated by sex and maturity.

Species	All Batoids			Mature Batoids			Immature Batoids		
	Male	Female	<i>P</i>	Males	Females	<i>P</i>	Males	Females	<i>P</i>
<i>Hypanus sabinus</i>	353	258	0.0001*	68	33	0.0006*	283	222	0.0075*
<i>Gymnura lessae</i>	303	216	0.0002*	179	120	0.0008*	114	90	0.1071
<i>Narcine bancroftii</i>	46	18	0.0006*	43	10	0.0001*	3	5	0.7266
<i>Hypanus say</i>	53	37	0.1133	20	9	0.0614	28	23	0.5758

Binomial test results for differences in sex ratios are shown for all individuals and for each life stage. Significant values p-values ($P < 0.05$) indicated with *.

Table 1.3 PERMANOVA results for all batoids whose numerical catch accounted for at least 5% of the total catch from trawls in and around Mobile Bay, February 2016 to November 2017.

Model(s)	Variable(s)	<i>df</i>	<i>F</i>	<i>R</i> ²	<i>P</i>	<i>Disp P</i>
Independent Variables	Trawl	4	1.2345	0.0130	0.2792	0.5051
	Year	1	9.6412	0.0249	0.0002*	0.5565
	Zone	3	14.1910	0.1017	0.0001*	0.1158
	Temperature	1	6.9425	0.0180	0.0011*	0.3243
	Day Length	1	22.5030	0.0562	0.0001*	0.1780
Interactions	Day Length x Year	1	2.8741	0.0070	0.0627	
	Day Length x Zone	3	12.5340	0.0783	0.0001*	
	Day Length x Temperature	1	5.1166	0.0125	0.0063*	
	Temperature x Year	1	4.6039	0.0116	0.0117*	
	Temperature x Zone	3	2.6105	0.0181	0.0201*	
	Zone x Year	3	3.1291	0.0217	0.0058*	
Final Model	Day Length	1	28.4473	0.0562	0.0001*	
	Zone	3	15.3326	0.0909	0.0001*	
	Year	1	8.6568	0.0171	0.0005*	
	Temperature	1	6.4107	0.0127	0.0020*	
	Day Length x Zone	3	11.5877	0.0687	0.0001*	
	Zone x Year	3	2.8019	0.0166	0.0136*	
	Day Length x Temperature	1	7.6067	0.0150	0.0005*	
	Residuals	366		0.7229		

Degrees of freedom (*df*), F-statistic (*F*), coefficient of determination (*R*²), p-value (*P*), and p-value of dispersion analysis (*Disp P*) are included for all independent variables and interaction terms. Significant p-values ($P < 0.05$) indicated with *.

Table 1.4 PERMANOVA results for mature *Gymnura lessae* caught from trawls in and around Mobile Bay, February 2016 to November 2017.

Model(s)	Variable(s)	<i>df</i>	<i>F</i>	<i>R</i> ²	<i>P</i>	<i>Disp P</i>
Independent Variables	Trawl	4	0.5302	0.0057	0.6979	0.7040
	Year	1	0.0068	0.0000	0.9375	0.9408
	Zone	3	15.2390	0.1092	0.0001*	0.0001*
	Temperature	1	32.6060	0.0800	0.0001*	0.2185
	Day Length	1	14.9610	0.0384	0.0004*	0.5610
Interactions	Day Length x Year	1	2.1998	0.0056	0.1427	
	Day Length x Zone	3	26.8630	0.1541	0.0001*	
	Day Length x Temperature	1	0.8769	0.0022	0.3483	
	Temperature x Year	1	0.7500	0.0018	0.3861	
	Temperature x Zone	3	6.2340	0.0390	0.0007*	
	Zone x Year	3	1.3117	0.0093	0.2666	
Final Model	Temperature	1	32.6060	0.0800	0.0001*	
	Residuals	375		0.9200		

Degrees of freedom (*df*), F-statistic (*F*), coefficient of determination (*R*²), p-value (*P*), and p-value of dispersion analysis (*Disp P*) are included for all independent variables and interaction terms. Significant p-values ($P < 0.05$) indicated with *.

Table 1.5 PERMANOVA results for immature *Gymnura lessae* caught from trawls in and around Mobile Bay, February 2016 to November 2017.

Model(s)	Variable(s)	<i>df</i>	<i>F</i>	<i>R</i> ²	<i>P</i>	<i>Disp P</i>
Independent Variables	Trawl	4	2.4157	0.0253	0.0511	0.0505
	Year	1	6.7263	0.0176	0.0121*	0.0111*
	Zone	3	12.6370	0.0923	0.0001*	0.0001*
	Temperature	1	0.1297	0.0004	0.7131	0.3774
	Day Length	1	26.5660	0.0662	0.0001*	0.1123
Interactions	Day Length x Year	1	0.0831	0.0002	0.7778	
	Day Length x Zone	3	4.5902	0.0308	0.0052*	
	Day Length x Temperature	1	16.1800	0.0373	0.0001*	
	Temperature x Year	1	7.0201	0.0181	0.0081*	
	Temperature x Zone	3	1.2839	0.0094	0.2838	
	Zone x Year	3	6.4374	0.0450	0.0004*	
Final Model	Day Length	1	28.6920	0.0662	0.0001*	
	Temperature	1	15.8360	0.0365	0.0002*	
	Day Length x Temperature	1	16.1800	0.0373	0.0001*	
	Residuals	373		0.8600		

Degrees of freedom (*df*), F-statistic (*F*), coefficient of determination (*R*²), p-value (*P*), and p-value of dispersion analysis (*Disp P*) are included for all independent variables and interaction terms. Significant p-values ($P < 0.05$) indicated with *.

Table 1.6 PERMANOVA results for *Hypanus sabinus* caught from trawls in and around Mobile Bay, February 2016 to November 2017.

Model(s)	Variable(s)	<i>df</i>	<i>F</i>	<i>R</i> ²	<i>P</i>	<i>Disp P</i>
Independent Variables	Trawl	4	1.1511	0.0121	0.3403	0.2886
	Year	1	18.0710	0.0456	0.0001*	0.0001*
	Zone	3	4.1629	0.0322	0.0067*	0.0321*
	Temperature	1	0.0068	0.0000	0.9327	0.6635
	Day Length	1	19.0250	0.0479	0.0001*	0.1056
Interactions	Day Length x Year	1	2.9248	0.0071	0.0934	
	Day Length x Zone	3	2.3803	0.0175	0.0669	
	Day Length x Temperature	1	0.3023	0.0008	0.5855	
	Temperature x Year	1	4.7104	0.0118	0.0299*	
	Temperature x Zone	3	1.4780	0.0114	0.2205	
	Zone x Year	3	1.7172	0.0128	0.1554	
Final Model	Day Length	1	19.4083	0.0479	0.0001*	
	Temperature	1	9.3169	0.0230	0.0033*	
	Residuals	377		0.9291		

Degrees of freedom (*df*), F-statistic (*F*), coefficient of determination (*R*²), p-value (*P*), and p-value of dispersion analysis (*Disp P*) are included for all independent variables and interaction terms. Significant p-values (*P* < 0.05) indicated with *.

Table 1.7 Results of CCA analysis on batoid catch data using significant response variables from the PERMANOVA analysis.

	<i>df</i>	<i>F</i>	<i>P</i>
Overall Model	6	11.9050	0.0001*
Canonical Axis			
CCA1	1	48.1566	0.0001*
CCA2	1	16.8799	0.0001*
Response Variables			
Day Length	1	32.6344	0.0001*
Channel	1	15.9434	0.0001*
Sand Island	1	6.5965	0.0001*
North Ft. Morgan	1	2.6093	0.0312*
Year	1	8.5342	0.0001*
Temperature	1	5.1121	0.0007*

Degrees of freedom (*df*), F-statistic (*F*), and p-value (*P*). Significant p-values ($P < 0.05$) indicated with *.

Table 1.8 Results of the negative binomial GLM for *Gymnura lessae* catch in the Channel zone modeled to test for differences in catch based on maturity stage with increasing day length.

Coefficients	Estimate	Std. Error	z value	<i>P</i>
Intercept	-10.1886	1.8292	-5.570	0.0001*
Day Length	0.8024	0.1439	5.576	0.0001*
Mature	-4.4506	2.6389	-1.687	0.0917
Day Length x Mature	0.3592	0.2067	1.737	0.0823

Significant p-values ($P < 0.05$) indicated with *.

Table 1.9 Top occupancy models for *Hypanus sabinus* for trawls near the mouth of Mobile Bay from 2016 to 2017 with covariates listed for the parameters occupancy (ψ), local colonization (γ), local extinction (ε), and detection (p).

Models	K	AIC	Δ AIC	AICwt	GoF P	\hat{c}
$\psi(\cdot) + \gamma(\cdot) + \varepsilon(\cdot) + p(\cdot)$	4	530.5	19.4	0.00	0.928	0.31
$\psi(\cdot) + \gamma(\text{year}) + \varepsilon(\text{year}) + p(\cdot)$	6	534.6	23.4	0.00	0.922	0.31
$\psi(\cdot) + \gamma(\cdot) + \varepsilon(\cdot) + p(\text{year})$	5	522.0	10.8	0.00	0.742	0.09
$\psi(\cdot) + \gamma(\text{month}) + \varepsilon(\text{month}) + p(\cdot)$	12	544.4	33.3	0.00	0.939	0.36
$\psi(\cdot) + \gamma(\text{day length}) + \varepsilon(\text{day length}) + p(\cdot)$	4	566.3	55.2	0.00	0.910	0.40
$\psi(\cdot) + \gamma(\cdot) + \varepsilon(\cdot) + p(\text{day length})$	5	515.5	4.3	0.10	0.428	0.87
$\psi(\cdot) + \gamma(\cdot) + \varepsilon(\cdot) + p(\text{date} + \text{date}^2)$	6	515.9	4.8	0.08	0.875	0.22
$\psi(\cdot) + \gamma(\cdot) + \varepsilon(\cdot) + p(\text{year} + \text{day length})^*$	6	511.2	0.0	0.82	0.919	0.13
$\psi(\cdot) + \gamma(\text{all}) + \varepsilon(\text{all}) + p(\text{all})$	12	521.7	10.5	0.00	0.846	0.10

∞ Number of parameters (K), AIC, Δ AIC, model weight (AICwt), goodness-of-fit test p-values (GOF P), and the overdispersion parameter (\hat{c}). Best fitting model indicated with *.

Table 1.10 Top occupancy models for *Gymnura lessae* for trawls near the mouth of Mobile Bay from 2016 to 2017 with covariates listed for the parameters occupancy (ψ), local colonization (γ), local extinction (ε), and detection (p).

Models	K	AIC	Δ AIC	AICwt	GoF P	\hat{c}
$\psi(\cdot) + \gamma(\cdot) + \varepsilon(\cdot) + p(\cdot)$	4	491.0	50.4	0.00	0.115	1.39
$\psi(\cdot) + \gamma(\text{year}) + \varepsilon(\text{year}) + p(\cdot)$	6	490.8	50.2	0.00	0.105	1.40
$\psi(\cdot) + \gamma(\cdot) + \varepsilon(\cdot) + p(\text{year})$	5	479.8	39.1	0.00	0.276	1.14
$\psi(\cdot) + \gamma(\text{month}) + \varepsilon(\text{month}) + p(\cdot)$	12	502.9	62.3	0.00	0.121	1.40
$\psi(\cdot) + \gamma(\text{day length}) + \varepsilon(\text{day length}) + p(\cdot)$	4	502.4	61.8	0.00	0.167	1.24
$\psi(\cdot) + \gamma(\cdot) + \varepsilon(\cdot) + p(\text{day length})$	5	453.8	13.1	0.00	0.229	0.96
$\psi(\cdot) + \gamma(\cdot) + \varepsilon(\cdot) + p(\text{date} + \text{date}^2)$	6	449.2	8.6	0.01	0.124	1.79
$\psi(\cdot) + \gamma(\cdot) + \varepsilon(\text{year}) + p(\text{year} + \text{day length} + \text{date} + \text{date}^2)^*$	9	440.7	0.0	0.88	0.689	0.05
$\psi(\cdot) + \gamma(\text{all}) + \varepsilon(\text{all}) + p(\text{all})$	12	444.8	4.2	0.11	0.616	0.04

30 Number of parameters (K), AIC, Δ AIC, model weight (AICwt), goodness-of-fit test p-values (GOF P), and the overdispersion parameter (\hat{c}). Best fitting model indicated with *.

Table 1.11 Top occupancy models for *Narcine bancroftii* for trawls near the mouth of Mobile Bay from 2016 to 2017 with covariates listed for the parameters occupancy (ψ), local colonization (γ), local extinction (ε), and detection (p).

Models	K	AIC	Δ AIC	AICwt	GoF P	\hat{c}
$\psi(\cdot) + \gamma(\cdot) + \varepsilon(\cdot) + p(\cdot)$	4	176.2	24.0	0.00	0.532	0.02
$\psi(\cdot) + \gamma(\text{year}) + \varepsilon(\text{year}) + p(\cdot)$	6	177.7	25.5	0.00	0.610	0.01
$\psi(\cdot) + \gamma(\cdot) + \varepsilon(\cdot) + p(\text{year})$	5	178.0	25.8	0.00	0.507	0.05
$\psi(\cdot) + \gamma(\text{month}) + \varepsilon(\text{month}) + p(\cdot)$	12	185.0	32.8	0.00	0.437	0.02
$\psi(\cdot) + \gamma(\text{day length}) + \varepsilon(\text{day length}) + p(\cdot)$	4	175.3	23.1	0.00	0.559	0.01
$\psi(\cdot) + \gamma(\cdot) + \varepsilon(\cdot) + p(\text{day length})$	5	171.9	19.7	0.00	0.085	1.50
$\psi(\cdot) + \gamma(\cdot) + \varepsilon(\cdot) + p(\text{date} + \text{date2})$	6	174.5	22.3	0.00	0.105	1.03
$\psi(\cdot) + \gamma(\cdot) + \varepsilon(\cdot) + p(\text{day length} + \text{date} + \text{date2})^*$	7	152.2	0.0	0.99	0.636	0.01
$\psi(\cdot) + \gamma(\text{all}) + \varepsilon(\text{all}) + p(\text{all})$	12	161.2	9.0	0.01	0.706	0.01

Number of parameters (K), AIC, Δ AIC, model weight (AICwt), goodness-of-fit test p-values (GOF P), and the overdispersion parameter (\hat{c}). Best fitting model indicated with *.

Table 1.12 Top occupancy models for *Hypanus say* for trawls near the mouth of Mobile Bay from 2016 to 2017 with covariates listed for the parameters occupancy (ψ), local colonization (γ), local extinction (ε), and detection (p).

Models	K	AIC	Δ AIC	AICwt	GoF P	\hat{c}
$\psi(\cdot) + \gamma(\cdot) + \varepsilon(\cdot) + p(\cdot)$	4	245.9	26.0	0.00	0.642	0.01
$\psi(\cdot) + \gamma(\text{year}) + \varepsilon(\text{year}) + p(\cdot)$	6	245.5	25.6	0.00	0.675	0.01
$\psi(\cdot) + \gamma(\cdot) + \varepsilon(\cdot) + p(\text{year})$	5	246.7	26.8	0.00	0.709	0.01
$\psi(\cdot) + \gamma(\text{month}) + \varepsilon(\text{month}) + p(\cdot)$	12	253.5	33.6	0.00	0.592	0.01
$\psi(\cdot) + \gamma(\text{day length}) + \varepsilon(\text{day length}) + p(\cdot)$	4	248.5	28.6	0.00	0.587	0.01
$\psi(\cdot) + \gamma(\cdot) + \varepsilon(\cdot) + p(\text{day length})$	5	232.2	12.3	0.00	0.480	0.06
$\psi(\cdot) + \gamma(\cdot) + \varepsilon(\cdot) + p(\text{date} + \text{date2})$	6	230.8	10.9	0.00	0.471	0.08
$\psi(\cdot) + \gamma(\cdot) + \varepsilon(\cdot) + p(\text{year} + \text{date} + \text{date2})^*$	7	219.9	0.0	0.78	0.468	0.09
$\psi(\cdot) + \gamma(\text{all}) + \varepsilon(\text{all}) + p(\text{all})$	12	222.5	2.6	0.22	0.326	0.20

Number of parameters (K), AIC, Δ AIC, model weight (AICwt), goodness-of-fit test p-values (GOF P), and the overdispersion parameter (\hat{c}). Best fitting model indicated with *.

Figures

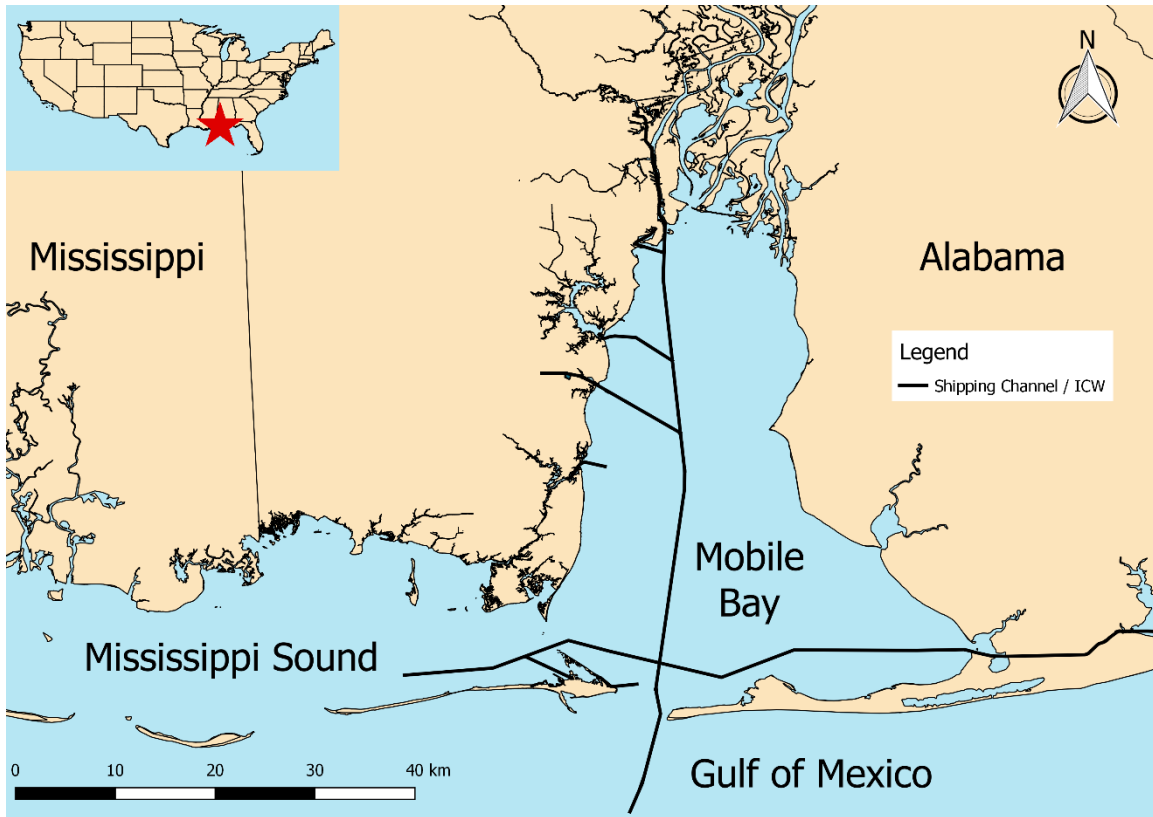


Figure 1.1 Map of Mobile Bay, Alabama.

The Mobile Bay shipping channel, which runs north to south, and the Intercoastal waterway (ICW), which runs east to west, are marked with a black line.

Rays of the Bay Trawl Zones – Mobile Bay

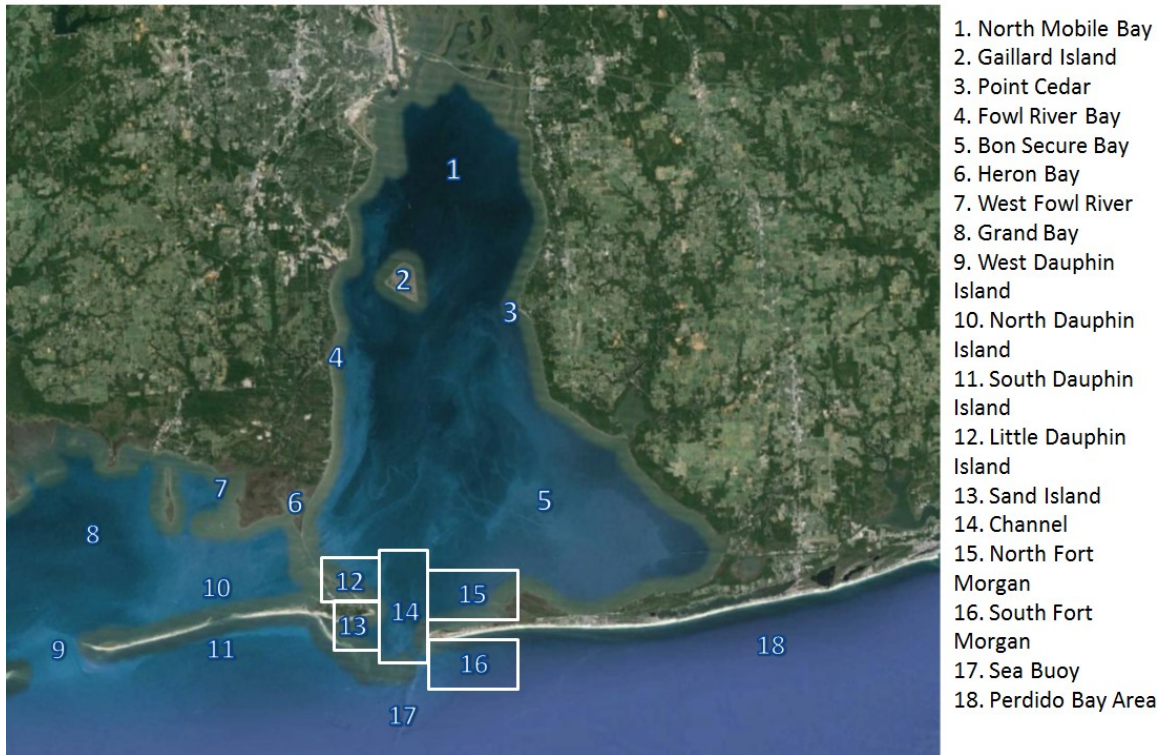


Figure 1.2 Copy of the partitioned map of Mobile Bay, Alabama, used to record trawl locations throughout the length of the survey.

Zones 12, 13, 14, and 15 were the only zones used in data analysis, as no other zones had greater than 50 sampling events throughout the length of the survey.

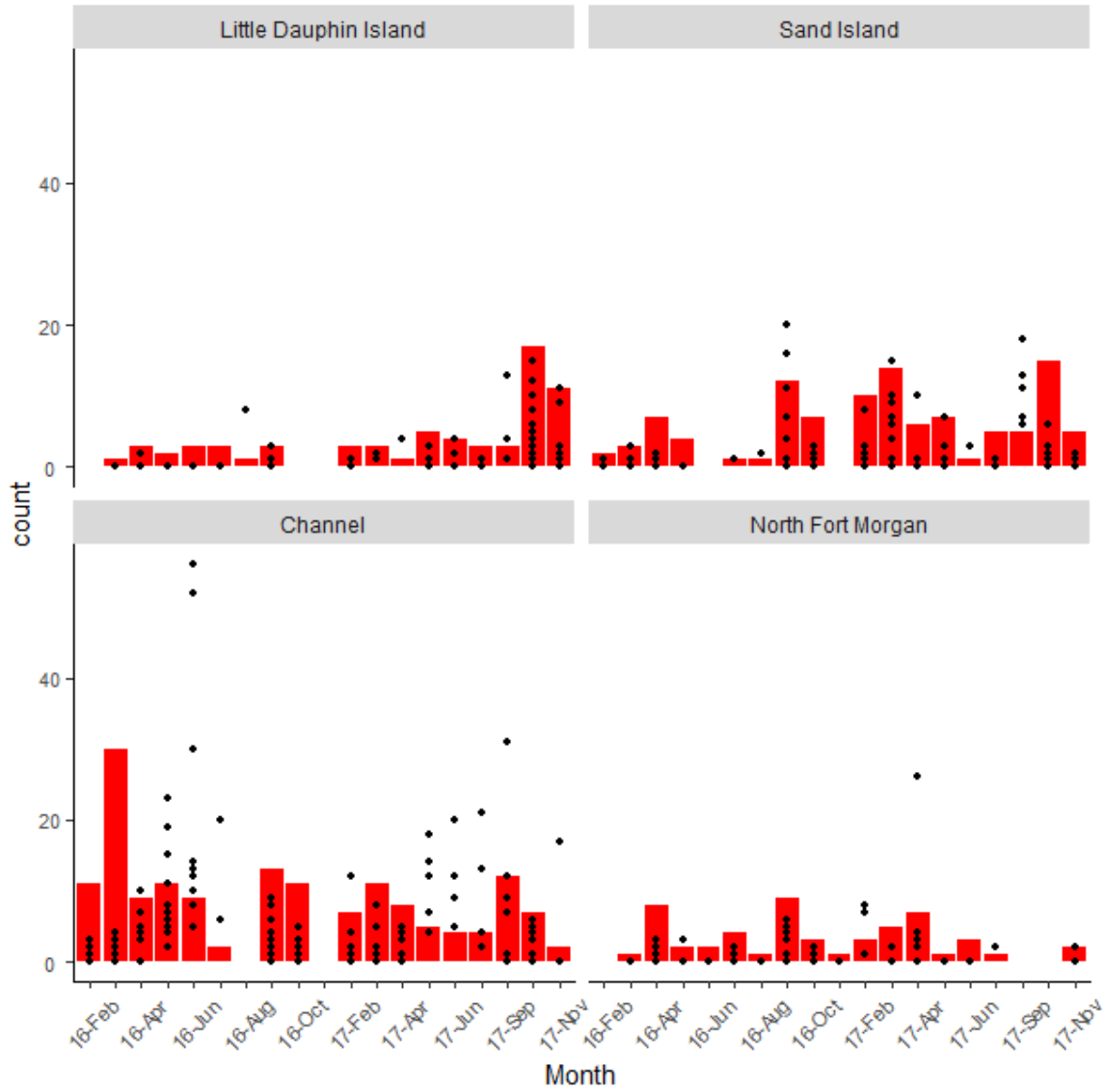


Figure 1.3 Number of trawls per month for each of the four sampling zones used in data analysis.

Red bars represent the total number of trawls performed and the black points represent the total number of batoids caught per month.



Figure 1.4 Image of the sea floor captured during the side-scan sonar survey of the Channel, including trawl scars marked with white lines.

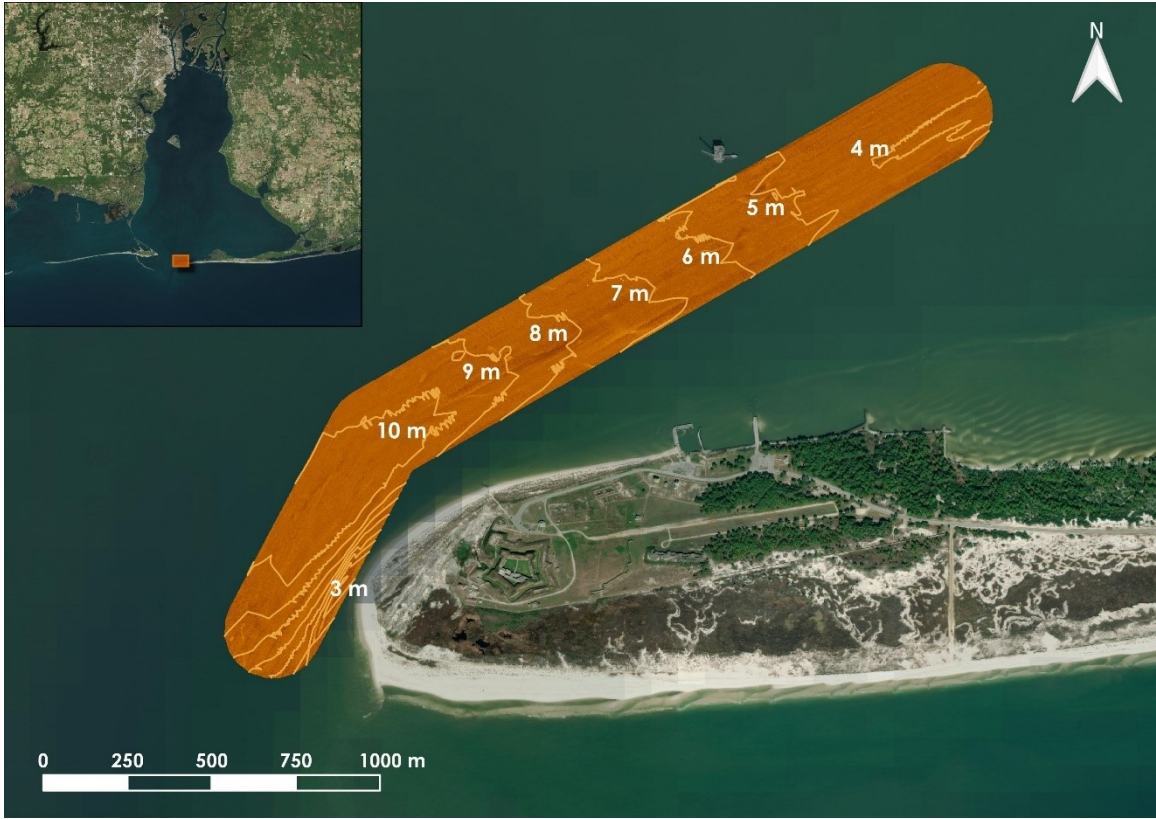


Figure 1.5 Image of the sea floor captured during the side-scan sonar survey of the Channel with outlined depth contours.



Figure 1.6 Image of the sea floor captured during the side-scan sonar survey of the Channel showing sediment composition.

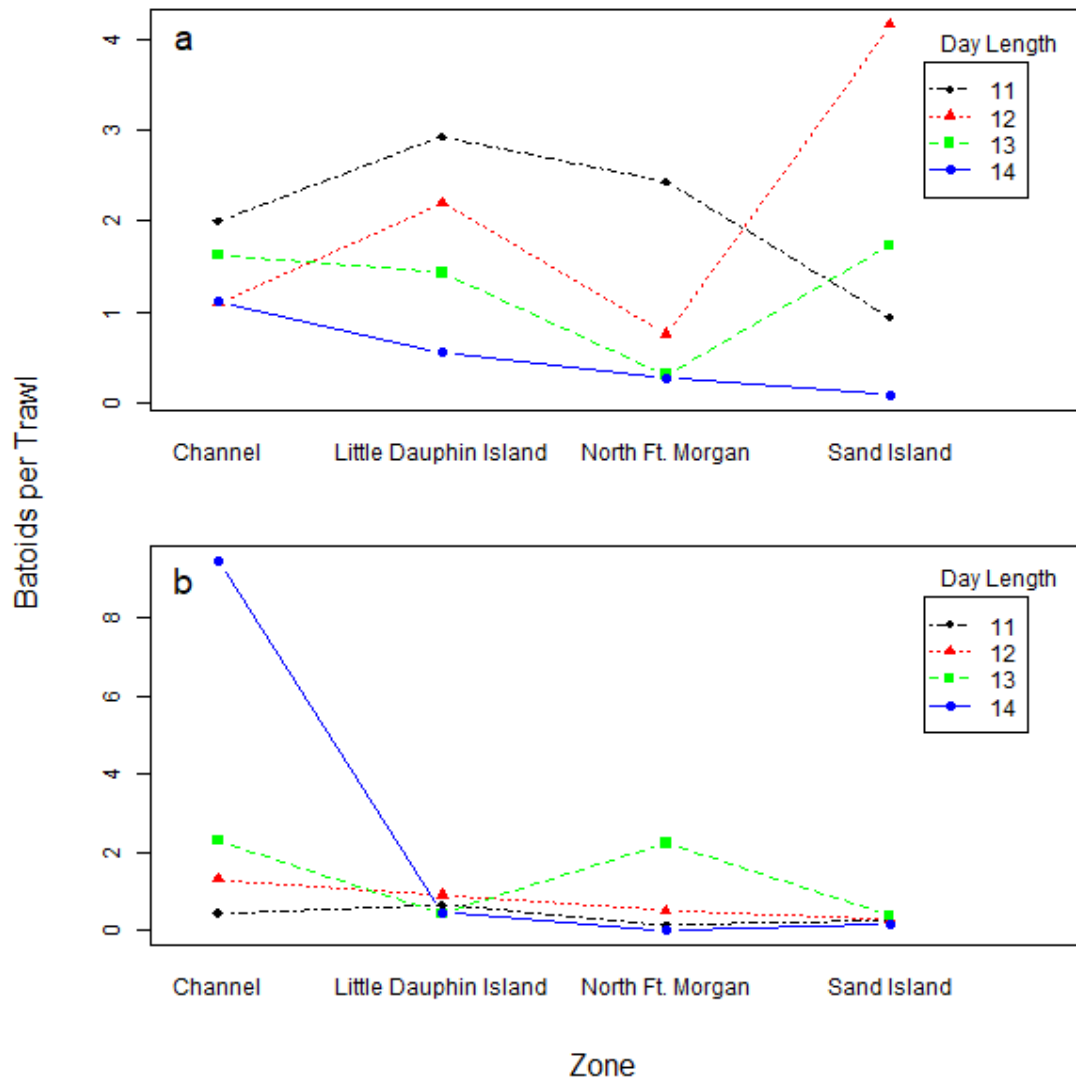


Figure 1.7 Interaction plots for a) *Hypanus sabinus* and b) *Gymnura lessae* catch for each zone plotted against day length pooled by hour.

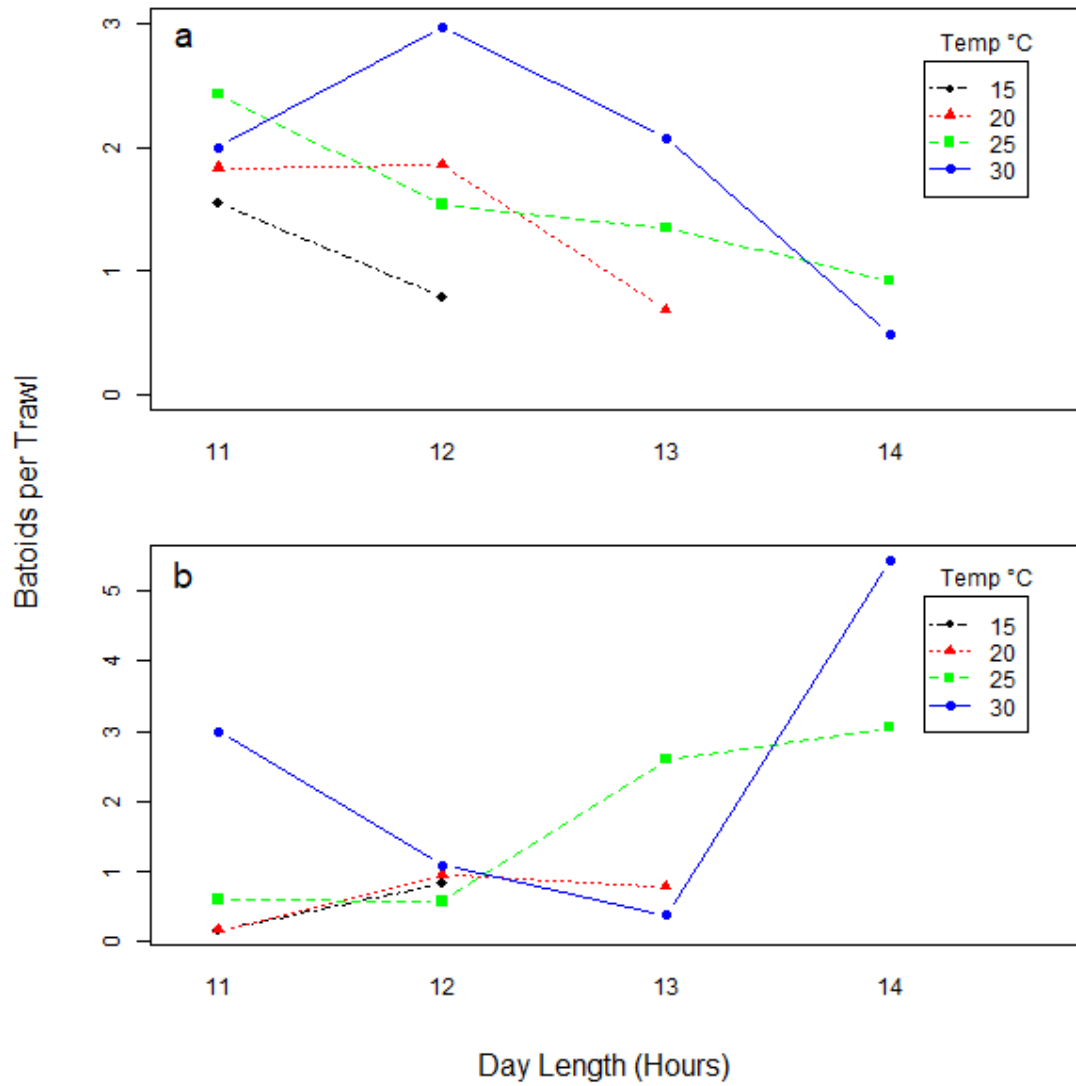


Figure 1.8 Interaction plots for a) *Hypanus sabinus* and b) *Gymnura lessae* catch for day length pooled by hour plotted by temperature binned by 5 °C increments.

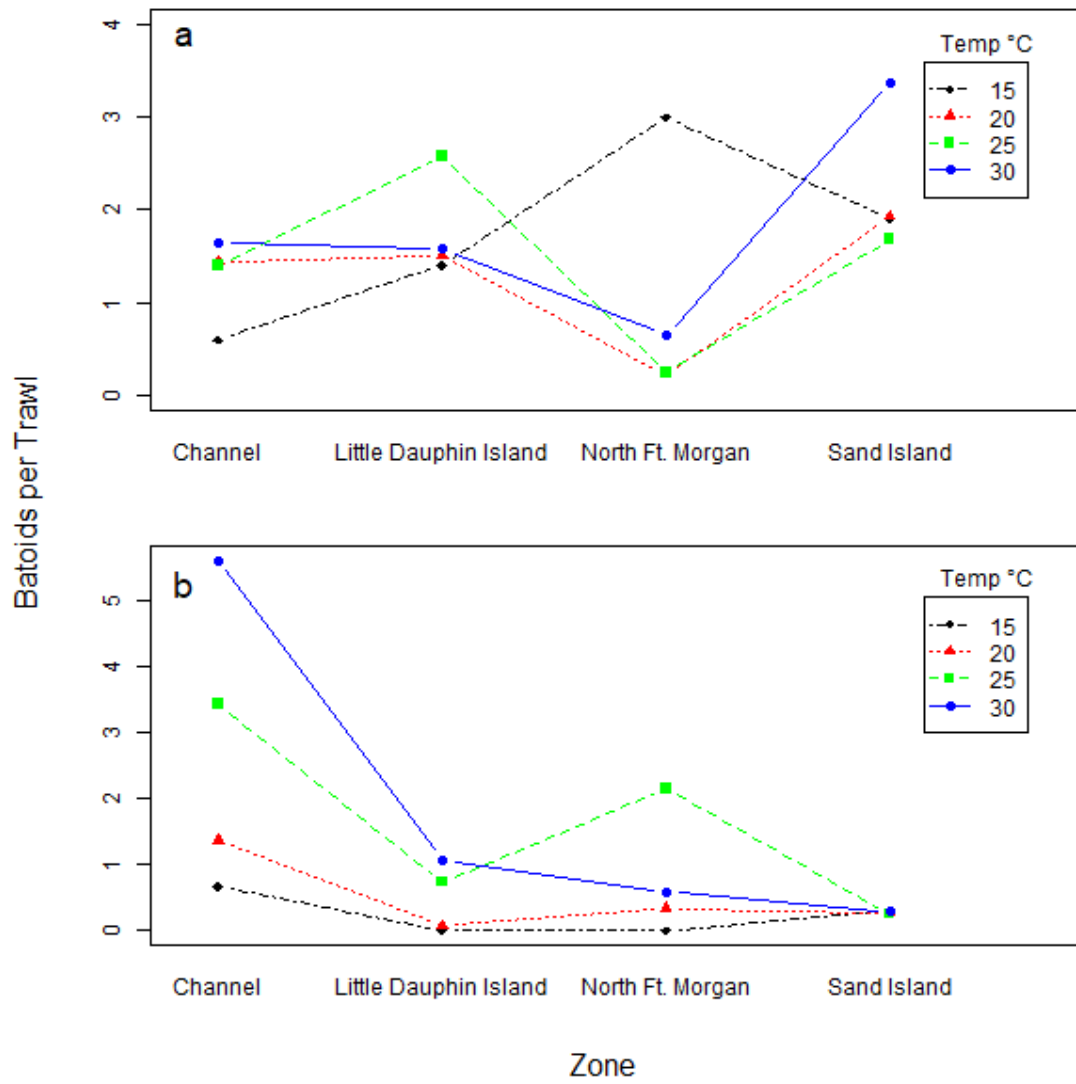


Figure 1.9 Interaction plots for a) *Hypanus sabinus* and b) *Gymnura lessae* catch for each zone plotted by temperature binned by 5 °C increments.

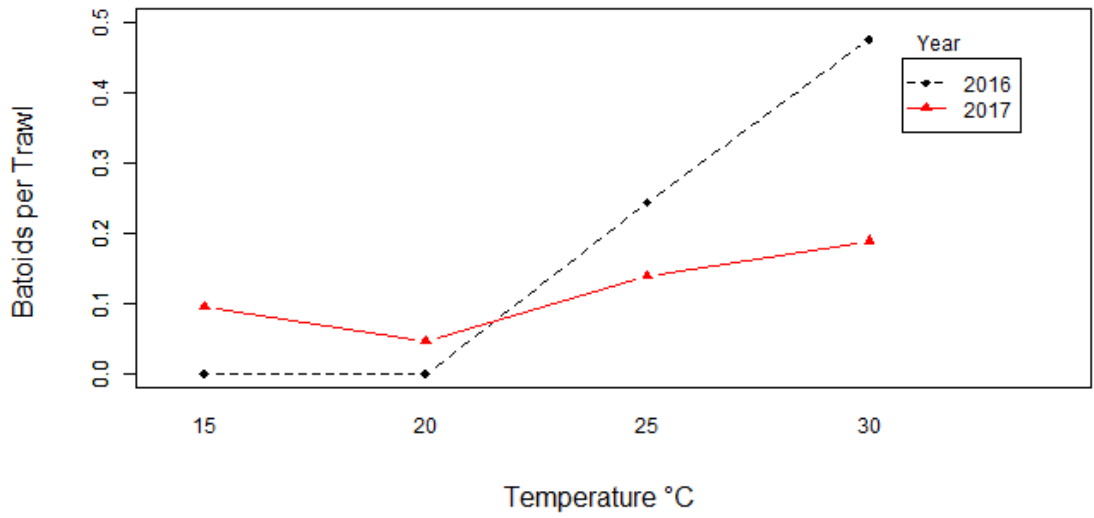


Figure 1.10 Interaction plots for *Narcine bancroftii* catch for temperature binned by 5 °C increments plotted by year.

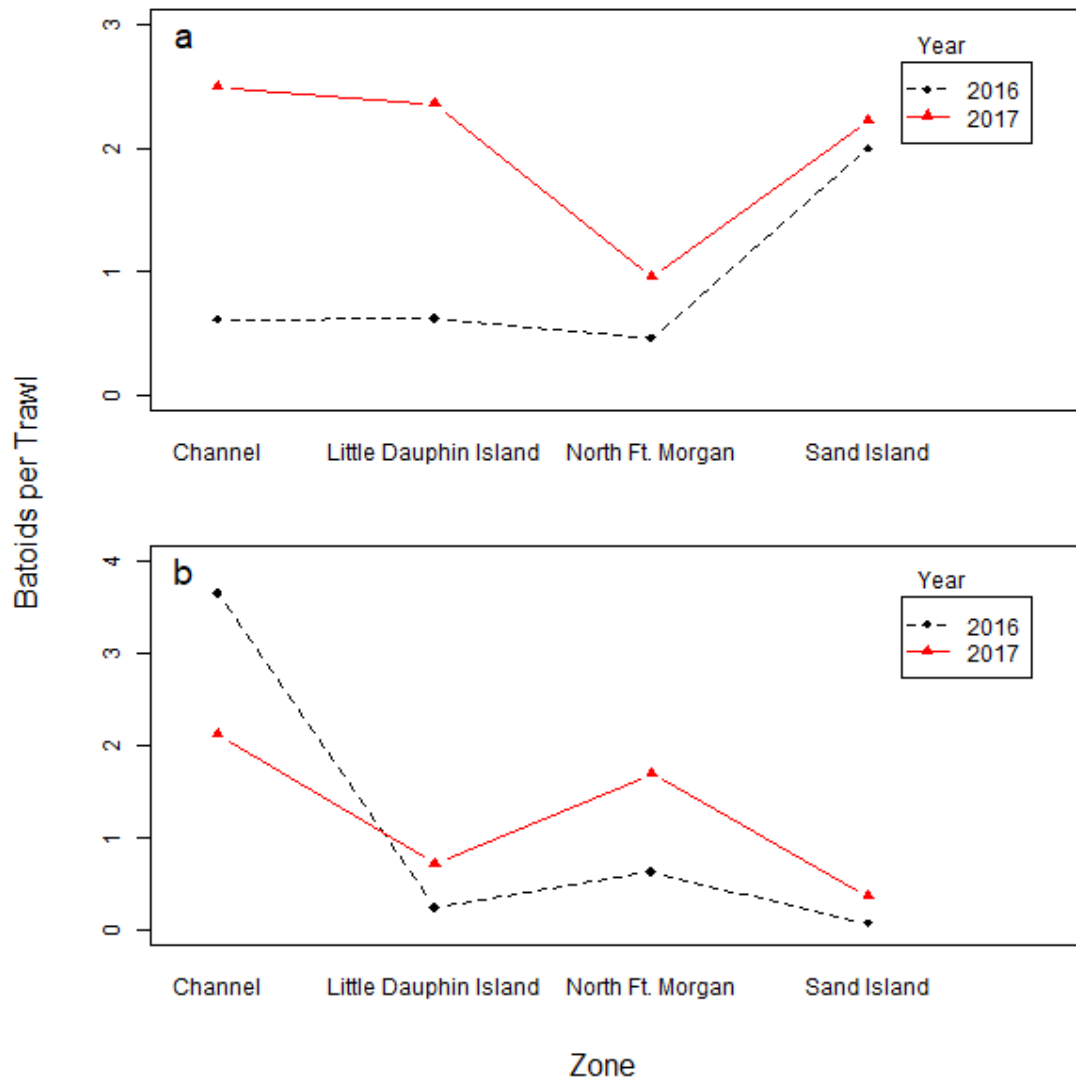


Figure 1.11 Interaction plots for a) *Hypanus sabinus* and b) *Gymnura lessae* catch for each zone plotted by year.

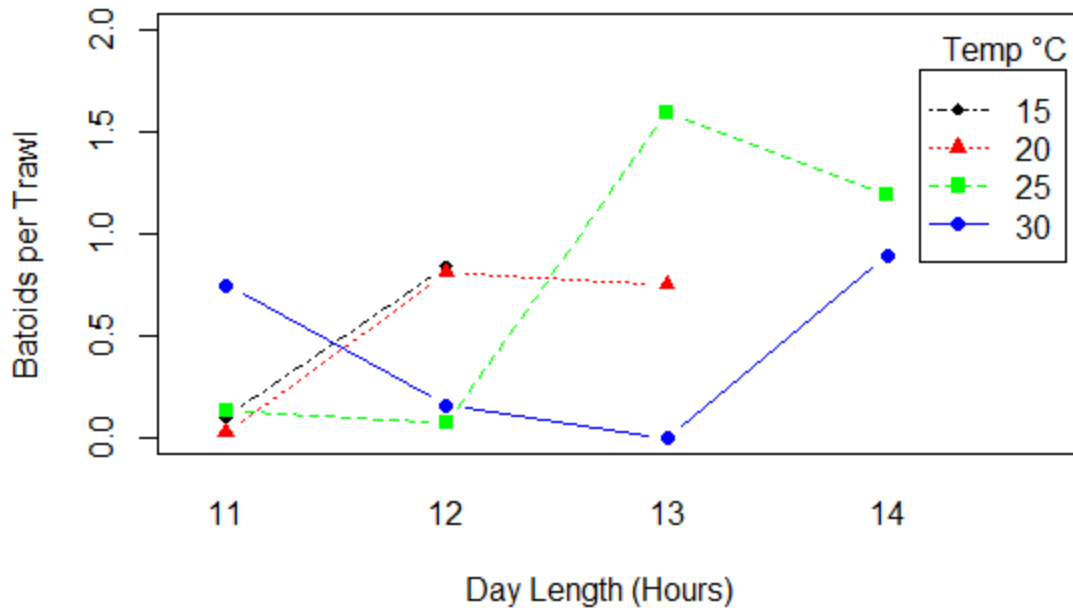


Figure 1.12 Interaction plots for immature *Gymnura lessae* catch for day length pooled by hour plotted against temperature binned by 5 °C increments.

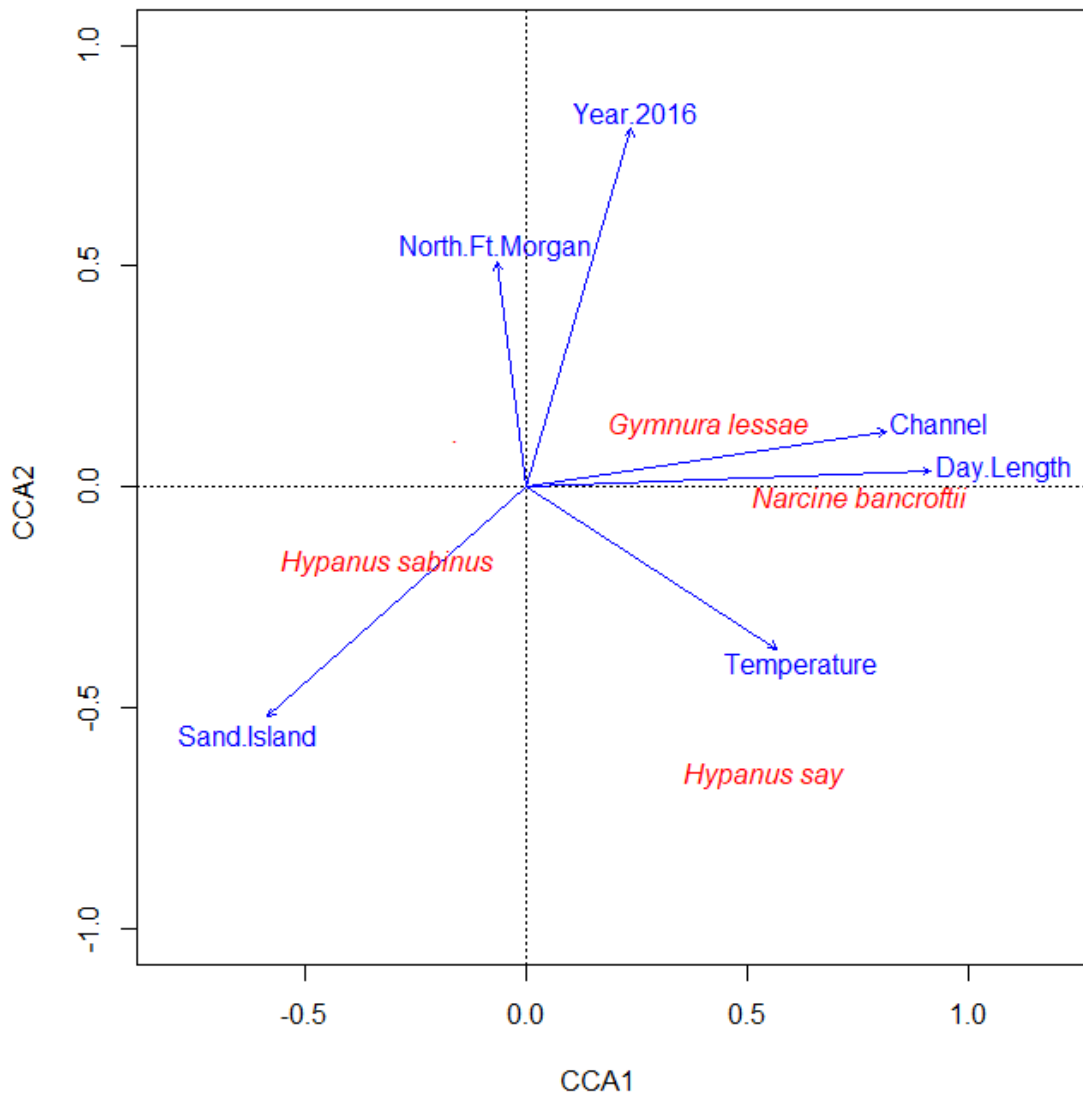


Figure 1.13 CCA biplot of the catch data showing the relationships between the response variables and batoid species for the variables found to be significant in the PERMANOVA analysis.

Spatial associations between the response variables (blue) and batoid species (red) indicate correlations, whereas their position on each axis is indicative of the relative amount of their explained variability.

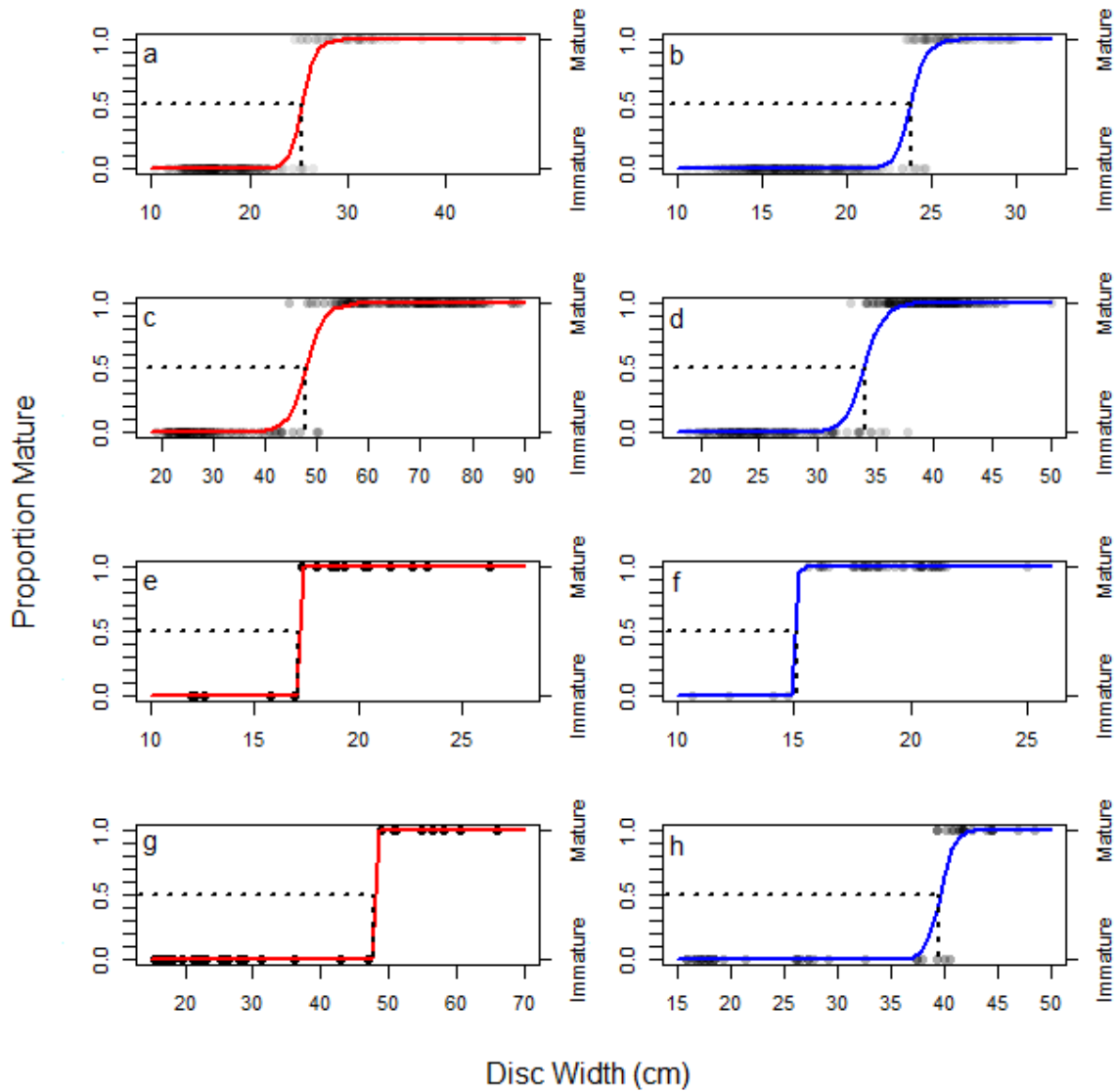


Figure 1.14 Logistic regression fit to sex-specific binomial maturity data for a) female *Hypanus sabinus*, b) male *Hypanus sabinus*, c) female *Gymnura lessae*, d) male *Gymnura lessae*, e) female *Narcine bancroftii*, f) male *Narcine bancroftii*, g) female *Hypanus say*, h) male *Hypanus say*.

Disc width at 50% maturity (DW₅₀) denoted with black dashed lines.

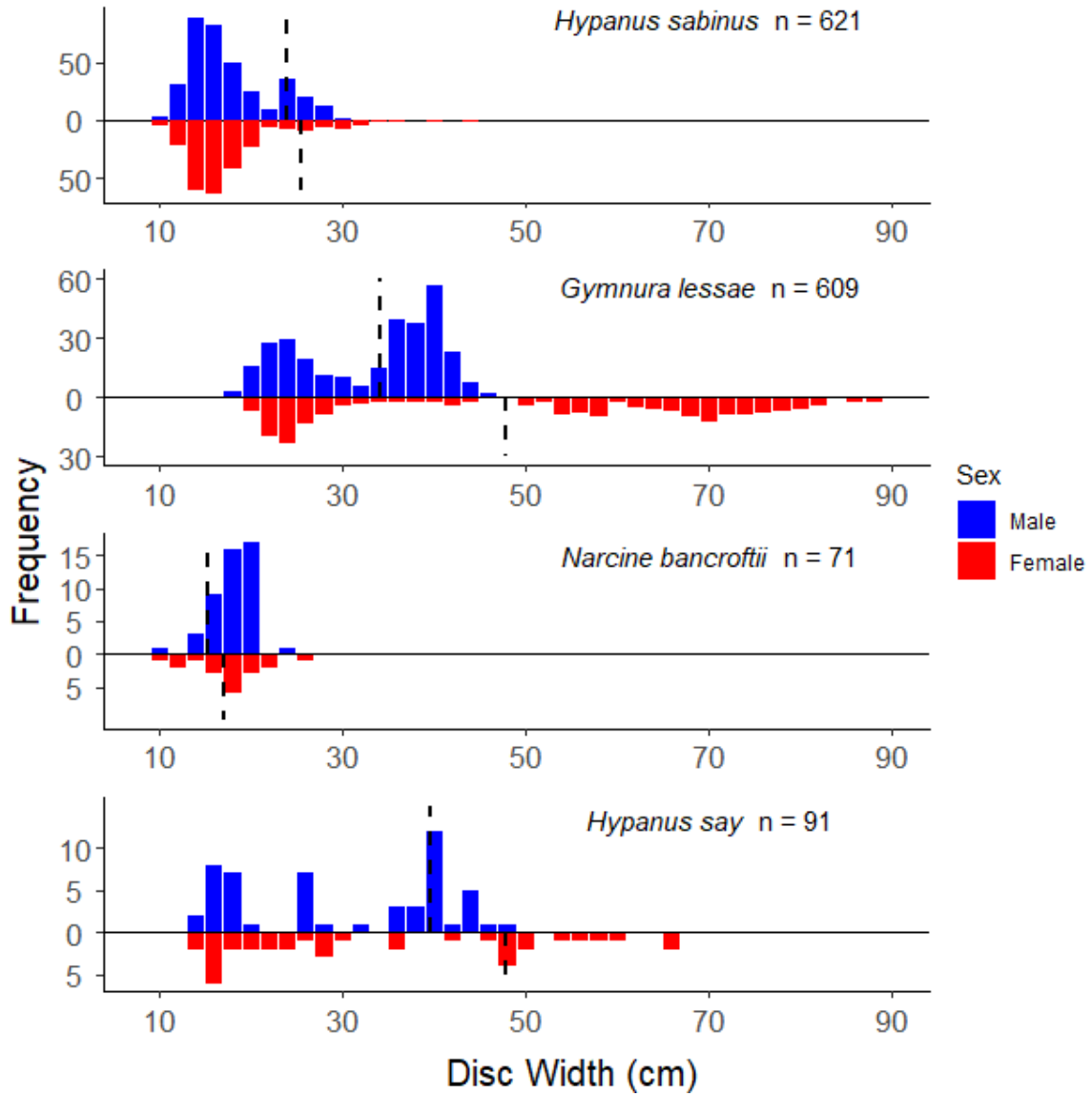


Figure 1.15 Length frequency plots for *Hypanus sabinus*, *Gymnura lessae*, *Narcine bancroftii*, and *Hypanus say*.

Males are shown in blue on top, females are shown in red below. 50% maturity (DW₅₀) is denoted with black dashed lines.



Figure 1.16 *Gymnura lessae* young sampled in early summer.



Figure 1.17 *Gymnura lessae* young sampled in late summer and presumably a few month in development, still yellow in color.

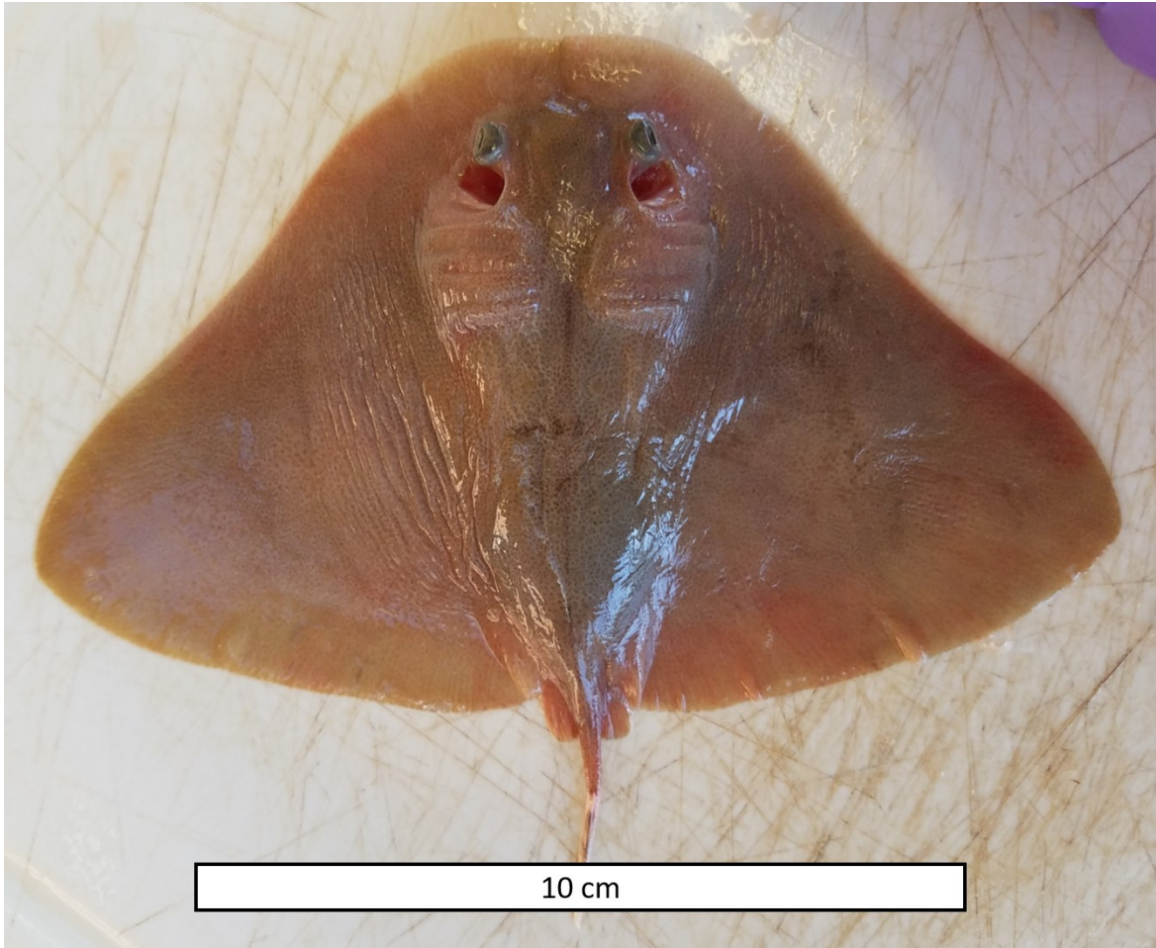


Figure 1.18 *Gymnura lessae* young sampled in October, which appears close to full term and is now brown in color.

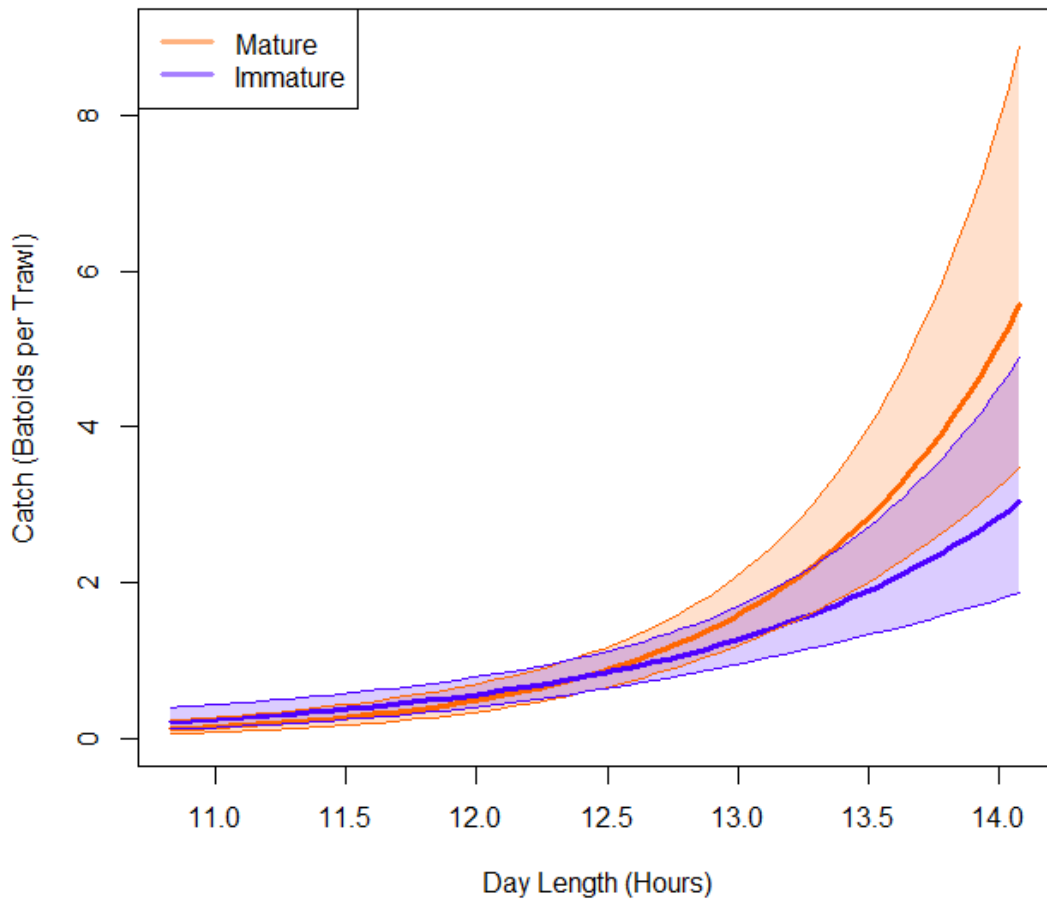


Figure 1.19 Estimates from the negative binomial GLM modeled for *Gymnura lessae* catch in the Channel zone with increasing day length to test for differences in catch based on maturity stage.

Estimates for mature *G. lessae* in orange and immature *G. lessae* in purple with the corresponding shaded areas representing 95% confidence intervals.

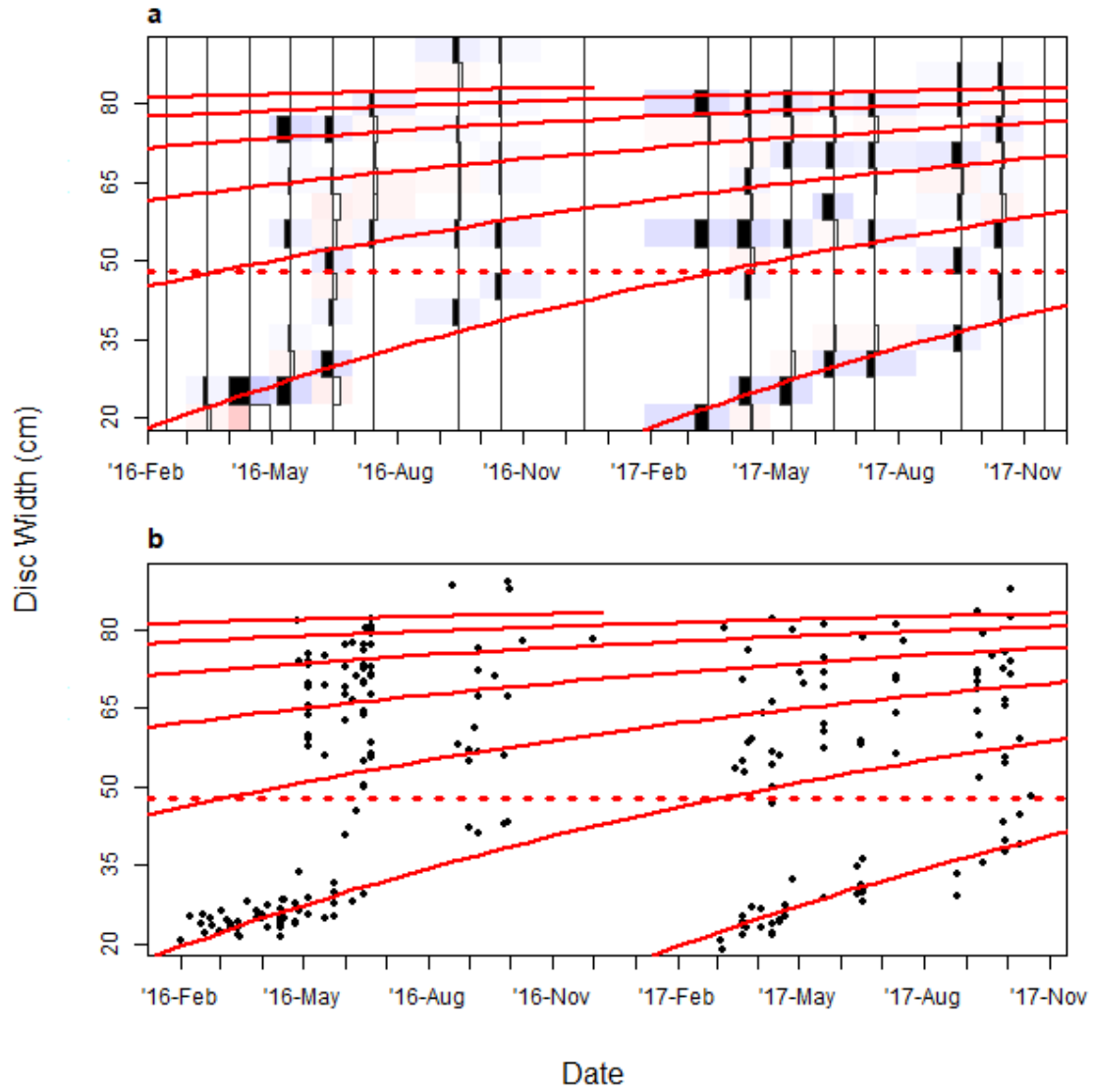


Figure 1.20 A von Bertalanffy growth function (VBGF) fit to female *Gymnura lessae* length frequency data using a simulated annealing algorithm, where $L_0 = 17.7$, $L_\infty = 86.7$, $k = 0.50$, and $t_0 = 0.07$, plotted over a) the binned and restructured data used to fit the VBGF and b) a scatter plot of individual disc widths plotted by date of capture.

Disc width at 50% maturity (DW_{50}) is denoted with a dashed horizontal line.

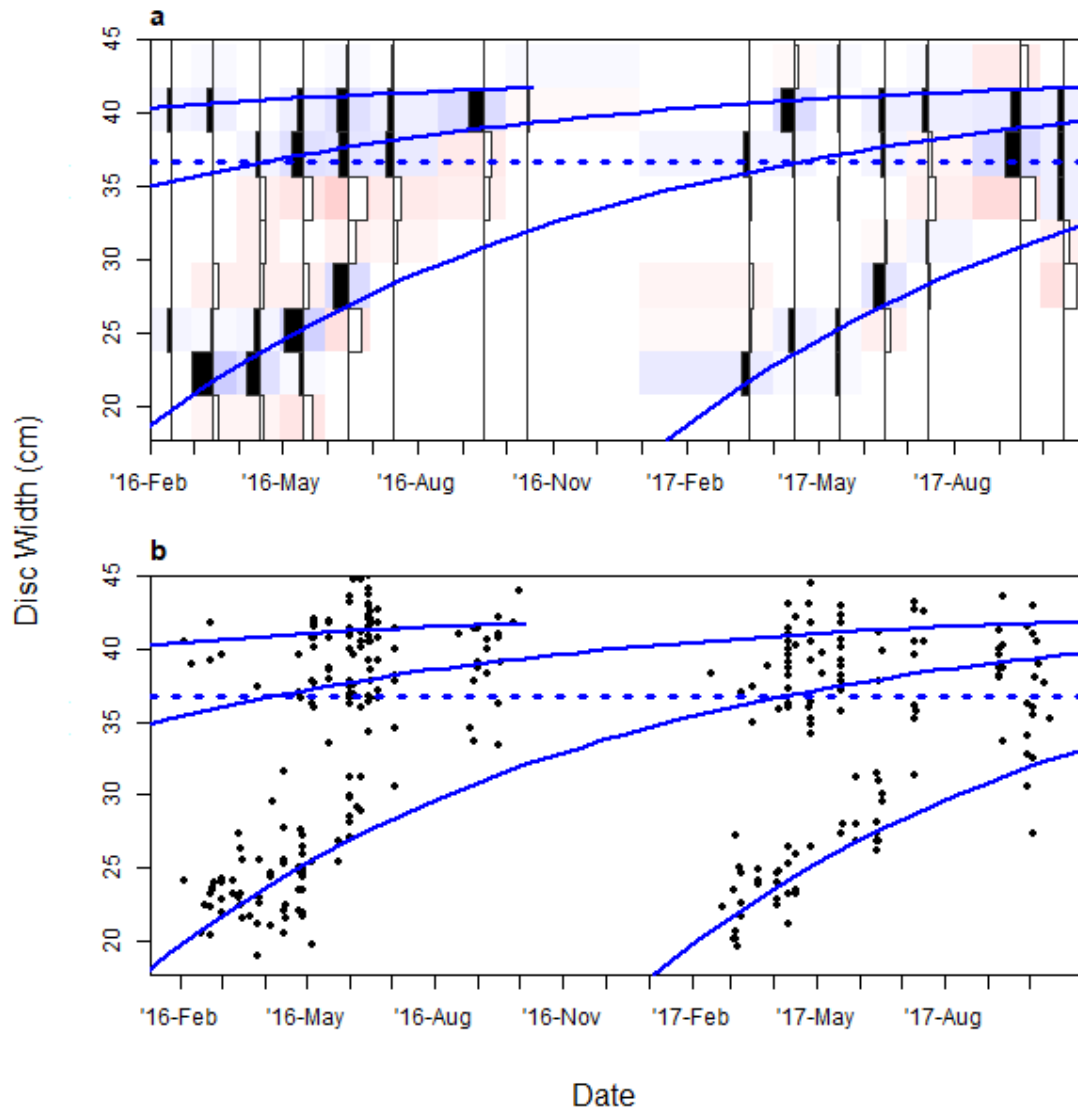


Figure 1.21 A von Bertalanffy growth function (VBGF) fit to male *Gymnura lessae* length frequency data using a simulated annealing algorithm, where $L_0 = 17.7$, $L_\infty = 42.9$, $k = 1.12$, and $t_0 = 0.05$, plotted over a) the binned and restructured data used to fit the VBGF and b) a scatter plot of individual disc widths plotted by date of capture.

Disc width at 50% maturity (DW_{50}) is denoted with a dashed horizontal line.

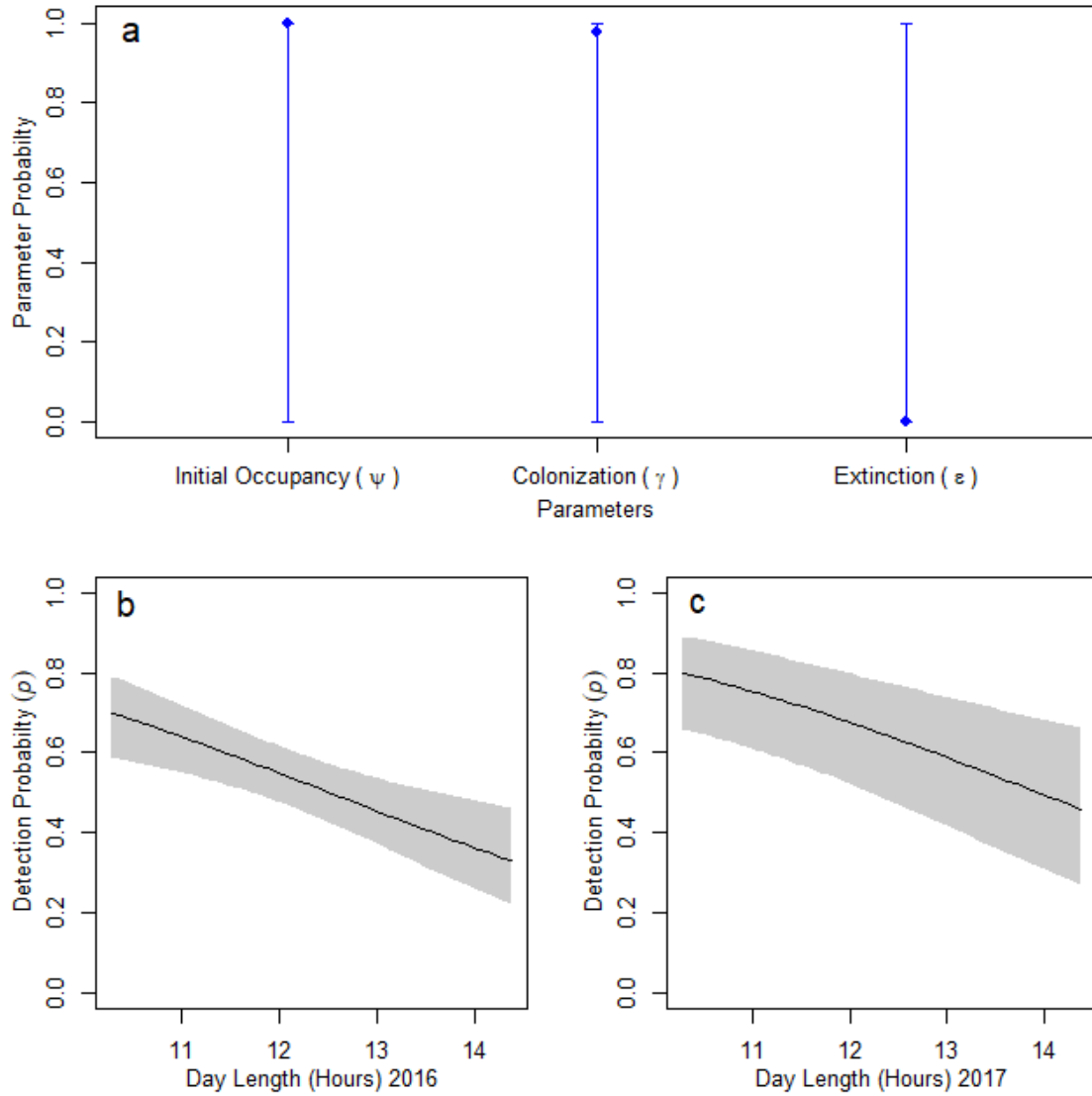


Figure 1.22 Outputs of the best fitting occupancy model for *Hypanus sabinus* for the parameters a) initial occupancy, local colonization, and local extinction probability, b) detection probability by day length for 2016, and c) 2017.

Black lines represent the estimated parameter values and the gray area and blue error bars represent 95% prediction intervals.

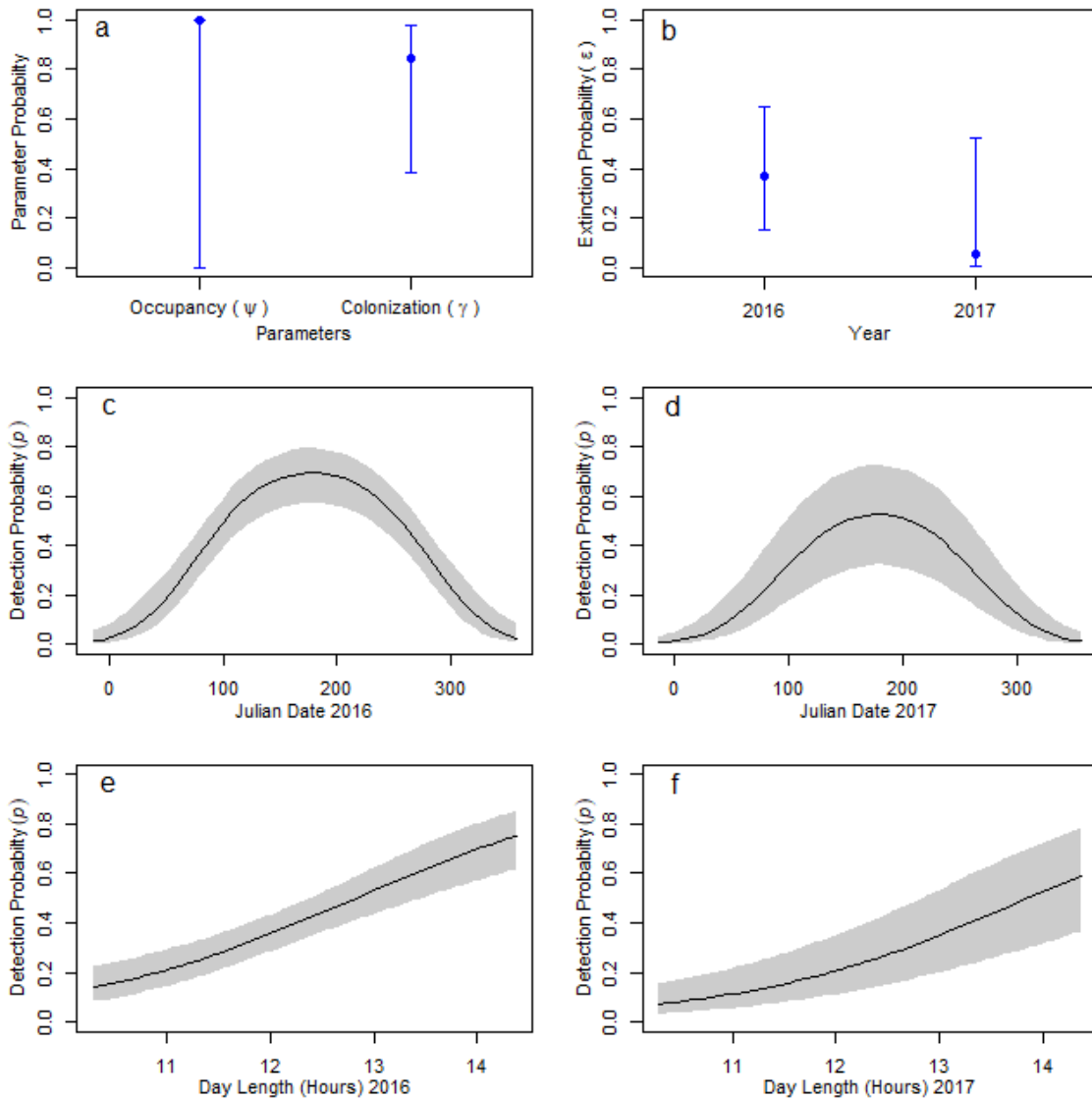


Figure 1.23 Outputs of the best fitting occupancy model for *Gymnura lessae* for the parameters a) initial occupancy and local colonization, b) local extinction probability by year, c) detection probability by date for 2016, d) 2017, e) detection probability by day length for 2016, and f) 2017.

Black lines represent the estimated parameter values and the gray area and blue error bars represent 95% prediction intervals.

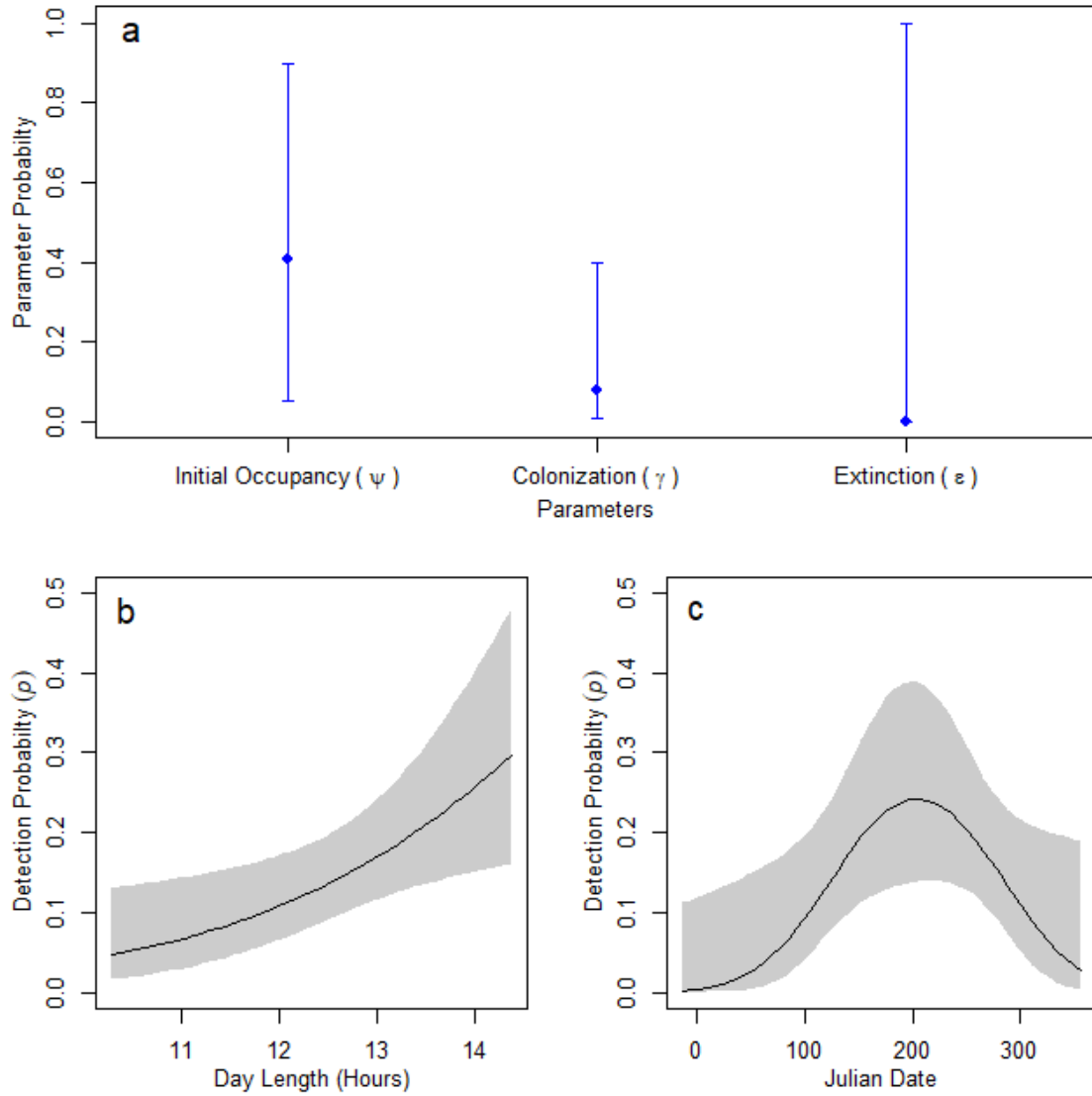


Figure 1.24 Outputs of the best fitting occupancy model for *Narcine bancroftii* for the parameters a) initial occupancy, local colonization, and local extinction probability, b) detection probability by day length, and c) detection probability by date.

Black lines represent the estimated parameter values and the gray area and blue error bars represent 95% prediction intervals.

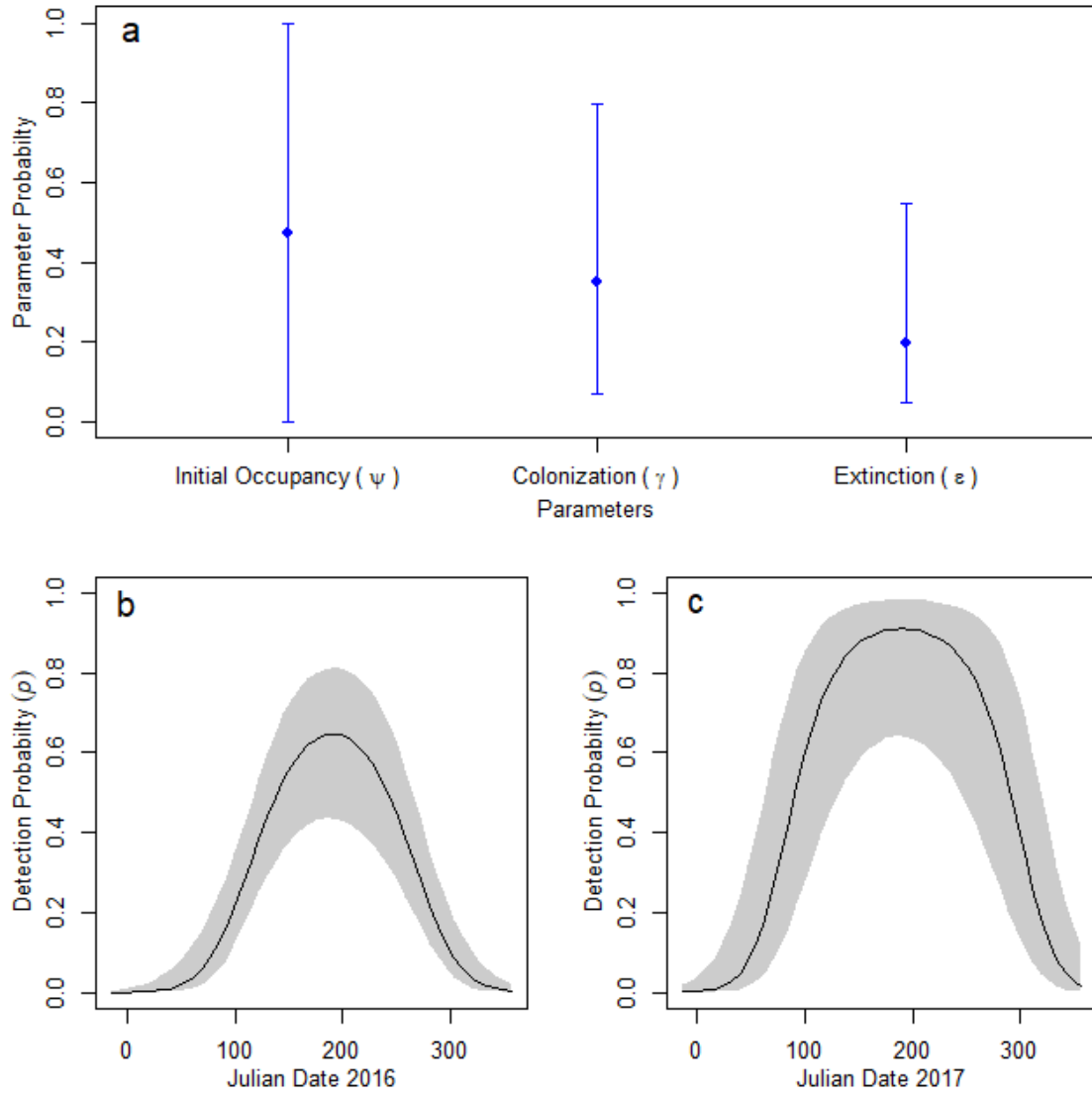


Figure 1.25 Outputs of the best fitting occupancy model for *Hypanus say* for the parameters a) initial occupancy, local colonization, and local extinction probability, b) detection probability by date for 2016, and c) detection probability by date for 2017.

Black lines represent the estimated parameter values and the gray area and blue error bars represent 95% prediction intervals.

CHAPTER II
DIETARY HABITS OF *GYMNURA LESSAE* REVEALED THROUGH DNA
METABARCODING OF STOMACH CONTENTS

Introduction

Understanding the diet of a species is vital for understanding trophic interactions and appropriately implementing ecosystem-based fisheries management (Chipps and Garvey 2007; Brown et al. 2012; Bizzarro et al. 2017). Without dietary information, changes in predator-prey interactions and food web dynamics can go unmonitored, resulting in poor management decisions due to erroneous assumptions (Kemper et al. 2017). Despite the clear need for dietary data, studies describing these interactions are often lacking (Bizzarro et al. 2007; Grüss et al. 2018). The most common method used to interpret a species' diet is to examine stomach contents, a methodological and straightforward means for obtaining a snapshot of what an individual has recently consumed (Hyslop 1980).

Recently, *G. micrura* was redescribed as three separate species: *G. micrura*, *G. sereti*, and *G. lessae* (Yokota and Carvalho 2017). As a result, the previous diet study on *G. micrura* does not describe the diet of the species of *Gymnura* found in the northern Gulf of Mexico, *G. lessae* (Yokota et al. 2013). *G. lessae* is a common species of batoid typically found on sandy and muddy bottoms along the coast, ranging from the northern

Caribbean Sea to the northeast Atlantic Ocean (Yokota and Carvalho 2017). Despite their relative abundance, studies report conflicting population trends. For example, Myers et al. (2007) note their populations have increased along the northwest Atlantic coast, citing the loss of apex predatory sharks, whereas Shepherd and Myers (2005) note population declines of over 99% in the northern Gulf of Mexico, resulting from shrimp fishery bycatch. However, subsequent studies have refuted some conclusions made by Shepherd and Myers (2005), finding that changes in sampling design were responsible for the declining catch of some species, as opposed to true population declines (Carlson et al. 2017). Clearly, much remains to be learned about *G. lessae* in the northern Gulf of Mexico.

The feeding behavior of *G. lessae* has only been described in captivity, where they are known to ambush passing prey from the sandy substrate by striking the prey with their pectoral fins, temporarily stunning the prey, and then pinning prey against the substratum for consumption (Schreiber 1997). A similar feeding behavior was seen in captive *G. altavela*, in which they were also seen to strike prey items using their pectoral fins (Henningsen 1996). This ambush feeding style has been observed in the wild with *G. natalensis*, which attempted to ambush approaching prey by positioning itself adjacent to an egg bed (Smale et al. 2001). Diet studies on other *Gymnura* species have found most to be teleost specialized feeders, which feed intermittently on relatively large prey (Jacobsen et al. 2009; Yokota et al. 2013). However, diet analysis on *Gymnura* species can be difficult due to high frequencies of empty stomachs and extended periods of digestion resulting in poor prey identification (Bizzarro 2005; Jacobsen et al. 2009; Yokota et al. 2013).

Otoliths can be a useful tool for identifying otherwise unknown teleosts as they are often one of the last structures to evacuate the stomach (Jobling and Breiby 1986; Granadeiro and Silva 2000). However, using free otoliths for prey identification can be biased, over-representing teleost species with larger and slower-digesting otoliths (Granadeiro and Silva 2000).

An increasingly common method to identify unknown prey items is through the analysis of DNA (Smith et al. 2005; Carreon-Martinez et al. 2011; Leray et al. 2015; Jakubavičiute et al. 2017). As technology and methods have advanced, DNA barcoding has become a cost-effective method to greatly increase prey species resolution (Carreon-Martinez et al. 2011; Pompanon et al. 2012). However, traditional DNA barcoding (i.e. Sanger sequencing) can be problematic when prey items are heavily degraded or when the prey sample is overwhelmed by the host species' DNA. Alternatively, DNA metabarcoding allows for the amplification of DNA from several different organisms in a single sample (Taberlet et al. 2012). This allows for the identification of a prey item, even when the sample is overwhelmed by host DNA. DNA metabarcoding can also allow for the identification of prey that has been completely assimilated, but with DNA remains in the stomach in only minute amounts.

Given the importance of dietary information to both single-species and ecosystem management, combined with the lack of information on *G. lessae*, a relatively abundant mesopredator, the goal of this study is to examine the diet of *G. lessae* in Mobile Bay and identify the impacts of using advanced genetic techniques in batoid dietary studies.

Methods

Sampling Methods

All *G. lessae* sampled in this study were collected during the same period and using the same methods described in Chapter 1, with the exception of rays sampled from two additional trawls conducted in May 2018. Ray stomachs were either excised and examined immediately after capture, or the ray was frozen at -20 °F until the stomach and other samples could be removed. All stomach contents were removed and examined using instruments sterilized with 10% bleach. If the stomach showed signs of regurgitation (e.g. the stomach was partially retracted into the esophagus), it was not examined and excluded from the study. All prey items were separated, identified to lowest possible taxa, counted, and weighed to the nearest 0.01 grams. Prey items that were not identified to species were stored in 200 proof ethanol for DNA metabarcoding. Highly digested prey material, such as free muscle and bones, were kept with the assumption that their identity would be revealed through DNA metabarcoding.

All free otoliths that were not associated with an intact prey item were counted and identified to lowest possible taxa using an in-house reference set and an additional otolith key specific to fishes from the Gulf of Mexico (Baremore and Bethea 2010). The otolith data were not included in the primary data analysis; however, these data were later analyzed to compare results to those from DNA metabarcoding. After free otoliths were separated by prey group, each count was divided by two and then rounded up as a conservative estimate of the original number of prey in the stomach. In addition, highly digested prey material, such as those mentioned previously, were not included as unidentified prey items when analyzing the otolith data, to avoid double counting in the

likely event that the otoliths in the stomach were from the same fish as the other digested material. From this point forward, the results of the diet analysis using DNA metabarcoding will be referred to as the metabarcoding data and the diet analysis using free otoliths will be referred to as the otolith data.

DNA Metabarcoding

All DNA extraction, PCR amplification, and post-PCR processing and pooling were done at the Genomics Core Lab at Texas A&M University-Corpus Christi (TAMUCC). DNA extractions were performed using an Omega Bio-tek E-Z 96 Tissue DNA kit following the standard tissue protocol, including the RNase treatment step. The samples were then eluted in a 200_μl Elution Buffer. For PCR amplification, the primers mLCOintF (Leray et al. 2013) and jgHC02198 (Geller et al. 2013) were used for any metazoan DNA in the sample (Table 2.1). These primers had 5 base pair (bp) barcodes on the 5' end to allow for pooling prior to library prep and then assignment back to the original sample during the bioinformatic processing. A *G. lessae* blocking primer was also used to reduce the amplification of any host DNA (Table 2.1).

The samples were amplified using a touchdown protocol that included an initial 3 min denaturation step at 95°C followed by 13 cycles of denaturation for 10 s at 95°C, annealing for 30 s at 62°C (-1°C per cycle), and elongation for 30 s at 72°C, followed by 27 cycles at an annealing temperature of 48°C, and a final 5 min elongation at 72°C (Leray et al. 2013). After PCR, all reactions were subjected to electrophoresis on a 1% agarose gel with Axygen 100bp ladder, and the resulting gel image was scored based on presence of the target band (~313 bp) and three undesirable results indicating improper

amplification: DNA smearing from high to low molecular weight, primer dimer, and non-target amplification. Samples that did not amplify properly the first time either had a DNA smear or primer dimer and were reamplified using a modified PCR protocol. If the DNA was smeared then the DNA template was reduced to 0.5 μ l and the water was increased by 0.5 μ l. Alternatively, if there was excessive primer dimer, the template DNA was increased to 2 μ l and the water was reduced by 1 μ l.

PCR products that showed amplification at the desired size (313 bp) were transferred to a new plate for purification with AMPure XP beads. The cleaned products were quantified at least twice with AccuBlue High Sensitivity dsDNA Quantitation solution on a SpectraMax M3 plate reader. Samples were then pooled so that an equal number of nanograms of PCR product came from each sample. Prior to sequencing, the library was adjusted to 2 nM using the Kapa Biosystems Library Quantification Kit on an ABI StepOnePlus real-time thermal cycler (Applied Biosystems Inc.) and checked for the desired fragment length distribution using an Advanced Analytical Fragment Analyzer and the High Sensitivity NGS kit. Pooled PCR products were concentrated and then used to create an Illumina library following the Illumina TruSeq protocol. The resulting library was sequenced on an Illumina MiSeq at the NYU School of Medicine's Genome Technology Center.

Bioinformatic processing and data analysis were performed at the Genomics Core Lab at Texas A&M University-Corpus Christi using the *charybdis* metabarcoding pipeline (<https://github.com/cbirdlab/charybdis>) on TAMUCC's high-performance computing cluster as described in Drymon et al. (in review). The *charybdis* pipeline uses OBITOOLS v1.2.9 (functions below in lower case italics without version numbers, Boyer

et al. 2016) with the addition of CROP v1.33 (Hao et al. 2011), VSEARCH v2.3.4 (Rognes et al. 2016), BLAST 2.6.0 (Edgar 2010), and GENOMETOOLS v1.5.9 (Gremme et al. 2013) together to cluster putative OTU's and assign them to taxa. Prior to this, for parallel processing, the raw Read 1 and Read 2 FASTQ files were divided into several smaller files using FASTQ SPLITTER v0.1.2 (<https://kirill-kryukov.com/study/tools/fastq-splitter/>). The read pairs were aligned and converted to FASTA format, using *illuminapairedend* and *obiconvert*, respectively. FASTA files were filtered using *obigrep*, removing read pairs with an alignment score lower than 40 or with less than 20 bp of overlapping sequence. Aligned read pairs were demultiplexed and assigned to samples according to the unique barcodes attached during PCR amplification using the function *ngsfilter*. All the sequences corresponding to each sample were sorted into unique FASTA files for further processing.

Duplicate read pairs were quantified and removed using *obiuniq*, leaving only the unique read pairs (variants) and their frequency. Singletons and variants that were likely to result from PCR errors were identified and removed using *obiclean*. PCR errors were defined as sequence variants that were, at most, half as frequent as a more abundant variant with one mismatch. Variants that differed in length from the expected 313 bp of COI by more than 15 nucleotides were filtered. Chimeric variants were identified and removed using the *uchime_denovo* function of VSEARCH. Variants were assigned to OTU using CROP with the block size set to 432 and the number of Markov chain Monte Carlo iterations was set to 10x the block size (4320), as recommended in the CROP manual.

Following bioinformatics processing, each prey sample was assigned a single, final OTU which represented the prey item from which the tissue was sampled. To be assigned a final OTU, the sample must have had at least 10 reads matching a single potential prey species and at least twice as many reads for that single species than any other species in the sample, apart from host reads. If those criteria were not met, the prey was assigned a final ID as an unidentified species from the potential prey class with the highest number of matches.

Data Analysis

Cumulative prey curves were created to determine if sufficient stomachs had been sampled to adequately describe the diet of *G. lessae* (Ferry and Cailliet 2007). All prey curves were generated using the Vegan Community Ecology package (Oksanen et al. 2018) in R. Sample size sufficiency was met once a prey curve reached an asymptote, which was defined as the slope of the curve being $b \leq 0.05$ (Ferry and Cailliet 2007; Brown et al. 2012).

Prey groups were quantified using single and compound indices, including average percent number (%N), average percent weight (%W), prey-specific number (%PN), prey-specific weight (%PW), and frequency of occurrence (%FO) (Hyslop 1980; Brown et al. 2012). %N and %W were standardized by stomach to treat each fish as an individual sampling unit (Chipps and Garvey 2007). The Prey-Specific Index of Relative Importance (%PSIRI) was used to create an unbiased metric to determine the relative importance of each prey group in the diet of *G. lessae*, as well as make comparisons to other studies (Brown et al. 2012). The formulas for %N, %W, %PN, %PW, %FO and

%PSIRI are as follows, where % A_{ij} is the percent abundance (by number or weight) of prey category i in stomach sample j , n_i is the number of stomachs containing prey i , and n is the total number of stomachs containing prey (Brown et al. 2012).

Average percent abundance (%N and %W)

$$\%A_i = \frac{\sum_{j=1}^n \%A_{ij}}{n} \quad (2.1)$$

Prey-specific abundance (%PN and %PW)

$$\%PA_i = \frac{\sum_{j=1}^n \%A_{ij}}{n_i} \quad (2.2)$$

Frequency of occurrence (%FO)

$$\%FO_i = \frac{n_i}{n} \quad (2.3)$$

Prey-Specific Index of Relative Importance (%PSIRI)

$$\%PSIRI = \frac{\%FO_i \times (\%PN_i + \%PW_i)}{2} \quad (2.4)$$

An index of vacuity was calculated by dividing the total number of stomachs without prey items by the total number of stomachs sampled (Hyslop 1980). The Bray-Curtis coefficient was used to create a similarity matrix for both dependent variables (%N and %W) with each individual ray stomach treated as an individual sampling event and prey species treated as the response variables (Clarke and Warwick 2001). Permutational multivariate analysis of variance (PERMANOVA) was run, as described in chapter 1, to test for differences in the dependent variables across the response variables sex, size (disc width), life history stage (immature and transitional vs mature), season (meteorological Spring, Summer, and Fall), day length, and water temperature. The variables sex, life history stage, and season were treated as factors and the variables size, day length, and water temperature were treated as covariates. Permutation tests for heterogeneity of

multivariate group dispersions were run and final models were assigned as described in chapter 1. A PERMANOVA was also run on a dataset of the metabarcoding and otolith data pooled together to test if the two sampling methods produced significantly different results when sampling method was treated as a response variable. Interaction plots were generated to help visualize any significant interactions. A canonical correspondence analysis (CCA) was used as in chapter 1 to help determine the association of prey items and the response variables. Canonical correspondence analysis outputs are strongly influenced by the inclusion of rare species; therefore, individual prey categories were only included in the model if they occurred in at least five stomachs, to help maximize the explanatory power of the model (Kemper et al. 2017).

Results

Sample Collection

531 *G. lessae* were sampled for stomach content analysis from February 2016 to May 2018, of which 316 were male (19.0-50.1 cm DW) and 215 were female (18.9-89.0 cm DW). The majority of rays sampled were sexually mature (57.3%), with 50% of males reaching maturity at 34 cm and females at 48 cm. For the metabarcoding data, of the 531 stomachs examined, 147 stomachs contained prey items, resulting in a 72.3% index of vacuity. A total of 163 prey items were found, all teleost; however, only twenty-one prey items were identified to species without the use of genetic techniques. For the otolith data, due to the removal of highly digested prey remains, only 133 stomachs were considered to contain prey, resulting in a 75.0% index of vacuity. From those stomachs,

198 distinct prey items were found, and 59% of those prey were identified to at least the genus level.

DNA Metabarcoding

143 prey items were metabarcoded, including five prey items whose identities were previously known to species. Of those prey items, DNA with at least a 98% match at the species level was found for twenty-nine different prey species, with twenty-six of those species and 99.999% of all individual reads representing species in the infraclass Teleostei. Final OTUs were assigned to 96 of the total 143 prey items, with all final OTUs representing teleost taxa. Final OTUs were assigned for thirteen different teleost species; one additional prey item was only identified to genus as a reference for that species was not available. For those that were not assigned final OTUs, 18 failed due to poor amplification of prey DNA and 29 did not meet our OTU assignment criteria. All five prey items whose identities were previously known were correctly identified with metabarcoding.

Sample Size Sufficiency

For the metabarcoding data, sample size was sufficient to adequately describe the diet of *G. lessae* at the species level for sexes combined ($b = 0.030$) and females ($b = 0.045$), but not males ($b = 0.091$, Figure 2.1). For the otolith data, cumulative prey curves were generated at the genus level and failed to reach an asymptote for all *G. lessae* ($b = 0.066$), male *G. lessae* ($b = 0.076$), or female *G. lessae* ($b = 0.080$) (Figure 2.2).

Diet Analysis

Metabarcoding increased prey species richness from six to thirteen and the total number of prey identified to species from twenty-eight to one hundred. Most stomachs contained only a single prey item (89.1%, $n = 130$). The maximum number of prey found in a single stomach was three. Unidentified teleosts made up the greatest portion of the %PSIRI, accounting for 33.1% (Table 2.2). Among identified prey, *Micropogonias undulatus* had the greatest %PSIRI, 17.5%, followed by *Anchoa hepsetus* and *Anchoa mitchilli*, with %PSIRI of 12.7% and 12.2% respectively. The families Sciaenidae and Engraulidae were the two most important prey families, with a combined %PSIRI of 86.1% when compared with other identified taxa.

For the otolith data, eleven different prey genera were identified (Table 2.3). As with the metabarcoding data, most stomachs contained a single prey item, but at a lower rate (67.2%, $n = 89$). The maximum number of prey found in a single stomach was five. Unidentified teleosts accounted for 40.0% of the %N and had a %FO of 56.3%. *Anchoa spp.* were the most common identified genus, 23%N, followed by *M. undulatus*, 18%N. The families Sciaenidae and Engraulidae were again the two most important prey families, with a combined %N of 94.2% when compared with other identified taxa. Prey in the families Sciaenidae made up a greater portion of the identified %N in the otolith data, 57.2%, than in the metabarcoding data, 48.5%. Prey in the family Engraulidae were similar for both the otolith data, 39.4%, and the metabarcoding data, 37.8%.

Five genera were present in the metabarcoding data that were absent in the otolith data. In addition, three prey groups that were only identified to genus in the otolith data were identified to species in the metabarcoding data. However, there were also three

genera present in the otolith data that were absent in the final OTUs of the metabarcoding data, though DNA for two of those species was found in low levels in the metabarcoding samples.

PERMANOVA

PERMANOVA analysis was done at the species level for the metabarcoding data and at genus level for the otolith data. Differences in diet based on location were not tested as 78.0% of *G. lessae* in this study were captured from a single site and 99.1% were captured from within eight kilometers of that site, so differences in the available prey were presumed to be minimal. For the metabarcoding data, none of the six variables (sex, maturity, size, temperature, season, and day length) were found to have heterogeneity of multivariate group dispersion. Sex, temperature, season, and day length were significant for both %N and %W (Table 2.4). Season had the greatest F statistic and R^2 value, and there was a significant sex x day length interaction (Table 2.4). The final models for %N and %W both included the variables season and sex, with no interaction effect. The final model explained 8.7% of the dietary variability for %N and 9.0% for %W.

For the otolith data, only size was found to have heterogeneity of multivariate group dispersion. Four of the variables (sex, size, temperature, and season) were found to be significant, as well as the interaction between sex x season and sex x day length (Table 2.5). The final model included season, sex, and their interaction. The final model explained 16.5% of the dietary variability. PERMANOVA analysis on the metabarcoding

and otolith data pooled together into one dataset found the type of sampling method, DNA metabarcoding versus free otoliths, to be insignificant (Table 2.6).

Interaction plots were created to help visualize the interaction term season x sex for both the metabarcoding (Figure 2.3) and the otolith data (Figure 2.4). Both datasets show an increase in *L. xanthurus* consumption by females in the Fall, an increase in *A. hepsetus* consumption in the summer, and a decline in *M. undulatus* consumption by males in the summer; however, the plots for female consumption of *M. undulatus* are very different. In the metabarcoding data, consumption of *M. undulatus* by females is constant across seasons, whereas for the otolith data, females show an increase in *M. undulatus* consumption in summer followed by a drastic decrease in the fall.

The interaction plots for the day length x sex interaction are similar as the interaction plots for season x sex (Figures 2.5-2.6). Both datasets show an overall decline in *L. xanthurus* consumption with increasing day length, increasing consumption of *Anchoa spp.* by males in the summer, and a gradual decline in *M. undulatus* consumption in males with increasing day length (Figures 2.5-2.6). For females, consumption of *M. undulatus* is similar in both plots, showing a gradual increase in *M. undulatus* consumption as days lengthen, with a slight decrease when day length reaches fourteen hours. There appears to be a difference between the metabarcoding and the otolith data with regards to *A. hepsetus* and *Anchoa spp.* consumption for females; however, this is potentially due to the inclusion of *A. mitchilli* with *A. hepsetus* in the otolith data.

The CCA model for the metabarcoding data using significant variables from the PERMANOVA analysis (season, sex, temperature, and day length) were significant for both %N and %W (Table 2.7). Both axes, CCA1 and CCA2, and the response variables

spring, summer, and sex were significant, but temperature and day length were not (Table 2.7). Both models explained 12.9% of the overall dietary variability. For all variables, sex explained the greatest amount of dietary variation and was highly correlated with the prey *L. xanthurus* (Figure 2.7). Other correlations were seen with the variable summer with *A. hepsetus* and the variable spring with *M. undulatus* (Figure 2.7).

For the otolith data, CCA models were created for significant variables from the PERMANOVA analysis for both the otolith (season, sex, temperature, and size) and metabarcoding (season, sex, temperature, and day length) data. Both models were significant, with the model including the otolith data variables explaining 14.6% of the overall dietary variability and the metabarcoding data variables explaining 16.6% (Table 2.8). Axis CCA1 was significant for both biplots, whereas axis CCA2 was for neither (Table 2.8). Sex and temperature were significant for both biplots, with summer and day length also being significant in the CCA model that used the metabarcoding data variables (Table 2.8). Sex explained the greatest amount of dietary variation of all response variables and was correlated with the prey *L. xanthurus* (Figure 2.8). *Anchoa* spp. were loosely correlated with summer, however summer was not significant in the model with the otolith variables (Table 2.8, Figure 2.8).

For the metabarcoding data, CCA models for %N and %W were also created for variables found to be significant from the PERMANOVA analysis of the otolith data (season, sex, temperature, and size). Both models were significant with %N explaining 13.0% of the overall dietary variability and %W explaining 13.1%. Axis CCA1 and the response variables sex, temperature, and summer were significant, but axis CCA2 and the variables fall and size were not (Table 2.9). These biplots were similar to the biplots

created for the models with the metabarcoding data variables, with sex explaining the greatest amount of dietary variation of all response variables and being highly correlated with the prey *L. xanthurus*, the variable summer being correlated with *A. hepsetus*, and the variable spring being correlated with *M. undulatus* (Figure 2.9).

Discussion

My analyses confirm that *G. lessae* in Mobile Bay are teleost specialized feeders. All prey were teleost, with most being from just two families (Engraulidae and Sciaenidae), consistent with trends described in *G. poecilura* in Mumbai, India and *G. altavela* in Brazil (Raje 2003; Silva and Vianna 2018). While studies investigating the diets of other *Gymnura* species often found non-teleost prey, these prey were generally determined to account for an insignificant portion of their diets (James 1966; Bizzarro 2005; Jacobsen et al. 2009; Yokota et al. 2013; Yemışken et al. 2017; Rastgoo et al. 2018). As seen with *G. micrura* and *G. australis*, there was generally only one, often large, prey item per stomach, which was oriented head first (Jacobsen et al. 2009; Yokota et al. 2013). This, combined with the ambush feeding style seen in captive *G. lessae* and other *Gymnura* spp., indicates that *G. lessae* bury themselves in substrate to ambush passing prey by striking them with their pectoral fins, stunning the prey, before then consuming it whole. Intermittent feeding on a small number of relatively large prey is common with ambush predators and is frequently seen in batoids that have the ability to stun their prey (Wetherbee et al. 2004; Jacobsen and Bennett 2013).

The results of the PERMANOVA analyses were similar for both the metabarcoding and the otolith data. Both techniques highlighted significant differences in

diet based on sex, water temperature, and season. Both datasets also had final models containing both the variables season and sex. The seasonal shift in diet was not surprising as the diets of batoids frequently vary seasonally due to changes in the available prey community (Platell et al. 1998; White et al. 2004; Szczepanski and Bengtson 2014). For *G. lessae* in Mobile Bay, this appears to be driven by increased consumption of *A. hepsetus* in summer. This change in prey consumption corresponds to a significant increase in the CPUE of *A. hepsetus* in Mobile Bay during the summer (Sean Powers, unpublished data). This increase in *A. hepsetus* consumption in the summer likely results in a decrease in the consumption of most other prey species since *G. lessae* generally only consume a single prey at a time. Consequently *A. hepsetus* may act as a temporary prey buffer for other prey species such as *M. undulatus* in this study area (Saunders et al. 2006).

Sex-specific differences in diet seem to be driven by increases in consumption of *L. xanthurus* by female *G. lessae*. This likely results from the difference in relative body size of *L. xanthurus* compared to the four other teleost species most commonly consumed by *G. lessae* (Figure 2.10). *L. xanthurus* in the sampling area are much deeper bodied than either *A. hepsetus* or *M. undulatus*, thus despite being one of the most common teleost in the area, are likely too large for most males to swallow whole. However, mature females appear large enough to consume them, thereby increasing the frequency of occurrence of *L. xanthurus* in their diet.

While sex was significant for the metabarcoding data, size was not. Size was found to be significant for heterogeneity of multivariate dispersion in the otolith data, which could be why it was significant in the otolith data, but not the metabarcoding data

(Anderson and Walsh 2013). In the metabarcoding data, smaller rays (<50 cm DW) consumed twice as many *A. mitchilli* (14.3%N vs 7.1%N) as larger rays (>50 cm DW). However, in the otolith data this difference is more extreme as smaller rays consumed more than six-fold as many *A. mitchilli* (42.3%N vs 6.9%N) as larger rays. This trend is not surprising with *G. lessae* given their feeding strategy; however, the otolith data finds this difference to be greater than the metabarcoding data.

Sex-specific differences in diet are sometimes seen in elasmobranchs; however, this is frequently attributed to differences in habitat use due to sexual segregation, which does not appear to be the case here (Springer 1967; O'Shea et al. 2013). While differences between male and female mouth width relative to disc width have not been reported, mouth widths of the largest *G. lessae* can be greater than three times as wide as smaller individuals (Yokota and Carvalho 2017). Of the six females in the metabarcoding data between the sizes of 40-50 cm, three of them were found to have consumed *L. xanthurus*; however, none of the twenty-nine males in that size range did. Similarly, with the otolith data, three of the six females between the sizes of 40-50 cm were found to have consumed *L. xanthurus*, whereas none of the twenty-one males did. Whether there is truly a behavioral difference between the feeding patterns of males and females of equal size or simply a gape limitation remains to be seen (Schmitt and Holbrook 1984).

The trends seen with *L. xanthurus* consumption by female *G. lessae* are most likely the result of a shift in prey availability. Unfortunately, unlike with *A. hepsetus*, this trend is not seen in the CPUE data from Mobile Bay (S. Powers, University of South Alabama, unpublished data). However, that sampling was done throughout Mobile Bay and not near the mouth of the bay. Thus, this sampling was also catching juvenile *L.*

xanthurus that migrate further into estuaries after hatching (Moser and Gerry 1989). However, an increase of *L. xanthurus* consumption in our sampling area during the fall could be a result of those same juveniles leaving the estuaries in the late summer to migrate to more open waters in the Gulf. These trends could also relate to *L. xanthurus* spawning activity in the winter or a competitive effect as both *L. xanthurus* and *M. undulatus* are often in direct competition for food resources (Parker 1971).

The PERMANOVA and CCA analyses only described a small portion of the observed dietary variability for *G. lessae*. Much of this unaccounted for variability likely stems from the unaccounted variability in the prey communities themselves. Many studies account for this by sampling the prey communities concurrently, as without a measure of the relative abundance of prey, determining whether a species is selecting for certain prey is difficult (Ajemian and Powers 2012; O’Shea et al. 2017). However, while I was not able to determine if *G. lessae* prefer certain teleost species over others, I was able to confirm that they prefer to consume large prey (Jacobsen et al. 2009; Yokota et al. 2013). Evidence for this is seen by the common occurrence of prey so large that they extend out into the batoid’s esophagus, coupled with a high percentage of empty stomachs (Figure 2.11). Furthermore, the smallest abundant prey species in this study, *A. mitchilli*, was generally positioned opposite of the largest prey species, *L. xanthurus*, in the CCA biplots.

While there were minute amounts of non-teleost DNA in the metabarcoding analysis, that DNA could likely be the result of secondary consumption, i.e. prey of prey, or accidental consumption (Sheppard et al. 2005). This is further supported by the complete absence of visible non-teleost prey remains in any stomach. Studies on other

Gymnura spp. often identify non-teleost prey, yet describe non-teleosts as an insignificant portion of the diet in Gymnurids. It is possible that the high abundance of teleost prey in the study area allows these *Gymnura* to be more selective in their prey consumption. Future work on diet in *Gymnura* relative to available prey is needed to further quantify the degree of dietary specialization in these batoids.

G. lessae are selecting for larger teleost prey, yet also consuming some of the most abundant teleost prey in the study area. One notable exception to this is the lack of Ariidae spp. consumption despite their relative abundance in the sampling area. *Bagre marinus* DNA was present in one stomach, but it comprised of only 0.18% of the total reads for that sample. In addition, both Ariidae spp. in the study area have large distinct otoliths, so their consumption would not be missed in the otolith data. Consumption of Ariidae spp. can be deadly for predators due to their large serrated venomous spines that can puncture internal organs such as the stomach (Ronje et al. 2017). Given that many *G. lessae* appear to stun prey by striking them with their pectoral fins, this behavior if used on an Ariidae spp. could result in external injuries to *G. lessae* (Henningsen 1996; Schreiber 1997).

Metabarcoding and otolith analysis were crucial in describing the diet of *G. lessae* in this study. While the metabarcoding data were better at explaining the total diversity of prey species in the diet of *G. lessae*, both datasets independently drew similar conclusions with regards to what prey genera they are consuming and what variables best explain the dietary variability. In addition, when both datasets were pooled together, PERMANOVA analysis found that the two sampling methods did not produce significantly different results. Considering the cost of both methods, future diet studies on

other *Gymnura* spp. should consider using otoliths in their analysis as opposed to exhausting resources to barcode unidentified teleost species. While analysis of otoliths was valuable in this study, the utility of otoliths in describing diet would be lessened if common teleost prey in the area had indistinguishable otoliths or if the species fed on more than just teleosts, potentially leading to under or overestimation of teleost vs non-teleost prey. I suggest that otolith data should at least be included as a complement to the primary diet analysis as it can provide valuable information not seen otherwise, e.g. male *G. lessae* infrequently consuming *L. xanthurus*, and the addition of three prey genera.

Though the otolith and metabarcoding data arrived at similar conclusions, the DNA metabarcoding provided a more complete view on what prey species *G. lessae* consumed. The DNA metabarcoding was successful in determining prey remains from samples with DNA that was likely too degraded to be amplified using traditional barcoding methods. It also provided insight into what prey species may have been recently consumed but are no longer present in the stomach. The lack of invertebrate DNA in metabarcoding data further confirmed that *G. lessae* are teleost specialized feeders. However, this power can introduce potential bias due to secondary consumption and amplification of DNA that was introduced to the stomach via the water column (Taberlet et al. 2012; Jakubavičiute et al. 2017). While the lack of invertebrate DNA in the samples implies that little DNA was added to the stomach during the trawl itself, DNA of other batoid species that were frequently placed in a temporary holding tank with *G. lessae* after capture were frequently found in the samples. Though *G. altavela* is known to occasionally consume elasmobranchs, I have no evidence to suggest this is the case with *G. lessae*, leading us to believe that this DNA is most likely environmental

contamination (Daiber and Booth 1960; Bizzarro 2005). Thus, care should be placed when analyzing metabarcoding data as DNA presence does not always mean consumption (Leray et al. 2015).

The relatively large size and teleost-specialized feeding of *G. lessae* suggests this fish plays an important role in its ecosystem. Its patchy distribution, but hyper abundance in areas with strong flow, imply that it prefers habitats where it can commonly encounter teleost prey that it can ambush from the substrate. The diet of *G. lessae* throughout the Gulf of Mexico likely reflect the most abundant small to medium sized teleost species in their region. Thus, while there were no commercially important teleost species found in their diets from this study, that may not be the case in other parts of their range.

Tables

Table 2.1 Primers used in this study.

Primer label	Sequence (5'–3')
mlCOIintF	GGWACWGGWTGAACWGTWTAYCCYCC
jgHC02198	TAIACYTCIGGRTGICCRAARAAYCA
SMBRblkCOIF	TACCCCCCATTAGCTGGTAACCTGG-C3

Table 2.2 Diet composition of *Gymnura lessae* collected in Mobile Bay from February 2016 to May 2018 using the results of DNA metabarcoding.

Order	Family	Species	%FO	%N	%PN	%W	%PW	%PSIRI
Unidentified Teleostei			34.0	33.3	98.0	32.8	96.6	33.1
Clupeiformes								
	Clupeidae	<i>Dorosoma petenense</i>	1.4	1.4	100.0	1.4	100.0	1.4
	Engraulidae	<i>Anchoa hepsetus</i>	12.9	12.6	97.4	12.8	99.4	12.7
		<i>Anchoa mitchilli</i>	12.9	12.0	92.7	12.4	95.6	12.2
		<i>Anchoa sp.</i>	0.7	0.6	88.0	0.3	50.0	0.5
Gobiiformes								
	Gobiidae	<i>Ctenogobius boleosoma</i>	1.4	1.0	75.0	1.2	91.4	1.1
Carangiformes								
	Carangidae	<i>Chloroscombrus chrysurus</i>	1.4	1.4	100.0	1.4	100.0	1.4
Pleuronectiformes								
	Achiridae	<i>Trinectes maculatus</i>	2.0	2.0	100.0	2.0	100.0	2.0
	Paralichthyidae	<i>Syacium papillosum</i>	2.7	2.7	100.0	2.7	100.0	2.7
		<i>Etropus crossotus</i>	0.7	0.7	100.0	0.7	100.0	0.7
Sciaeniformes								
	Sciaenidae	<i>Micropogonias undulatus</i>	17.7	17.3	98.1	17.7	99.9	17.5
		<i>Leiostomus xanthurus</i>	6.1	6.1	100.0	6.1	100.0	6.1
		<i>Cynoscion arenarius</i>	4.8	4.4	92.9	4.3	90.5	4.4
		<i>Menticirrhus americanus</i>	4.1	4.1	100.0	4.1	100.0	4.1
		<i>Larimus fasciatus</i>	0.7	0.3	50.0	0.0	2.8	0.2

Frequency of occurrence (%FO), average percent number (%N), average percent weight (%W), prey-specific number (%PN), prey-specific weight (%PW), and the Prey-Specific Index of Relative Importance (%PSIRI).

Table 2.3 Diet composition of *Gymnura lessae* collected in Mobile Bay from February 2016 to May 2018 using free otoliths as a measure of prey species consumption.

Order	Family	Genus / Species	%FO	%N
Unidentified Teleostei			56.3	40.9
Clupeiformes				
	Engraulidae	<i>Anchoa spp.</i>	30.3	23.3
Gadiformes				
	Phycidae	<i>Urophycis sp.</i>	0.8	0.5
Carangiformes				
	Carangidae	<i>Ctenogobius boleosoma</i>	0.8	0.5
Pleuronectiformes				
	Achiridae	<i>Trinectes maculatus</i>	0.8	0.5
	Paralichthyidae	<i>Syacium papillosum</i>	0.8	0.5
Sciaeniformes				
	Sciaenidae	<i>Micropogonias undulatus</i>	26.9	18.2
		<i>Leiostomus xanthurus</i>	15.1	10.6
		<i>Cynoscion spp.</i>	3.4	2.0
		<i>Menticirrhus spp.</i>	3.4	2.0
		<i>Bairdiella chrysoura</i>	0.8	0.5
		<i>Stellifer lanceolatus</i>	0.8	0.5

Frequency of occurrence (%FO) and average percent number (%N).

Table 2.4 PERMANOVA models for the diet composition of *Gymnura lessae* using the results of DNA metabarcoding.

Model(s)	Variable(s)	df	%N				%W			
			F	R ²	P	Disp P	F	R ²	P	Disp P
Independent Variables	Sex	1	2.7802	0.0276	0.0128*	0.2002	2.9234	0.0290	0.0113*	0.1541
	Maturity	1	1.0299	0.0104	0.3827	0.5530	1.0054	0.0102	0.4148	0.6306
	Size	1	1.3653	0.0137	0.2020	0.5204	1.3686	0.0138	0.2053	0.6158
	Temperature	1	2.3466	0.0234	0.0291*	0.6099	2.3987	0.0239	0.0274*	0.7719
	Season	2	3.0945	0.0600	0.0009*	0.8213	3.1748	0.0614	0.0003*	0.8175
	Day Length	1	2.1468	0.0214	0.0444*	0.5730	2.1999	0.0220	0.0415*	0.7630
Interactions	Sex x Maturity	1	1.1228	0.0111	0.3257		1.1226	0.0111	0.3279	
	Sex x Temp	1	1.5908	0.0155	0.1288		1.6530	0.0160	0.1197	
	Sex x Season	2	1.6129	0.0303	0.0799		1.6746	0.0313	0.0654	
	Sex x Day Length	1	2.0807	0.0202	0.0469*		2.1609	0.0209	0.0441*	
	Sex x Size	1	1.6544	0.0163	0.1206		1.6006	0.0158	0.1348	
	Size x Temp	1	1.7518	0.0172	0.0971		1.7088	0.0168	0.1087	
	Size x Season	2	1.5168	0.0290	0.1022		1.5448	0.0295	0.0972	
	Size x Day Length	1	0.7571	0.0076	0.6101		0.7939	0.0079	0.5787	
Size x Maturity	1	0.9492	0.0096	0.4542		0.9426	0.0095	0.4573		
Final Model	Season	2	3.1647	0.0594	0.0002*		3.2397	0.0614	0.0007*	
	Sex	1	2.9378	0.0276	0.0098*		2.9819	0.0283	0.0079*	
	Residuals	96		0.9130			0.9103			

Degrees of freedom (*df*), F-statistic (*F*), coefficient of determination (*R*²), p-value (*P*), and p-values of dispersion analysis (*Disp P*) are included for percent number (%N) and percent weight (%W) data. Significant p-values (*P* < 0.05) indicated with *.

Table 2.5 PERMANOVA models for the diet composition of *Gymnura lessae* using free otoliths as a measure of prey species consumption.

Model(s)	Variable(s)	<i>df</i>	%N			
			<i>F</i>	<i>R</i> ²	<i>P</i>	<i>Disp P</i>
Independent Variables	Sex	1	9.2890	0.0945	0.0001*	0.1376
	Maturity	1	0.7199	0.0080	0.5558	0.7685
	Size	1	4.2497	0.0456	0.0052*	0.0096*
	Temperature	1	3.3883	0.0367	0.0149*	0.4750
	Season	2	2.0867	0.0453	0.0447*	0.0542
	Day Length	1	1.3213	0.0146	0.2446	0.4789
	Interactions	Sex x Maturity	1	1.5624	0.0158	0.1712
Sex x Temp		1	1.0053	0.0101	0.3794	
Sex x Season		2	2.1909	0.0431	0.0365*	
Sex x Day Length		1	2.7488	0.0274	0.0348*	
Sex x Size		1	1.1266	0.0114	0.3167	
Size x Temp		1	0.8915	0.0093	0.4543	
Size x Season		2	1.1561	0.0241	0.3225	
Size x Day Length		1	1.2880	0.0137	0.2623	
Size x Maturity		1	0.9550	0.0098	0.4255	
Final Model	Season	2	2.3043	0.0453	0.0262*	
	Sex	1	7.7954	0.0766	0.0001*	
	Season x Sex	2	2.1909	0.0431	0.0365*	
	Residuals	85		0.8351		

Degrees of freedom (*df*), F-statistic (*F*), coefficient of determination (*R*²), p-value (*P*), and p-values of dispersion analysis (*Disp P*) for the percent number (%N) data. Significant p-values (*P* < 0.05) indicated with *.

Table 2.6 PERMANOVA results for the metabarcoding and otolith data pooled into a single dataset to test for differences in diet based on sampling method.

Variable	%N				
	<i>df</i>	<i>F</i>	<i>R</i> ²	<i>P</i>	<i>Disp P</i>
Sampling Method	1	1.4510	0.0076	0.1967	0.5264

Degrees of freedom (*df*), F-statistic (*F*), coefficient of determination (*R*²), p-value (*P*), and p-values of dispersion analysis (*Disp P*) for the percent number (%N) data. Significant p-values (*P* < 0.05) indicated with *.

Table 2.7 Results of CCA analysis on the metabarcoding data based on the response variables found to be significant in the metabarcoding data PERMANOVA analysis.

	%N			%W		
	<i>df</i>	<i>F</i>	<i>P</i>	<i>df</i>	<i>F</i>	<i>P</i>
Overall Model	5	2.3673	0.0003*	5	2.3738	0.0004*
Canonical Axis						
CCA1	1	5.8089	0.0023*	1	5.8579	0.0021*
CCA2	1	4.0509	0.0401*	1	4.0730	0.0345*
Response Variables						
Spring	1	3.0944	0.0059*	1	3.1238	0.0061*
Summer	1	4.0789	0.0011*	1	4.0957	0.0015*
Sex	1	3.1950	0.0052*	1	3.2438	0.0038*
Temperature	1	0.8549	0.5245	1	0.8269	0.5406
Day Length	1	0.6134	0.6927	1	0.5786	0.7269

Degrees of freedom (*df*), F-statistic (*F*), and p-value (*P*) for percent number (%N) and percent weight (%W) data. Significant p-values (*P* < 0.05) indicated with *.

Table 2.8 Results of CCA analysis on the otolith data based on the response variables found to be significant in both the otolith and metabarcoding data PERMANOVA analysis.

	Otolith Variables			Metabarcoding Variables		
	<i>df</i>	<i>F</i>	<i>P</i>	<i>df</i>	<i>F</i>	<i>P</i>
Overall Model	5	2.7449	0.0001*	5	3.1808	0.0001*
Canonical Axis						
CCA1	1	9.7593	0.0002*	1	10.8828	0.0001*
CCA2	1	1.8623	0.7485	1	3.3378	0.2001
Response Variables						
Sex	1	7.5757	0.0001*	1	6.4543	0.0001*
Size	1	1.7617	0.1310	-	-	-
Temperature	1	2.8384	0.0190*	1	2.1502	0.0693
Spring	1	0.6648	0.6203	1	1.0872	0.3861
Summer	1	0.8839	0.4728	1	2.3810	0.0454*
Day Length	-	-	-	1	3.8310	0.0052*

Degrees of freedom (*df*), F-statistic (*F*), and P value (*P*) for percent number (%N) for the otolith data. Significant values indicated with *.

Table 2.9 Results of CCA analysis on the metabarcoding data based on the response variables found to be significant in the otolith data PERMANOVA analysis.

	%N			%W		
	<i>df</i>	<i>F</i>	<i>P</i>	<i>df</i>	<i>F</i>	<i>P</i>
Overall Model	5	2.3673	0.0003*	5	2.3738	0.0004*
Canonical Axis						
CCA1	1	5.7932	0.0034*	1	5.8594	0.0023*
CCA2	1	3.8007	0.0561	1	3.8219	0.0527
Response Variables						
Sex	1	3.7196	0.0019*	1	3.7739	0.0025*
Size	1	1.1912	0.3117	1	1.1592	0.3348
Temperature	1	2.6004	0.0209*	1	2.6729	0.0157*
Spring	1	1.7232	0.1227	1	1.7330	0.1231
Summer	1	2.6992	0.0180*	1	2.6758	0.0182*

Degrees of freedom (*df*), F-statistic (*F*), and p-value (*P*) for percent number (%N) and percent weight (%W) data. Significant p-values ($P < 0.05$) indicated with *.

Figures

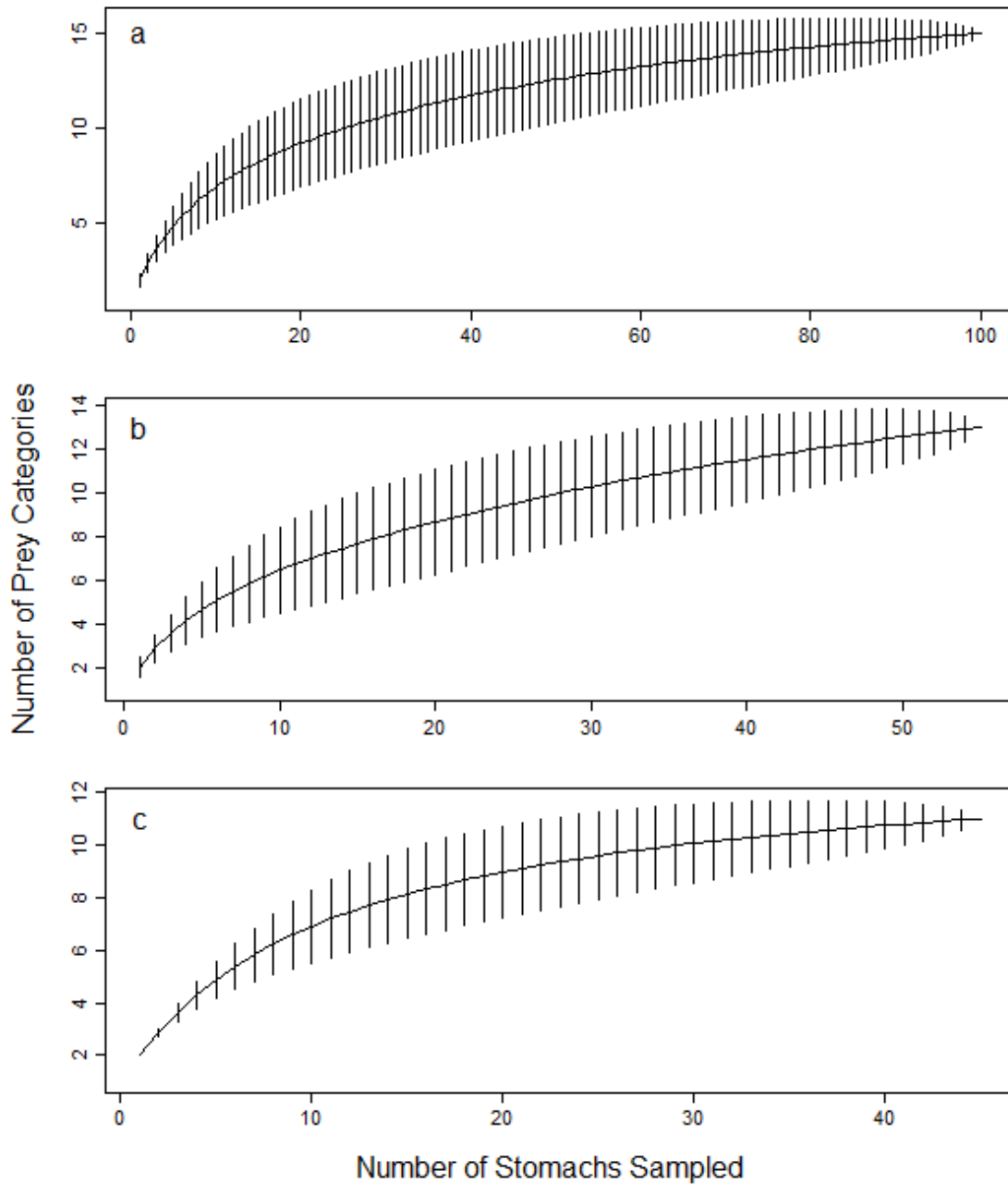


Figure 2.1 Cumulative prey curves for *Gymnura lessae* sampled from February 2016 to May 2018 based on the metabarcoding data with prey categories representing distinct species for increasing number of ray stomachs sampled for a) all stomachs, b) stomachs from males, and c) stomachs from females.

Curve b failed to reach an asymptote. Error bars represent standard deviation.

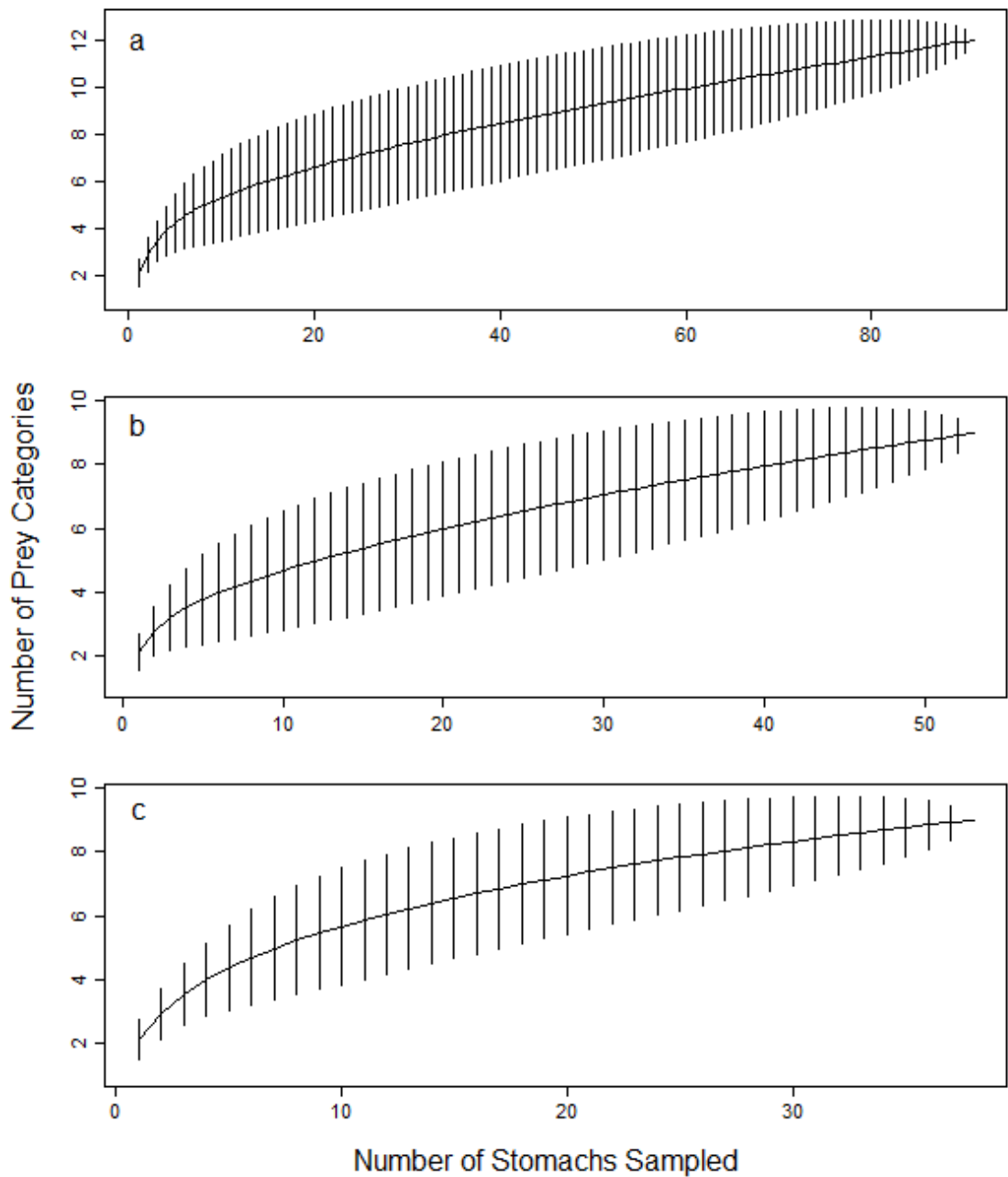


Figure 2.2 Cumulative prey curves for *Gymnura lessae* sampled from February 2016 to May 2018 based on the otolith data with prey categories representing distinct species for increasing number of ray stomachs sampled for a) all stomachs, b) stomachs from males, and c) stomachs from females.

All curves failed to reach an asymptote. Error bars represent standard deviation.

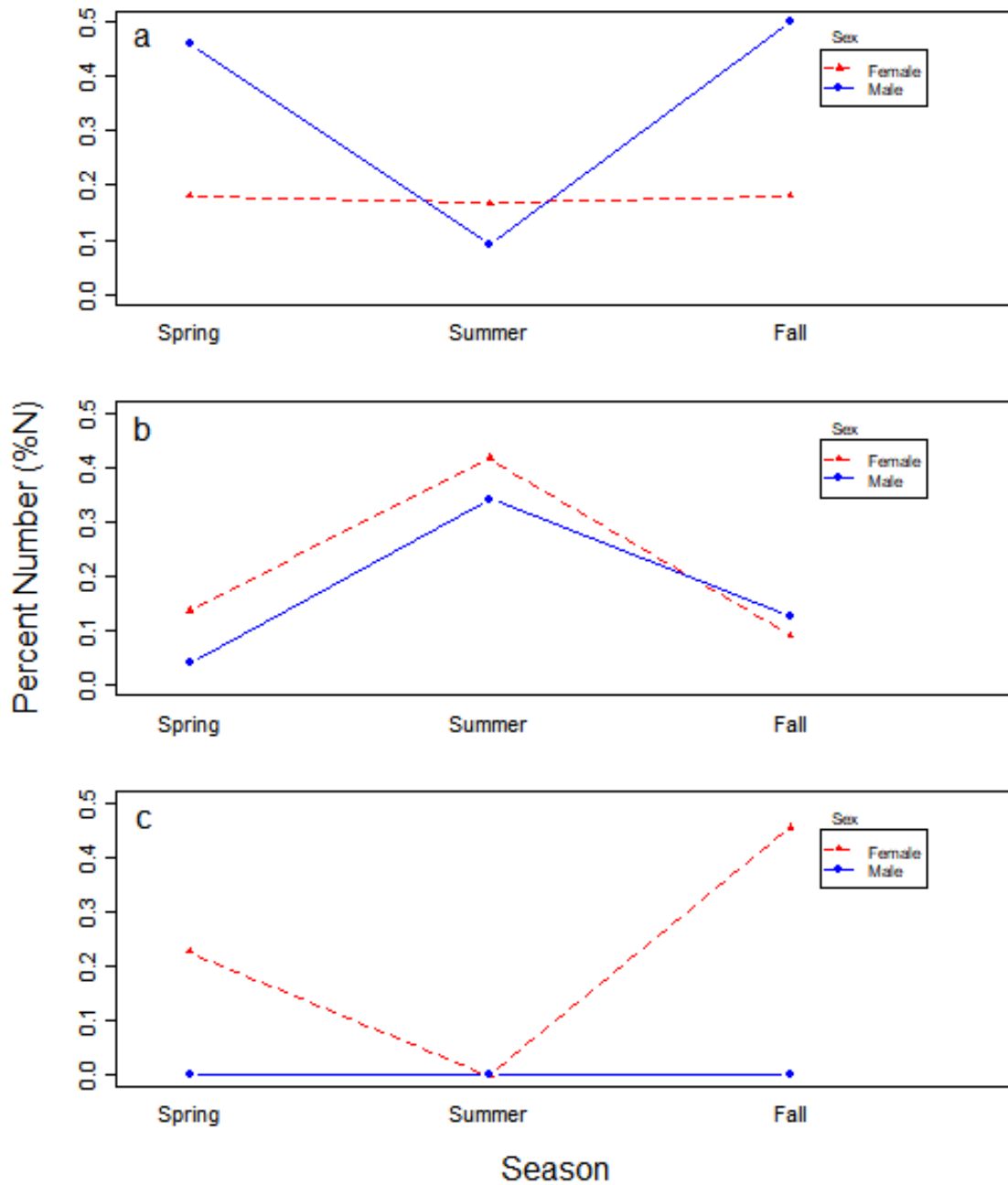


Figure 2.3 Interaction plots for the metabarcoding data comparing the variables season and sex using mean prey consumption, represented by %N, for the prey species a) *Micropogonias undulatus*, b) *Anchoa hepsetus*, and c) *Leiostomus xanthurus* plotted against season.

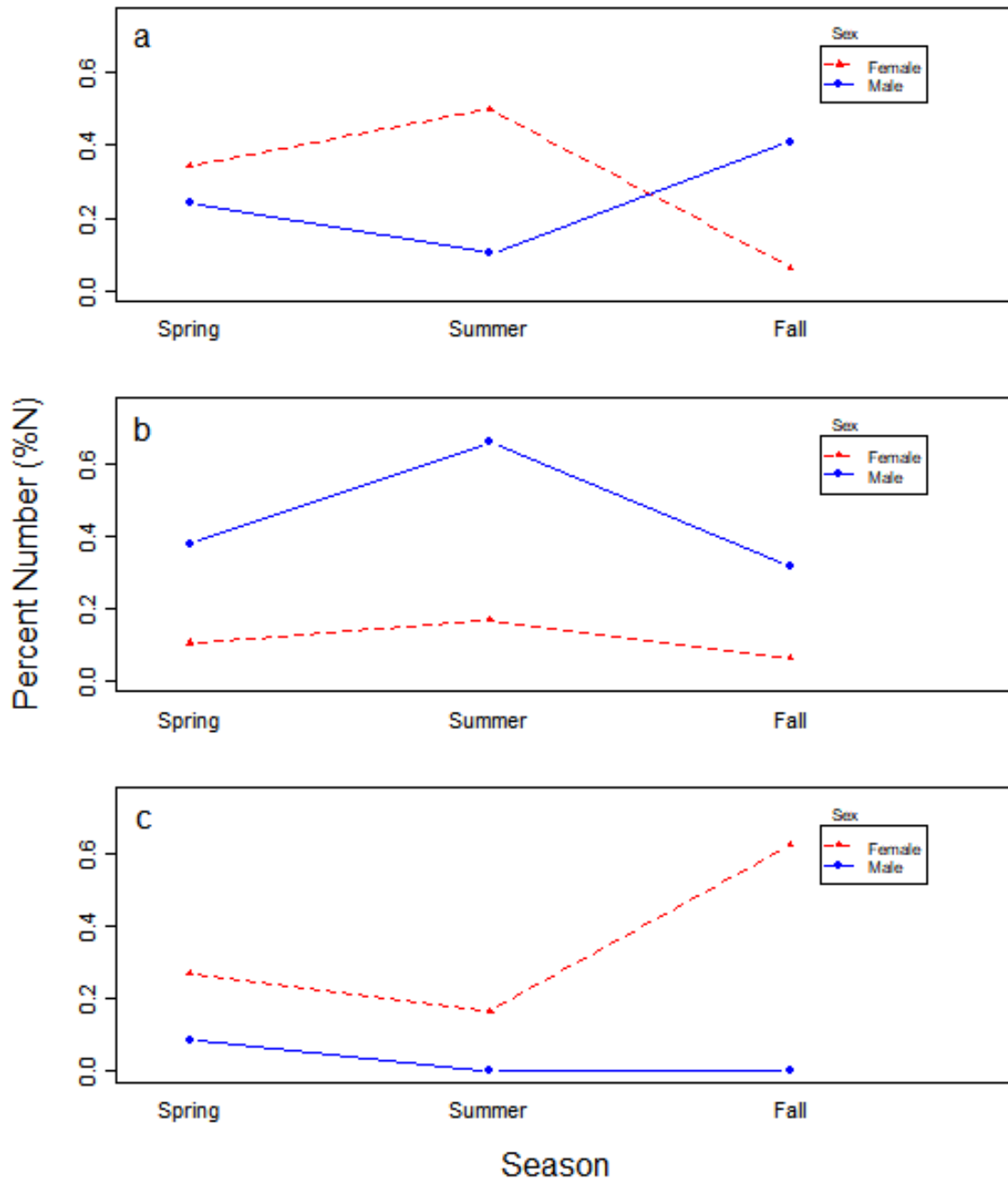


Figure 2.4 Interaction plots for the otolith data comparing the variables season and sex using mean prey consumption, represented by %N, for the prey species a) *Micropogonias undulatus*, b) *Anchoa spp.*, and c) *Leiostomus xanthurus* plotted against season.

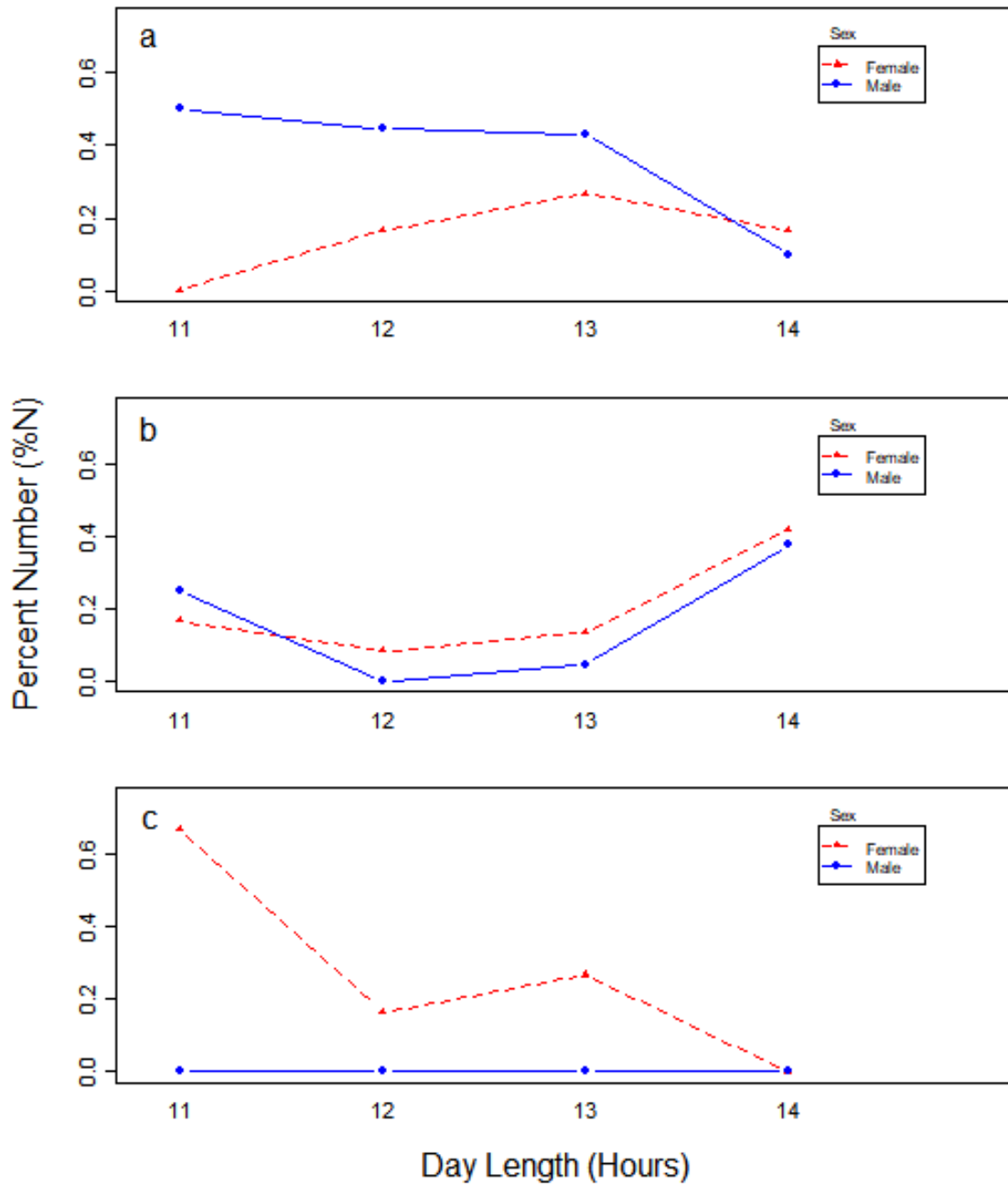


Figure 2.5 Interaction plots for the metabarcoding data comparing the variables day length and sex using mean prey consumption, represented by %N, for the prey species a) *Micropogonias undulatus*, b) *Anchoa hepsetus*, and c) *Leiostomus xanthurus* plotted against day length pooled by hour.

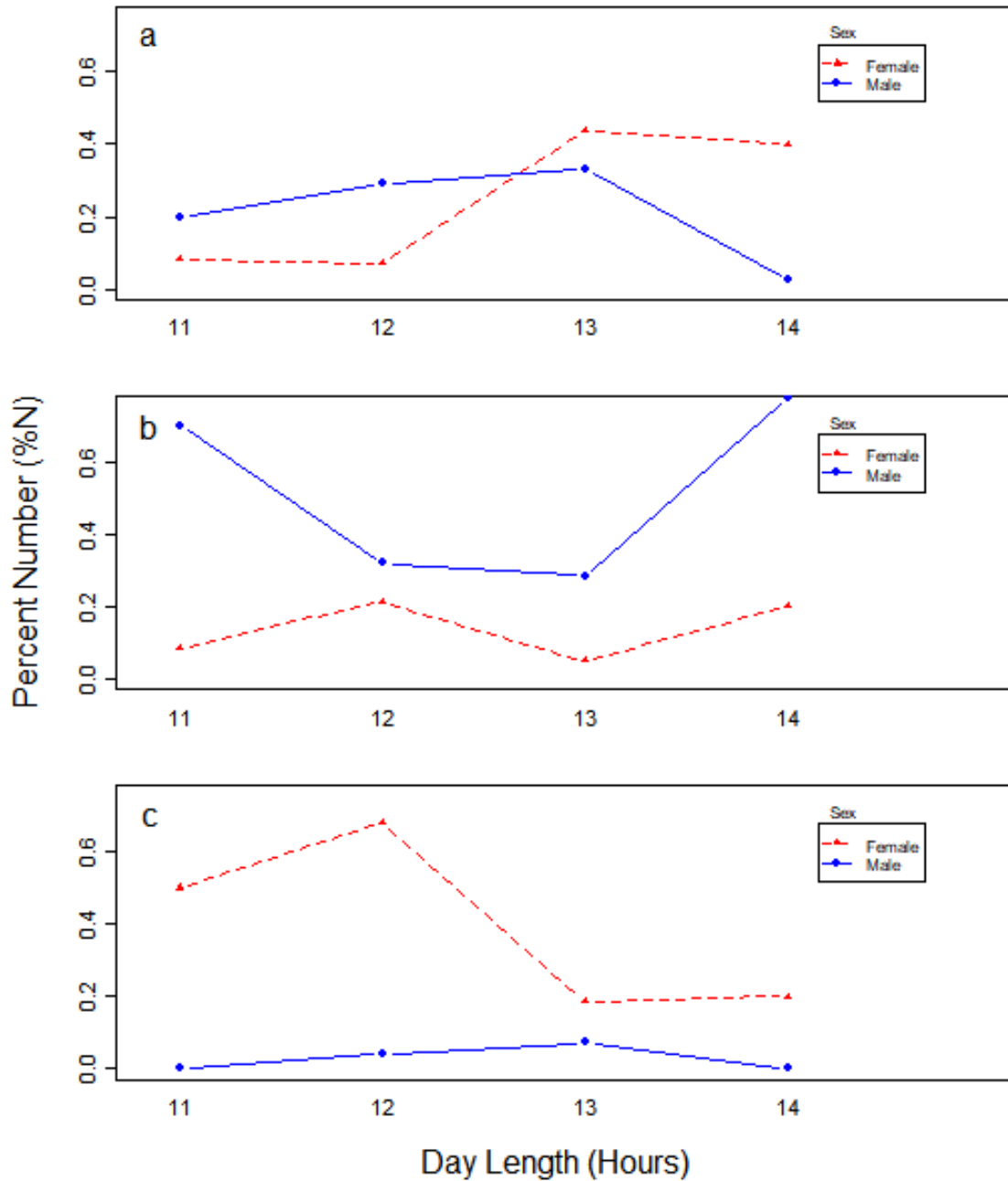


Figure 2.6 Interaction plots for the otolith data comparing the variables day length and sex using mean prey consumption, represented by %N, for the prey species a) *Micropogonias undulatus*, b) *Anchoa hepsetus*, and c) *Leiostomus xanthurus* plotted against day length pooled by hour.

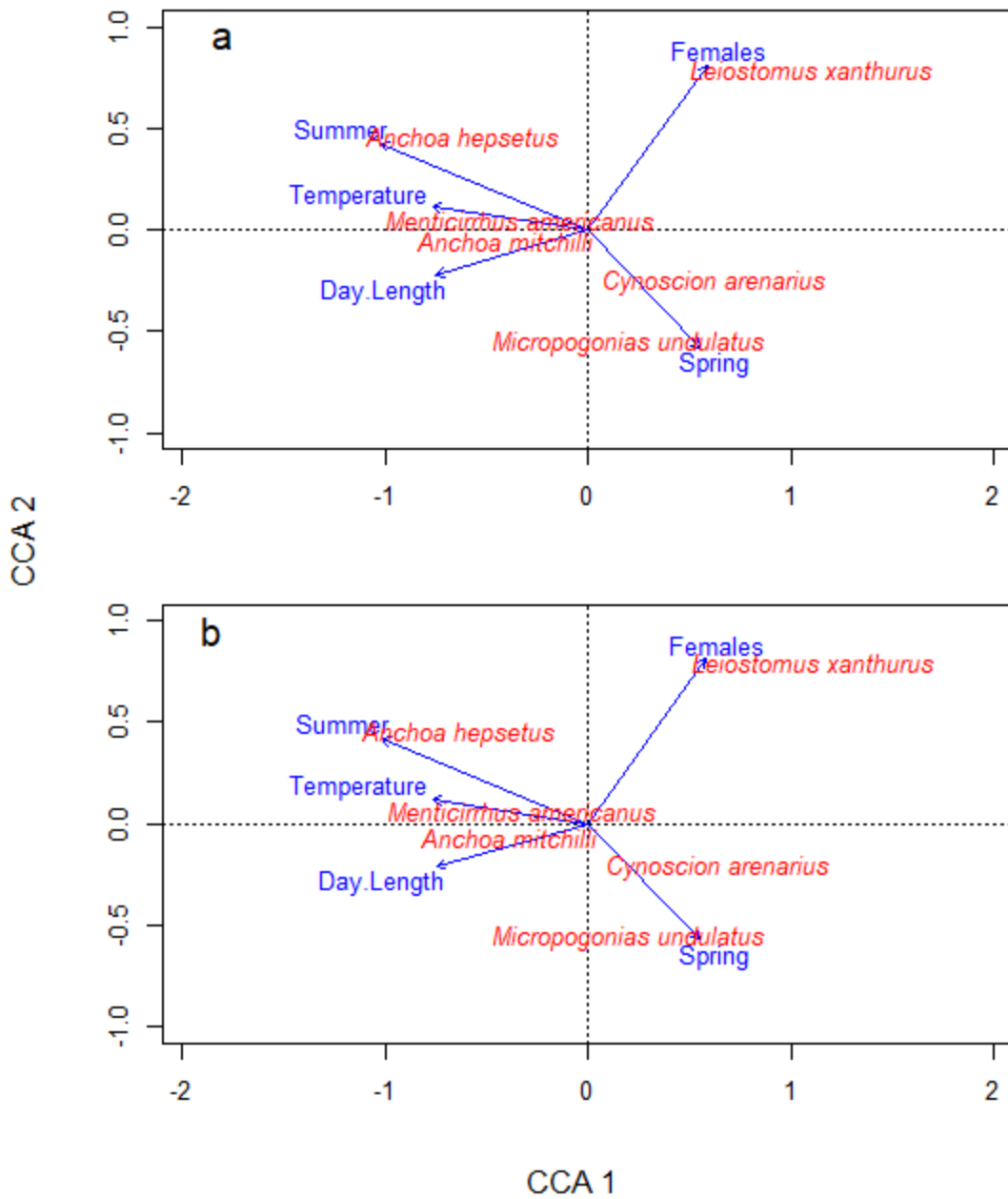


Figure 2.7 CCA biplots of the metabarcoding data showing the relationships between the response variables found to be significant in the metabarcoding data PERMANOVA analysis and prey species for a) percent number, %N, and b) percent weight, %W, for *Gymnura lessae*.

Spatial associations between the response variables (blue) and prey species (red) indicate correlations, whereas their position on each axis is indicative of the relative amount of their explained dietary variability.

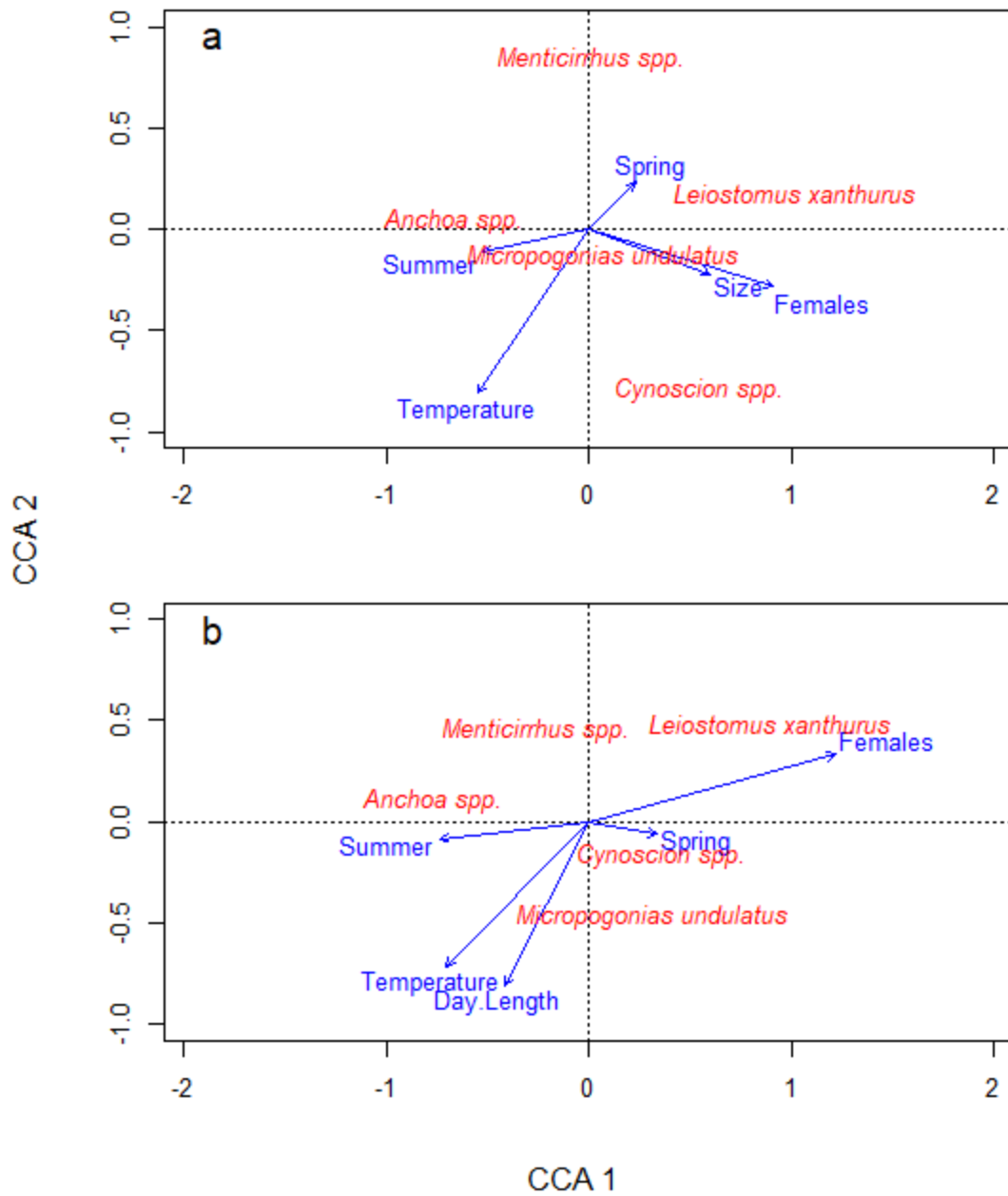


Figure 2.8 CCA biplots of the otolith data showing the relationships between the response variables and prey species / genus for %N showing the variables found to be significant in the PERMANOVA analysis for a) the otolith data and b) the metabarcoding data for *Gymnura lessae*.

Spatial associations between the response variables (blue) and prey (red) indicate correlations, whereas their position on each axis is indicative of the relative amount of their explained dietary variability.

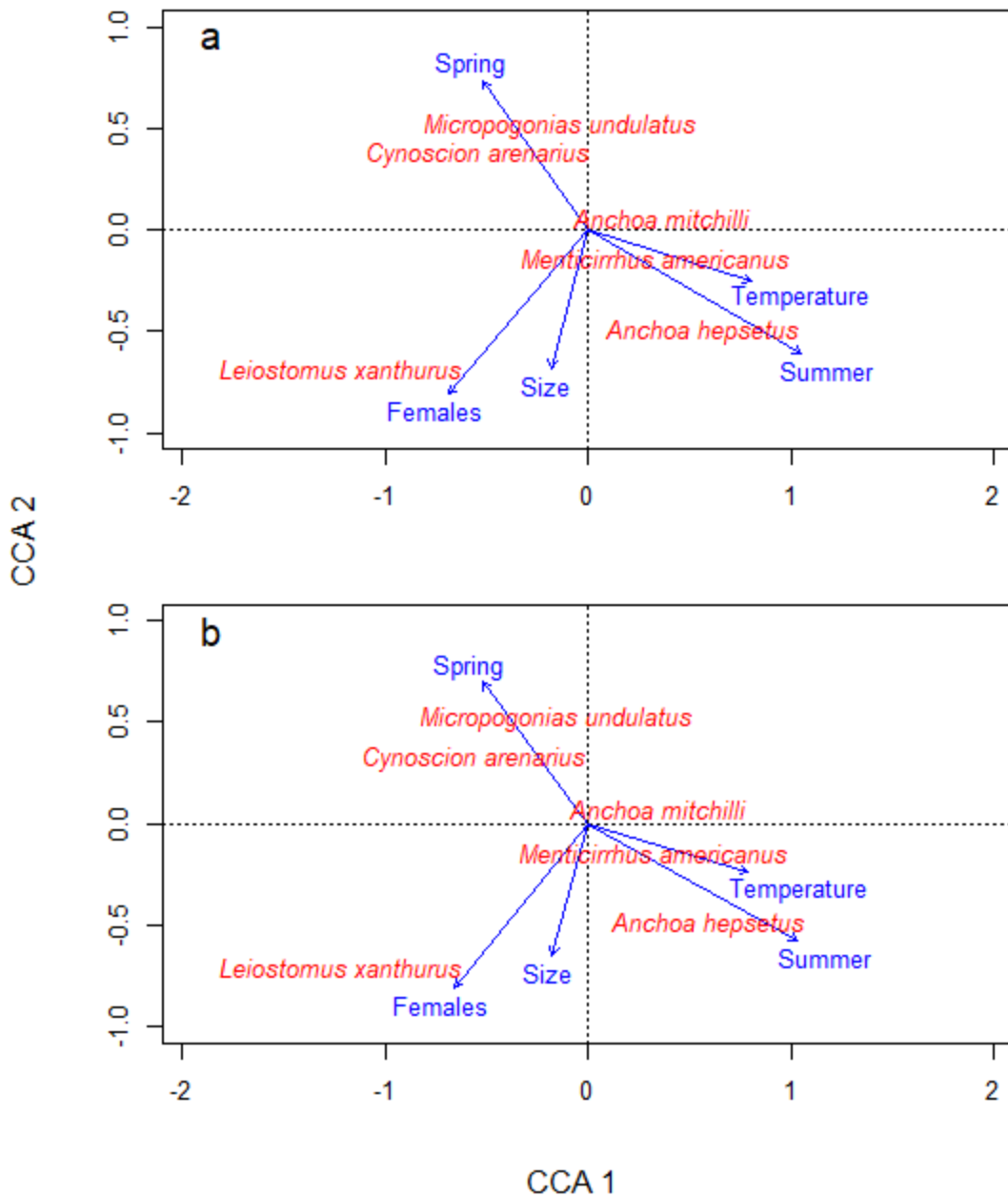


Figure 2.9 CCA biplots of the metabarcoding data showing the relationships between the response variables found to be significant in the otolith data PERMANOVA analysis and prey species for a) percent number, %N, and b) percent weight, %W, for *Gymnura lessae*.

Spatial associations between the response variables (blue) and prey species (red) indicate correlations, whereas their position on each axis is indicative of the relative amount of their explained dietary variability.



Figure 2.10 Snapshot of trawl contents taken during sampling showing differences in relative body size of *Leiostomus xanthurus*, larger bodied fish with distinct black spot located above pectoral fin, compared to *Anchoa hepsetus*, semi-translucent fish with a distinct horizontal silver stripe, and *Micropogonias undulatus*, smaller bodied fish without distinct black spot located above its pectoral fin.

Anchoa mitchilli was not pictured due to being too small to be caught in trawl net.

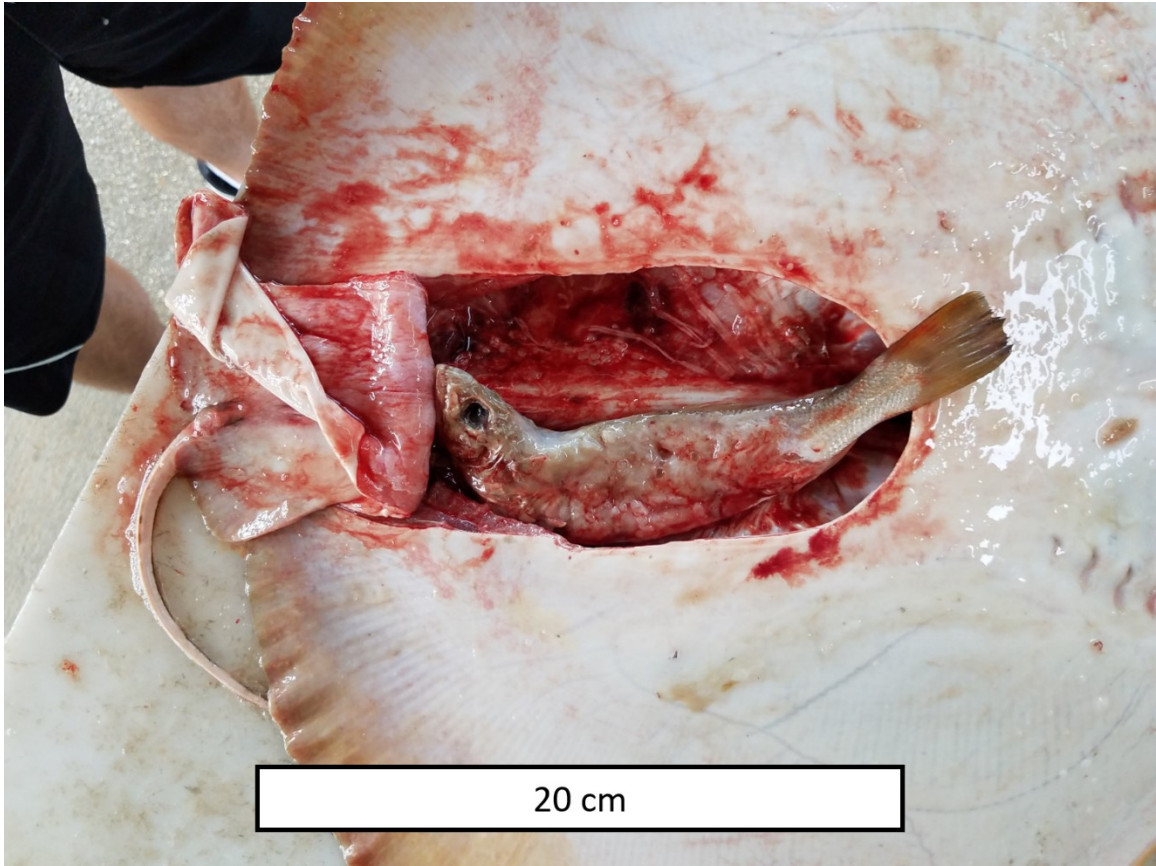


Figure 2.11 Picture of a prey item, *Cynoscion arenarius*, relative to the body cavity of the *Gymnura lessae* that consumed it, which was too large to fit completely into the batoids stomach resulting in only partial digestion of the prey.

REFERENCES

- Adams, K. R., L. C. Fetterplace, A. R. Davis, M. D. Taylor, and N. A. Knott. 2018. Sharks, rays and abortion: The prevalence of capture-induced parturition in elasmobranchs. *Biological Conservation* 217:11–27. Elsevier.
- Ajemian, M. J., and S. P. Powers. 2012. Habitat-specific feeding by cownose rays (*Rhinoptera bonasus*) of the northern Gulf of Mexico. *Environmental Biology of Fishes* 95(1):79–97.
- Ajemian, M. J., and S. P. Powers. 2016. Seasonality and ontogenetic habitat partitioning of cownose rays in the northern Gulf of Mexico. *Estuaries and Coasts* 39(4):1234–1248. *Estuaries and Coasts*.
- Anderson, M. J., and D. C. I. Walsh. 2013. PERMANOVA , ANOSIM , and the Mantel test in the face of heterogeneous dispersions : What null hypothesis are you testing ? *Ecological Monographs* 83(4):557–574.
- Arnold, T. W. 2010. Uninformative parameters and model selection using Akaike’s information criterion. *Journal of Wildlife Management* 74(6):1175–1178.
- Barley, S. C., M. G. Meekan, and J. J. Meeuwig. 2017. Species diversity, abundance, biomass, size and trophic structure of fish on coral reefs in relation to shark abundance. *Marine Ecology Progress Series* 565:163-179.
- Baremore, I. E., and D. M. Bethea. 2010. A guide to otoliths from fishes of the Gulf of Mexico.
- Bigelow, H. B., & Schroeder, W. C. 1953. Fishes of the western north Atlantic. Part 2 (sawfishes, skates, rays, chimaeroids).
- Bizzarro, J. J. 2005. Fishery biology and feeding ecology of rays in Bahía Almejas, Mexico. M.S. Thesis, Moss Landing Marine Laboratories/California State University, San Francisco:468.
- Bizzarro, J. J., H. J. Robinson, C. S. Rinewalt, and D. A. Ebert. 2007. Comparative feeding ecology of four sympatric skate species off central California, USA. *Environmental Biology of Fishes* 80(2–3):197–220.

- Bizzarro, J. J., M. M. Yoklavich, and W. W. Wakefield. 2017. Diet composition and foraging ecology of U.S. Pacific Coast groundfishes with applications for fisheries management. *Environmental Biology of Fishes* 100(4):375–393. *Environmental Biology of Fishes*.
- Boyer, F., C. Mercier, A. Bonin, Y. Le Bras, P. Taberlet, and E. Coissac. 2016. obitools: a unix-inspired software package for DNA metabarcoding. *Molecular ecology resources*, 16(1):176-182.
- Braak, C. J. F. F., and P. F. M. M. Verdonschot. 1995. Canonical correspondence analysis and related multivariate methods in aquatic ecology. *Aquatic Sciences* 57(3):255–289.
- Brown, S. C., J. J. Bizzarro, G. M. Cailliet, and D. A. Ebert. 2012. Breaking with tradition: Redefining measures for diet description with a case study of the Aleutian skate *Bathyraja aleutica* (Gilbert 1896). *Environmental Biology of Fishes* 95(1):3–20.
- Burnham, K. P., and D. R. Anderson. 2003. Model selection and multimodel inference: a practical information-theoretic approach. Springer Science & Business Media.
- Carlson, J. K., A. G. Pollack, W. B. Driggers III, J. I. Castro, A. B. Brame, and J. L. Lee. 2017. Revised analyses suggest that the lesser electric ray *Narcine bancroftii* is not at risk of extinction. *Endangered Species Research* 32:177–186.
- Carreon-Martinez, L., T. B. Johnson, S. A. Ludsin, and D. D. Heath. 2011. Utilization of stomach content DNA to determine diet diversity in piscivorous fishes. *Journal of Fish Biology* 78(4):1170–1182.
- Carvalho, M.R. de, M.E. McCord, and R.A. Myers. 2007. *Narcine bancroftii*. The IUCN Red List of Threatened Species 2007: e.T63142A12622582. Downloaded on 09 January 2019.
- Chipps, S. R., and J. E. Garvey. 2007. Assessment of diets and feeding patterns. Analysis and interpretation of freshwater fisheries data:473–514.
- Clarke, K. R., and R. M. Warwick. 2001. Change in marine communities: an approach to statistical analysis and interpretation, 2nd edition.
- Cowan, J. L. W., J. R. Pennock, and W. R. Boynton. 1996. Seasonal and interannual patterns of sediment-water nutrient and oxygen fluxes in Mobile Bay, Alabama (USA): regulating factors and ecological significance. *Marine Ecology Progress Series* 141(1–3):229–245.
- Craig, J. K., P. C. Gillikin, M. A. Magelnicki, and L. N. May. 2010. Habitat use of cownose rays (*Rhinoptera bonasus*) in a highly productive, hypoxic continental shelf ecosystem. *Fisheries Oceanography*, 19(4):301-317.

- Cu-Salazar, N., J. C. Pérez-Jiménez, I. Méndez-Loeza, and M. Mendoza-Carranza. 2014. Reproductive parameters of females of butterfly ray *Gymnura micrura* (Elasmobranchii) in the southern Gulf of Mexico. *Hidrobiológica* 24(2):109–117.
- Daiber, F. C., and R. A. Booth. 1960. Notes on the Biology of the Butterfly Rays, *Gymnura altavela* and *Gymnura mucrura*. *Copeia* 1960(2):137–139.
- Dedman, S., R. Officer, D. Brophy, M. Clarke, and D. G. Reid. 2015. Modelling abundance hotspots for data-poor Irish Sea rays. *Ecological Modelling* 312:77–90.
- Drymon J.M., P.T. Cooper, S.P. Powers, M.M. Miller, S. Magnuson, E. Krell, and C. Bird. 2019. Genetic identification of depredator species in commercial and recreational fisheries. Manuscript submitted for publication.
- Dulvy, N. K., S. L. Fowler, J. A. Musick, R. D. Cavanagh, P. M. Kyne, L. R. Harrison, J. K. Carlson, L. N. K. Davidson, S. V. Fordham, M. P. Francis, C. M. Pollock, C. A. Simpfendorfer, G. H. Burgess, K. E. Carpenter, L. J. Compagno, D. A. Ebert, C. Gibson, M. R. Heupel, S. R. Livingstone, J. C. Sanciangco, J. D. Stevens, S. Valenti, and W. T. White. 2014. Extinction risk and conservation of the world’s sharks and rays. *eLife* 3:1–35.
- Edgar, R.C., 2010. Search and clustering orders of magnitude faster than BLAST. *Bioinformatics*, 26(19):2460-2461.
- Ferry, L. A., and G. M. Cailliet. 2007. Sample size and data analysis: are we characterizing and comparing diet properly? *GUTSHOP*'96:71.
- Fish, A. C., C. E. Moorman, C. S. Deperno, J. M. Schillaci, G. R. Hess, A. C. Fish, C. E. Moorman, and C. S. Deperno. 2018. Predictors of Bachman’s sparrow occupancy at its northern range limit. *Southeastern Naturalist* 17(1):104–116.
- Fiske, I., and R. B. Chandler. 2011. unmarked : An R Package for Fitting Hierarchical Models of Wildlife Occurrence and Abundance. *Journal of Statistical Software* 43(10).
- Flowers, K. I., M. J. Ajemian, K. Bassos-Hull, K. A. Feldheim, R. E. Hueter, Y. P. Papastamatiou, and D. D. Chapman. 2016. A review of batoid philopatry, with implications for future research and population management. *Marine Ecology Progress Series* 562:251–261.
- Fodrie, F. J., K. L. Heck, S. P. Powers, W. M. Graham, and K. L. Robinson. 2010. Climate-related, decadal-scale assemblage changes of seagrass-associated fishes in the northern Gulf of Mexico. *Global Change Biology*, 16(1):48-59.
- Fox, J., and S. Weisberg. 2011. An {R} Companion to applied regression. *R package*.

- Frisk, M. G. 2010. Life history strategies of batoids. Pages 290-323. *Sharks and Their Relatives II*. CRC Press.
- Funicelli, N. A. 1975. Taxonomy, feeding, limiting factors, and sex ratios of *Dasyatis sabina*, *Dasyatis americana*, *Dasyatis sayi*, and *Narcine brasiliensis*. Ph.D. Dissertation, Univ. S. Miss., Hattiesburg, Mississippi:258.
- Geller, J., C. P. Meyer, M. Parker, and H. Hawk. 2013. Redesign of PCR primers for mitochondrial cytochrome c oxidase subunit I for marine invertebrates and application in all-taxa biotic surveys. *Molecular Ecology Resources* 13(5):851–861.
- Granadeiro, J. P., and M. A. Silva. 2000. The use of otoliths and vertebrae in the identification and size-estimation of fish in predator-prey studies. *Cybium* 24(4):383–393.
- Gremme, G., S. Steinbiss, and S. Kurtz. 2013. GenomeTools: a comprehensive software library for efficient processing of structured genome annotations. *IEEE/ACM Transactions on Computational Biology and Bioinformatics (TCBB)*, 10(3):645-656.
- Grubbs, R. D., J. K. Carlson, J. G. Romine, T. H. Curtis, W. D. McElroy, C. T. McCandless, C. F. Cotton, and J. A. Musick. 2016. Critical assessment and ramifications of a purported marine trophic cascade. *Scientific Reports* 6:20970.
- Grubbs, R. D., J. A. Musick, C. L. Conrath, and J. G. Romine. 2005. Long-term movements, migration, and temporal delineation of a summer nursery for juvenile sandbar sharks in the Chesapeake Bay region. *American Fisheries Society Symposium* 50:87–107.
- Grüss, A., H. Perryman A., E. Babcock A., S. R. Sagarese, J. T. Thorson, C. H. Ainsworth, E. J. Anderson, K. Brennan, M. D. Campbell, M. C. Christman, S. Cross, M. D. Drexler, J. M. Drymon, C. L. Gardner, D. S. Hanisko, J. M. Hendon, C. C. Koenig, M. Love, F. Martinez-Andrade, J. Morris, B. T. Noble, M. A. Nuttall, J. Osborne, C. Pattengill-Semmens, A. G. Pollack, T. T. Sutton, and T. S. Switzer. 2018. Monitoring programs of the U.S. Gulf of Mexico: inventory, development and use of a large monitoring database to map fish and invertebrate spatial distributions. *Reviews in Fish Biology and Fisheries* 28(104):1–25.
- Hao, X., R. Jiang, and T. Chen. 2011. Clustering 16S rRNA for OTU prediction: a method of unsupervised Bayesian clustering. *Bioinformatics* 27(5):611–618.
- Henningsen, A. D. 1996. Captive husbandry and bioenergetics of the spiny butterfly ray, *Gymnura altavela* (Linnaeus). *Zoo Biology* 15(2):135–142.
- Hilbe, J. M. 2011. *Negative binomial regression*. Cambridge University Press.

- Humphries, N. E., S. J. Simpson, V. J. Wearmouth, and D. W. Sims. 2016. Two's company, three's a crowd: fine-scale habitat partitioning by depth among sympatric species of marine mesopredator. *Marine Ecology Progress Series* 561:173–187.
- Hyslop, E. J. 1980. Stomach contents analysis—a review of methods and their application. *Journal of Fish Biology* 17(4):411–429.
- Jacobsen, I. P., and M. B. Bennett. 2013. A comparative analysis of feeding and trophic level ecology in stingrays (Rajiformes; Myliobatoidei) and electric rays (Rajiformes: Torpedinoidei). *PLoS ONE* 8(8).
- Jacobsen, I. P., J. W. Johnson, and M. B. Bennett. 2009. Diet and reproduction in the Australian butterfly ray *Gymnura australis* from northern and north-eastern Australia. *Journal of Fish Biology* 75(10):2475–2489.
- Jakubavičiute, E., U. Bergström, J. S. Eklöf, Q. Haenel, and S. J. Bourlat. 2017. DNA metabarcoding reveals diverse diet of the three-spined stickleback in a coastal ecosystem. *PLoS ONE* 12(10):1–16.
- James, P. S. B. R. 1966. Notes on the biology and fishery of the butterfly ray, *Gymnura poecilura* (Shaw) from the Palk Bay and Gulf of Mannar. *Indian Journal of Fisheries* 13(1 & 2):150–157.
- Jobling, M., and A. Breiby. 1986. The use and abuse of fish otoliths in studies of feeding habits of marine piscivores. *Sarsia* 71(3–4):265–274.
- Johnson, M. R., and F. F. Snelson Jr. 1996. Reproductive life history of the Atlantic stingray, *Dasyatis sabina* (Pisces, Dasyatidae), in the freshwater St. Johns River, Florida. *Bulletin of Marine Science* 59(1):74–88.
- Kajiura, S. M., L. J. Macesic, T. L. Meredith, K. L. Cocks, and L. J. Dirk. 2009. Commensal foraging between double-crested cormorants and a southern stingray. *The Wilson Journal of Ornithology* 121(3):646–648.
- Kemper, J. M., J. J. Bizzarro, and D. A. Ebert. 2017. Dietary variability in two common Alaskan skates (*Bathyraja interrupta* and *Raja rhina*). *Marine Biology* 164(52).
- Last, P. R., W. T. White, M. R. de Carvalho, B. Séret, M. F. W. Stehmann, and G. J. P. Naylor. 2016. *Rays of the world*. Csiro Publishing.
- Leray, M., C. P. Meyer, and S. C. Mills. 2015. Metabarcoding dietary analysis of coral dwelling predatory fish demonstrates the minor contribution of coral mutualists to their highly partitioned, generalist diet. *PeerJ* 3:e1047.

- Leray, M., J. Y. Yang, C. P. Meyer, S. C. Mills, N. Agudelo, V. Ranwez, J. T. Boehm, and R. J. Machida. 2013. A new versatile primer set targeting a short fragment of the mitochondrial COI region for metabarcoding metazoan diversity: Application for characterizing coral reef fish gut contents. *Frontiers in Zoology* 10(1):1–14.
- MacKenzie, D. I., J. D. Nichols, J. E. Hines, M. G. Knutson, and A. B. Franklin. 2003. Estimating site occupancy, colonization, and local extinction when a species is detected imperfectly. *Ecology* 84(8):2200–2207.
- Mazerolle, M. J. 2017. Package ‘AICcmodavg’. *R package*.
- Mildenberger, T. K., M. H. Taylor, and M. Wolff. 2017. TropFishR: an R package for fisheries analysis with length-frequency data. *Methods in Ecology and Evolution* 8(11):1520–1527.
- Moser, M. L., and L. R. Gerry. 1989. Differential effects of salinity changes on two estuarine fishes, *Leiostomus xanthurus* and *Micropogonias undulatus*. *Estuaries* 12(1):35–41.
- Myers, R. A., J. K. Baum, T. D. Shepherd, S. P. Powers, and C. H. Peterson. 2007. Cascading effects of the loss of apex predatory sharks from a coastal ocean. *Science* 315:1846–1850.
- Neer, J. A., and B. A. Thompson. 2005. Life history of the cownose ray, *Rhinoptera bonasus*, in the northern Gulf of Mexico, with comments on geographic variability in life history traits. *Environmental Biology of Fishes* 73(3):321–331.
- O’Shea, O. R., M. Thums, M. van Keulen, R. M. Kempster, and M. G. Meekan. 2013. Dietary partitioning by five sympatric species of stingray (Dasyatidae) on coral reefs. *Journal of Fish Biology* 82(6):1805–1820.
- O’Shea, O. R., M. Thums, M. van Keulen, and M. G. Meekan. 2012. Bioturbation by stingrays at Ningaloo Reef, Western Australia. *Marine and Freshwater Research* 63(3):189–197.
- O’Shea, O. R., B. E. Wueringer, M. M. Winchester, and E. J. Brooks. 2017. Comparative feeding ecology of the yellow ray *Urobatis jamaicensis* (Urotrygonidae) from The Bahamas. *Journal of Fish Biology* 92:73–84.
- Ogle, D. H., P. Wheeler, and A. Dinno. 2018. FSA: fisheries stock analysis. *R package version 0.8.22.9000*.
- Oksanen, A. J., F. G. Blanchet, M. Friendly, R. Kindt, P. Legendre, D. Mcglinn, P. R. Minchin, R. B. O. Hara, G. L. Simpson, P. Solymos, M. H. H. Stevens, and E. Szoecs. 2018. Package ‘vegan.’ *Community Ecology Package, Version 2.5-1*.

- Park, K., C. K. Kim, and W. W. Schroeder. 2007. Temporal variability in summertime bottom hypoxia in shallow areas of Mobile Bay, Alabama. *Estuaries and Coasts* 30(1):54–65.
- Parker, J. C. 1971. The biology of the spot, *Leiostomus xanthurus* Lacepede; and Atlantic croaker, *Micropogon undulatus* (Linnaeus), in two Gulf of Mexico nursery areas. Texas A&M University Sea Grant Publication TAMU-SG-71-210:182.
- Pauly, D., and N. David. 1981. ELEFAN I, a BASIC program for the objective extraction of growth parameters from length-frequency data. *Meeresforschung* 28(4):205-211.
- Platell, M. E., I. C. Potter, and K. R. Clarke. 1998. Resource partitioning by four species of elasmobranchs (Batoidea: Urolophidae) in coastal waters of temperate Australia. *Marine Biology* 131(4):719–734.
- Pompanon, F., B. E. Deagle, W. O. C. Symondson, D. S. Brown, S. N. Jarman, and P. Taberlet. 2012. Who is eating what: diet assessment using next generation sequencing. *Molecular Ecology* 21(8):1931–1950.
- Pörtner, H. O. 2008. Ecosystem effects of ocean acidification in times of ocean warming: a physiologist's view. *Marine Ecology Progress Series* 373:203–217.
- Preisser, E. L., J. L. Orrock, and O. J. Schmitz. 2007. Predator hunting mode and habitat domain alter nonconsumptive effects in predator–prey interactions. *Ecology* 88(11):2744-2751.
- QGIS Development Team. 2018. QGIS Geographic Information System. Open Source Geospatial Foundation Project. <http://qgis.osgeo.org>.
- R Core Team. 2016. A language and environment for statistical computing. R Foundation for Statistical Computing, Vienna, Austria. <https://www.R-project.org>.
- Raje, S. G. 2003. Some aspects of biology of four species of rays off Mumbai water. *Indian Journal of Fisheries* 50(1):89–96.
- Rastgoo, A. R., J. Navarro, and T. Valinassab. 2018. Comparative diets of sympatric batoid elasmobranchs in the Gulf of Oman. *Aquatic Biology*, 27:35-41.
- Rognes, T., T. Flouri, B. Nichols, C. Quince, and F. Mahé. 2016. VSEARCH: a versatile open source tool for metagenomics. *PeerJ* 4:e2584.
- Ronje, E. I., K. P. Barry, C. Sinclair, M. A. Grace, N. Barros, J. Allen, B. Balmer, A. Panike, C. Toms, K. D. Mullin, and R. S. Wells. 2017. A common bottlenose dolphin (*Tursiops truncatus*) prey handling technique for marine catfish (Ariidae) in the northern Gulf of Mexico. *PLoS ONE* 12(7):1–19.

- Rudloe, A. 1989. Habitat preferences, movement, size frequency patterns and reproductive seasonality of the lesser electric ray, *Narcine brasiliensis*. *Northeast Gulf Science* 10(2):103–112.
- Saunders, R., M. A. Hachey, and C. W. Fay. 2006. Maine's diadromous fish community: Past, present, and implications for Atlantic salmon recovery. *Fisheries* 31(11):537–547.
- Schmitt, R. J., and S. J. Holbrook. 1984. Gape-limitation, foraging tactics and prey size selectivity of two microcarnivorous species of fish. *Oecologia* 63(1):6–12.
- Schreiber, C. M. 1997. Captive husbandry of smooth butterfly rays (*Gymnura micrura*). *American Zoo and Aquarium Association Regional Conference Proceedings*:122–126.
- Schroeder, W. W., and W. J. Wiseman Jr. 1988. The Mobile Bay estuary: stratification, oxygen depletion, and jubilees. *Hydrodynamics of Estuaries. Volume II. Estuarine Case Studies*. Pages 41–52
- Schwartz, F. J. 1990. Mass migratory congregations and movements of several species of cownose rays, genus *Rhinoptera*: A world-wide review.
- Shepherd, T. D., and R. A. Myers. 2005. Direct and indirect fishery effects on small coastal elasmobranchs in the northern Gulf of Mexico. *Ecology Letters* 8(10):1095–1104.
- Sheppard, S. K., J. Bell, K. D. Sunderland, J. Fenlon, D. Skervin, and W. O. C. Symondson. 2005. Detection of secondary predation by PCR analyses of the gut contents of invertebrate generalist predators. *Molecular Ecology* 14(14):4461–4468.
- Silva, F. G., and M. Vianna. 2018. Diet and reproductive aspects of the endangered butterfly ray *Gymnura altavela* raising the discussion of a possible nursery area in a highly impacted environment. *Brazilian Journal of Oceanography* 66(3):315–324.
- Smale, M. J., W. H. H. Sauer, and M. J. Roberts. 2001. Behavioural interactions of predators and spawning chokka squid off South Africa: Towards quantification. *Marine Biology* 139(6):1095–1105.
- Smart, J. J., A. Chin, A. J. Tobin, and C. A. Simpfendorfer. 2016. Multimodel approaches in shark and ray growth studies: strengths, weaknesses and the future. *Fish and Fisheries*, 17(4), 955-971.
- Smith, P. J., S. M. Mcveagh, V. Allain, and C. Sanchez. 2005. DNA identification of gut contents of large pelagic fishes. *Journal of Fish Biology* 67(4):1178–1183.

- Snelson Jr, F. F., S. E. Williams-Hooper Jr, and T. H. Schmid. 1988. Reproduction and ecology of the Atlantic stingray, *Dasyatis sabina*, in Florida coastal lagoons. *Copeia* 3(3):729–739.
- Snelson Jr, F. F., S. E. Williams-Hooper Jr, and T. H. Schmid. 1989. Biology of the bluntnose stingray, *Dasyatis sayi*, in Florida coastal lagoons. *Bulletin of Marine Science* 45(1):15–25.
- Springer, S. 1967. Social organization of shark population. Pages 149–174 *Sharks, skates, and rays*.
- Strong Jr, W. R., F. F. Snelson Jr, and S. H. Gruber. 1990. Hammerhead shark predation on stingrays: an observation of prey handling by *Sphyrna mokarran*. *Copeia* 1990(3):836–840.
- Szczepanski, J. A., and D. A. Bengtson. 2014. Quantitative food habits of the bullnose ray, *Myliobatis freminvillii*, in Delaware Bay. *Environmental Biology of Fishes* 97(9):981–997.
- Taberlet, P., E. Coissac, F. Pompanon, C. Brochmann, and E. Willerslev. 2012. Towards next-generation biodiversity assessment using DNA metabarcoding. *Molecular Ecology* 21(8):2045–2050.
- Thrush, S. F., R. D. Pridmore, J. E. Hewitt, and V. J. Cummings. 1991. Impact of ray feeding disturbances on sandflat macrobenthos: do communities dominated by polychaetes or shellfish respond differently? *Marine Ecology Progress Series* 69(3):245–252.
- Tilley, A., J. López-Angarita, and J. R. Turner. 2013. Effects of scale and habitat distribution on the movement of the southern stingray *Dasyatis americana* on a Caribbean atoll. *Marine Ecology Progress Series* 482:169–179.
- VanBlaricom, G. R. 1982. Experimental analyses of structural regulation in a marine sand community exposed to oceanic swell. *Ecological Monographs* 52(3):283–305.
- Venables, W. N., and B. D. Ripley. 2002. *Statistics and computing. Modern applied statistics with S*. Springer, New York, USA.
- Vaudo, J. J., and M. R. Heithaus. 2011. Dietary niche overlap in a nearshore elasmobranch mesopredator community. *Marine Ecology Progress Series* 425:247–260.
- Wetherbee, B. M., E. Cortés, and J. J. Bizzarro. 2004. Food consumption and feeding habits. Pages 225–246 *Biology of Sharks and their Relatives*.

- White, W. T., M. E. Platell, and I. C. Potter. 2004. Comparisons between the diets of four abundant species of elasmobranchs in a subtropical embayment: Implications for resource partitioning. *Marine Biology* 144(3):439–448.
- Xiang, Y., S. Gubian, B. Suomela, and J. Hoeng. 2013. Generalized simulated annealing for global optimization: the GenSA Package. *R Journal* 5(1):13–28.
- Yemişken, E., M. G. Forero, P. Megalofonou, L. Eryilmaz, and J. Navarro. 2018. Feeding habits of three Batoids in the Levantine Sea (north-eastern Mediterranean Sea) based on stomach content and isotopic data. *Journal of the Marine Biological Association of the United Kingdom*, 98(1): 89-96.
- Yokota, L., and M. R. de Carvalho. 2017. Taxonomic and morphological revision of butterfly rays of the *Gymnura micrura* (Bloch & Schneider 1801) species complex, with the description of two new species (Myliobatiformes: Gymnuridae). *Zootaxa* 4332(1):1–74.
- Yokota, L., R. Goitein, M. D. Gianeti, and R. T. P. Lessa. 2012. Reproductive biology of the smooth butterfly ray *Gymnura micrura*. *Journal of Fish Biology* 81(4):1315–1326.
- Yokota, L., R. Goitein, M. D. Gianeti, and R. T. P. Lessa. 2013. Diet and feeding strategy of smooth butterfly ray *Gymnura micrura* in northeastern Brazil. *Journal of Applied Ichthyology* 29(6):1325–1329.
- Zaret, T. M., and A. S. Rand. 1971. Competition in tropical stream fishes: support for the competitive exclusion principle 52(2):336–342.

APPENDIX A

FT. MORGAN SIDE-SCAN SONAR ANALYSIS CRUISE REPORTED

(CRUISE WI201808-L1)

Introduction

The Ft. Morgan side-scan sonar cruise reported (Cruise WI201808-L1) was completed by Trey Spearman of the University of South Alabama on January 10, 2019. All work was funded by the University of South Alabama, Department of Marine Sciences, and the Dauphin Island Sea Lab, Fisheries Ecology Lab. The waters around Ft. Morgan Peninsula, AL are frequently trawled by the R/V *Alabama Discovery*, in part, assisting Matt Jargowsky in sampling species going towards completing his master's degree. This area has not been previously side-scanned by the Dauphin Island Sea Lab, though a survey in 1993 was conducted by East Carolina University to examine the condition of the USS *Tecumseh*. This acoustic survey (side-scan sonar) covered an area 300 meters wide and 3,060 meters long following the shore off Ft. Morgan (Figure A.1). The purpose of this survey was to collect data on bottom features, contours and sediment composition to better inform Mr. Jargowsky in a crucial area of sample collections.

Methods

The Ft. Morgan survey was completed aboard the R/V *E. O. Wilson* on August 24, 2018. A total of 22 transects were completed within the survey area at this time (Figure A.2), and sonar data analysis was conducted within SonarWiz7 utilizing all data collected. The workflow of sonar analysis can be simplified into these major groups: (1) importing data into SonarWiz7; (2) fine-tuning data appearance, including adjustments to gain normalization, bottom tracking, and transect alignment; (3) identifying targets with vertical relief; and (4) identifying broad-scale bottom features, including changes in

sediment composition. Upon completion of the analysis, the contact and feature shapefiles as well as the GeoTiff files were imported into QGIS 3.0 and clipped by the area of interest's extents, giving them a cleaner appearance.

Results

A total of 16 targets (Table A.1) were documented in the Ft. Morgan Sonar Survey within the bounds of the survey area (Figure A.3). Of these, 9 have a high probability of being either mounds of sediment or schools of fish lying just above the sea floor, and they are labeled as a natural contact. Another contact, a sand wave field, was also labeled as natural. The remaining contacts were labeled as artificial (n = 5) or unknown (n = 1). A few of the artificial contacts are also present on current nautical charts, including the USS *Tecumseh*'s marker buoy and a small sunken boat (not to be confused with the *Tecumseh* wreck). The full contact analysis is located at the end of this report (Table A.2).

Broad bottom features were classified into two major groups: changes in sediment composition and trawl paths identified by seafloor scarring. A large sand wave field dominates the southernmost tip of the survey, with a width of over 340 m and a length of over 460 m. This feature expands past the spatial extent of this survey; therefore, it is unknown how far the sand wave field continues. There is another subtler shift in sediment across the northern portion of the survey. Following the northern shoreline of the peninsula is a shift from a sandier sediment nearshore to a muddier sediment farther from shore. This is visualized in the side-scan mosaic in a visible line over 1 kilometer long having the landward side as a "brighter" (stronger) acoustic return, and the seaward

side a “darker” return. The distinct line fades away as it moves westward across the survey area. With only having images from the side-scan mosaic this is as precise a classification as can be derived, and only sediment samples would give a true sediment composition.

Faint trawl scarring is seen across much of the area, usually as shallow markings dug into the sea floor ranging from 45 – 500 meters in length. While it is possible that water current could play a role in digging paths cut into the sediment by tidal changes, these lines follow the same trawl path given to us at the beginning of the sonar survey by captains that trawl this area, and they do not necessarily follow the curved shape of the peninsula (as the sediment does).

Depth contours were constructed utilizing the bottom returns of each transect. Transects were 30 meters apart, giving course-grade resolution to the data, yet a clear shape can be seen. The deepest portion of the survey area was at the bend just north of the sand wave fields at just over 10 meters deep. The sand waves shallowed quickly as we moved south of the deep hole with the shallowest point of the survey just south of the *Tecumseh* marker buoy (3 meters deep). The northern side shallowed much more gradually up to 4 meters deep.

Tables

Table A.1 Contacts in the report.

FtMorganContact0001	8/24/2018 6:39:12 PM	30° 13.52710" N	088° 01.83612" W
FtMorganContact0002	8/24/2018 6:05:10 PM	30° 13.78479" N	088° 01.78960" W
FtMorganContact0003	8/24/2018 6:14:34 PM	30° 13.77943" N	088° 01.77373" W
FtMorganContact0004	8/24/2018 5:53:31 PM	30° 13.89136" N	088° 01.75082" W
FtMorganContact0005	8/24/2018 3:16:22 PM	30° 13.93606" N	088° 01.61235" W
FtMorganContact0006	8/24/2018 3:16:27 PM	30° 13.93974" N	088° 01.60350" W
FtMorganContact0007	8/24/2018 6:58:17 PM	30° 13.80418" N	088° 01.59928" W
FtMorganContact0008	8/24/2018 6:57:04 PM	30° 13.92705" N	088° 01.59101" W
FtMorganContact0009	8/24/2018 2:27:42 PM	30° 13.90314" N	088° 01.56296" W
FtMorganContact0010	8/24/2018 6:53:33 PM	30° 14.05023" N	088° 01.53987" W
FtMorganContact0011	8/24/2018 2:22:24 PM	30° 13.95758" N	088° 01.53612" W
FtMorganContact0012	8/24/2018 3:18:38 PM	30° 14.00937" N	088° 01.40475" W
FtMorganContact0013	8/24/2018 3:20:07 PM	30° 14.10236" N	088° 01.30984" W
FtMorganContact0014	8/24/2018 1:42:08 PM	30° 14.22592" N	088° 01.20468" W
FtMorganContact0015	8/24/2018 4:00:16 PM	30° 14.26434" N	088° 01.15678" W
FtMorganContact0016	8/24/2018 4:41:46 PM	30° 14.27228" N	088° 00.94669" W

Table A.2 Full contact analysis.

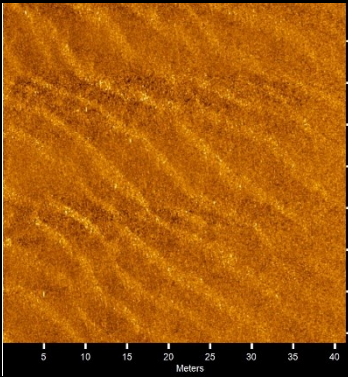
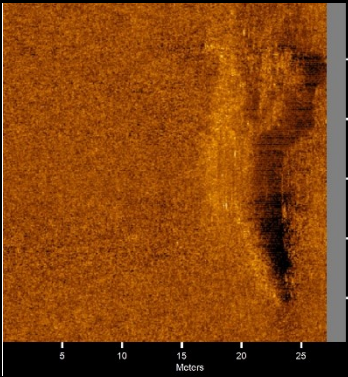
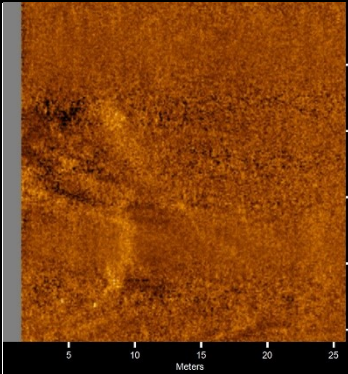
Target Image	Target Info	User Entered Info
	<p>FtMorganContact001</p> <ul style="list-style-type: none"> • Sonar Time at Target: 8/24/2018 6:39:12 PM • Click Position 30° 13.52710" N 088° 01.83612" W (WGS84) • Map Projection: UTM84-16N • Range to target: 31.68 Meters • Fish Height: 7.54 Meters • Heading: 237.200 Degrees 	<p>Dimensions and attributes</p> <ul style="list-style-type: none"> • Target Width: 0.00 Meters • Target Height: 0.00 Meters • Target Length: 0.00 Meters • Target Shadow: 0.00 Meters • Classification1: sand waves • Classification2: natural • Block: • Description: Length > 460m. Width > 340m.
	<p>FtMorganContact002</p> <ul style="list-style-type: none"> • Sonar Time at Target: 8/24/2018 6:05:10 PM • Click Position 30° 13.78479" N 088° 01.78960" W (WGS84) • Map Projection: UTM84-16N • Range to target: 41.88 Meters • Fish Height: 10.55 Meters • Heading: 8.000 Degrees 	<p>Dimensions and attributes</p> <ul style="list-style-type: none"> • Target Width: 7.77 Meters • Target Height: 0.80 Meters • Target Length: 21.90 Meters • Target Shadow: 3.52 Meters • Classification1: unknown • Classification2: natural • Block: • Description: sediment mound or low-lying school of fish
	<p>FtMorganContact003</p> <ul style="list-style-type: none"> • Sonar Time at Target: 8/24/2018 6:14:34 PM • Click Position 30° 13.77943" N 088° 01.77373" W (WGS84) • Map Projection: UTM84-16N • Range to target: 45.48 Meters • Fish Height: 10.28 Meters • Heading: 225.590 Degrees 	<p>Dimensions and attributes</p> <ul style="list-style-type: none"> • Target Width: 7.00 Meters • Target Height: 0.32 Meters • Target Length: 9.34 Meters • Target Shadow: 1.51 Meters • Classification1: unknown • Classification2: natural • Block: • Description: sediment mound or low-lying school of fish

Table A.2 (Continued)

	<p>FtMorganContact0004</p> <ul style="list-style-type: none"> • Sonar Time at Target: 8/24/2018 5:53:31 PM • Click Position 30° 13.89136" N 088° 01.75082" W (WGS84) • Map Projection: UTM84-16N • Range to target: 40.19 Meters • Fish Height: 10.21 Meters • Heading: 232.000 Degrees 	<p>Dimensions and attributes</p> <ul style="list-style-type: none"> • Target Width: 1.87 Meters • Target Height: 0.47 Meters • Target Length: 4.15 Meters • Target Shadow: 1.98 Meters • Classification1: unknown • Classification2: natural • Block: • Description: sediment mound or low-lying school of fish
	<p>FtMorganContact0005</p> <ul style="list-style-type: none"> • Sonar Time at Target: 8/24/2018 3:16:22 PM • Click Position 30° 13.93606" N 088° 01.61235" W (WGS84) • Map Projection: UTM84-16N • Range to target: 45.93 Meters • Fish Height: 10.49 Meters • Heading: 29.500 Degrees 	<p>Dimensions and attributes</p> <ul style="list-style-type: none"> • Target Width: 1.39 Meters • Target Height: 0.30 Meters • Target Length: 2.26 Meters • Target Shadow: 1.40 Meters • Classification1: unknown • Classification2: natural • Block: • Description: sediment mound or low-lying school of fish
	<p>FtMorganContact0006</p> <ul style="list-style-type: none"> • Sonar Time at Target: 8/24/2018 3:16:27 PM • Click Position 30° 13.93974" N 088° 01.60350" W (WGS84) • Map Projection: UTM84-16N • Range to target: 40.84 Meters • Fish Height: 10.48 Meters • Heading: 26.100 Degrees 	<p>Dimensions and attributes</p> <ul style="list-style-type: none"> • Target Width: 1.11 Meters • Target Height: 0.14 Meters • Target Length: 1.91 Meters • Target Shadow: 0.59 Meters • Classification1: unknown • Classification2: natural • Block: • Description: sediment mound or low-lying school of fish
	<p>FtMorganContact0007</p> <ul style="list-style-type: none"> • Sonar Time at Target: 8/24/2018 6:58:17 PM • Click Position 30° 13.80418" N 088° 01.59928" W (WGS84) • Map Projection: UTM84-16N • Range to target: 40.37 Meters • Fish Height: 9.05 Meters • Heading: 222.000 Degrees 	<p>Dimensions and attributes</p> <ul style="list-style-type: none"> • Target Width: 2.71 Meters • Target Height: 0.19 Meters • Target Length: 19.40 Meters • Target Shadow: 0.90 Meters • Classification1: buoy • Classification2: artificial • Block: • Description: Tecumseh Marker Bouy

Table A.2 (Continued)

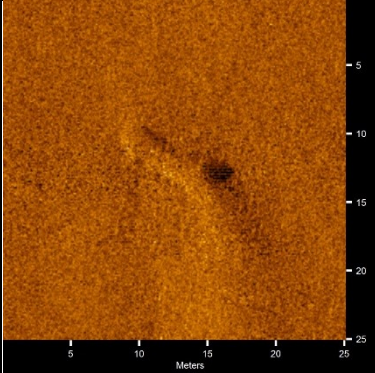
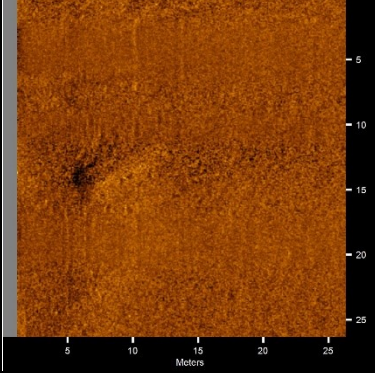
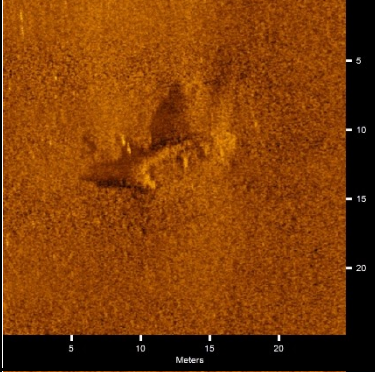
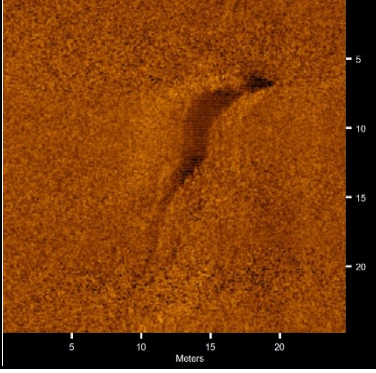
	<p>FtMorganContact0008</p> <ul style="list-style-type: none"> • Sonar Time at Target: 8/24/2018 6:57:04 PM • Click Position 30° 13.92705" N 088° 01.59101" W (WGS84) • Map Projection: UTM84-16N • Range to target: 33.05 Meters • Fish Height: 10.00 Meters • Heading: 230.790 Degrees 	<p>Dimensions and attributes</p> <ul style="list-style-type: none"> • Target Width: 2.34 Meters • Target Height: 0.63 Meters • Target Length: 12.58 Meters • Target Shadow: 2.32 Meters • Classification1: unknown • Classification2: natural • Block: • Description: sediment mound or low-lying school of fish
	<p>FtMorganContact0009</p> <ul style="list-style-type: none"> • Sonar Time at Target: 8/24/2018 2:27:42 PM • Click Position 30° 13.90314" N 088° 01.56296" W (WGS84) • Map Projection: UTM84-16N • Range to target: 41.91 Meters • Fish Height: 9.40 Meters • Heading: 33.390 Degrees 	<p>Dimensions and attributes</p> <ul style="list-style-type: none"> • Target Width: 2.71 Meters • Target Height: 0.40 Meters • Target Length: 6.68 Meters • Target Shadow: 1.92 Meters • Classification1: unknown • Classification2: natural • Block: • Description: sediment mound or low-lying school of fish
	<p>FtMorganContact0010</p> <ul style="list-style-type: none"> • Sonar Time at Target: 8/24/2018 6:53:33 PM • Click Position 30° 14.05023" N 088° 01.53987" W (WGS84) • Map Projection: UTM84-16N • Range to target: 22.02 Meters • Fish Height: 9.08 Meters • Heading: 13.500 Degrees 	<p>Dimensions and attributes</p> <ul style="list-style-type: none"> • Target Width: 2.55 Meters • Target Height: 1.39 Meters • Target Length: 7.47 Meters • Target Shadow: 4.30 Meters • Classification1: wreck • Classification2: artificial • Block: • Description: Sunken Boat
	<p>FtMorganContact0011</p> <ul style="list-style-type: none"> • Sonar Time at Target: 8/24/2018 2:22:24 PM • Click Position 30° 13.95758" N 088° 01.53612" W (WGS84) • Map Projection: UTM84-16N • Range to target: 28.66 Meters • Fish Height: 10.43 Meters • Heading: 261.090 Degrees 	<p>Dimensions and attributes</p> <ul style="list-style-type: none"> • Target Width: 4.54 Meters • Target Height: 0.95 Meters • Target Length: 17.65 Meters • Target Shadow: 3.05 Meters • Classification1: unknown • Classification2: natural • Block: • Description: sediment mound or low-lying school of fish

Table A.2 (Continued)

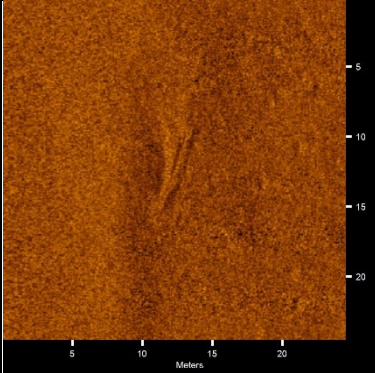
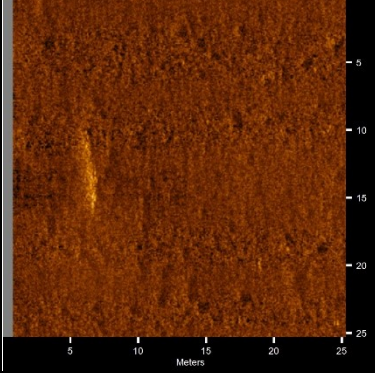
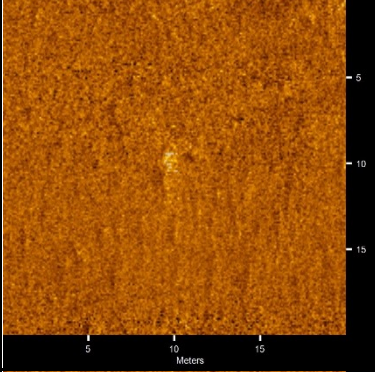
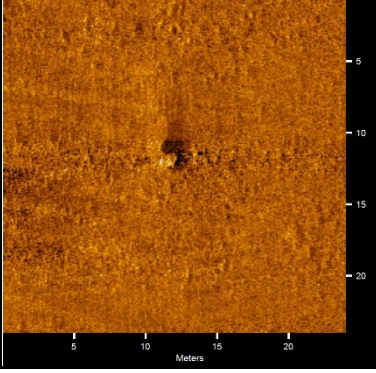
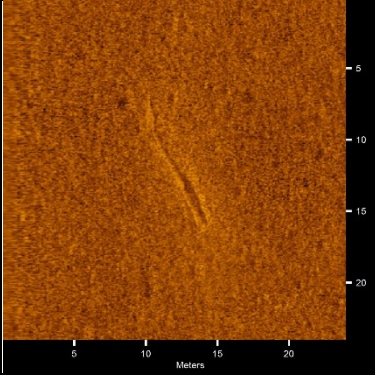
	<p>FtMorganContact0012</p> <ul style="list-style-type: none"> • Sonar Time at Target: 8/24/2018 3:18:38 PM • Click Position 30° 14.00937" N 088° 01.40475" W (WGS84) • Map Projection: UTM84-16N • Range to target: 18.19 Meters • Fish Height: 9.49 Meters • Heading: 26.690 Degrees 	<p>Dimensions and attributes</p> <ul style="list-style-type: none"> • Target Width: 2.23 Meters • Target Height: 0.29 Meters • Target Length: 7.20 Meters • Target Shadow: 0.65 Meters • Classification1: unknown • Classification2: unknown • Block: • Description:
	<p>FtMorganContact0013</p> <ul style="list-style-type: none"> • Sonar Time at Target: 8/24/2018 3:20:07 PM • Click Position 30° 14.10236" N 088° 01.30984" W (WGS84) • Map Projection: UTM84-16N • Range to target: 44.96 Meters • Fish Height: 8.38 Meters • Heading: 31.000 Degrees 	<p>Dimensions and attributes</p> <ul style="list-style-type: none"> • Target Width: 1.24 Meters • Target Height: 0.05 Meters • Target Length: 6.24 Meters • Target Shadow: 0.30 Meters • Classification1: unknown • Classification2: natural • Block: • Description: possibly a school of fish
	<p>FtMorganContact0014</p> <ul style="list-style-type: none"> • Sonar Time at Target: 8/24/2018 1:42:08 PM • Click Position 30° 14.22592" N 088° 01.20468" W (WGS84) • Map Projection: UTM84-16N • Range to target: 31.77 Meters • Fish Height: 7.18 Meters • Heading: 257.400 Degrees 	<p>Dimensions and attributes</p> <ul style="list-style-type: none"> • Target Width: 0.65 Meters • Target Height: 0.13 Meters • Target Length: 1.05 Meters • Target Shadow: 0.60 Meters • Classification1: unknown • Classification2: artificial • Block: • Description:
	<p>FtMorganContact0015</p> <ul style="list-style-type: none"> • Sonar Time at Target: 8/24/2018 4:00:16 PM • Click Position 30° 14.26434" N 088° 01.15678" W (WGS84) • Map Projection: UTM84-16N • Range to target: 33.56 Meters • Fish Height: 6.77 Meters • Heading: 31.800 Degrees 	<p>Dimensions and attributes</p> <ul style="list-style-type: none"> • Target Width: 1.01 Meters • Target Height: 0.35 Meters • Target Length: 1.22 Meters • Target Shadow: 1.85 Meters • Classification1: unknown • Classification2: artificial • Block: • Description:

Table A.2 (Continued)

	<p>FtMorganContact0016</p> <ul style="list-style-type: none">• Sonar Time at Target: 8/24/2018 4:41:46 PM• Click Position 30° 14.27228" N 088° 00.94669" W (WGS84)• Map Projection: UTM84-16N• Range to target: 12.81 Meters• Fish Height: 5.60 Meters• Heading: 35.000 Degrees	<p>Dimensions and attributes</p> <ul style="list-style-type: none">• Target Width: 0.91 Meters• Target Height: 0.00 Meters• Target Length: 9.53 Meters• Target Shadow: 0.00 Meters• Classification1: scar• Classification2: artificial• Block:• Description: anchor scar
---	---	--

Figures



Figure A.1 Survey extent of the Ft. Morgan Sonar Survey outlined in orange.

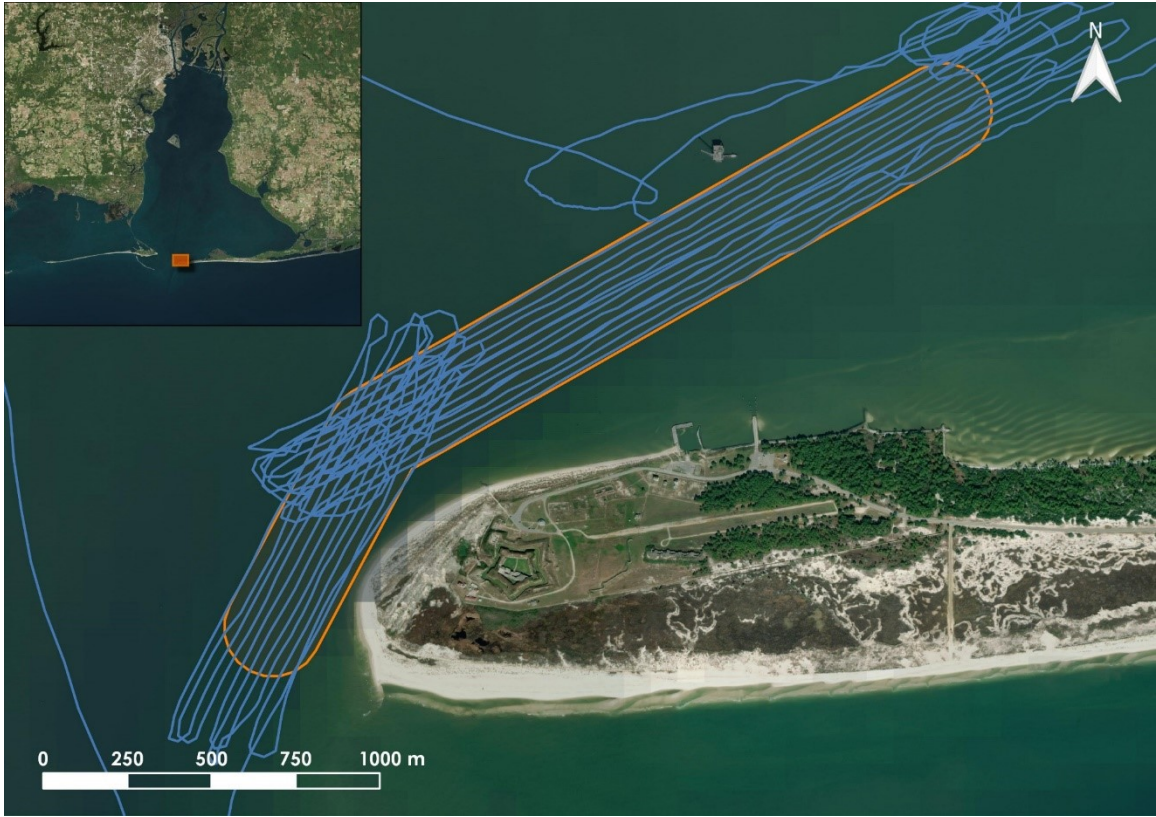


Figure A.2 Actual cruise track for the Ft. Morgan Sonar Survey.



Figure A.3 Contacts identified within the Ft. Morgan Sonar Survey.